eman ta zabal zazu

Universidad del País Vasco

Euskal Herriko Unibertsitatea

Faculty of Medicine and Nursing. Department of Neurosciences

EXPLORING MICROGLIAL TARGETS IN EXPERIMENTAL MULTIPLE SCLEROSIS

DOCTORAL THESIS

Alejandro Montilla López

Thesis supervisors: María Domercq García and Carlos Matute Almau

University of the Basque Country (UPV/EHU)

Leioa, 2022

Part of the results presented in this Doctoral Thesis have been published in the following articles:

Montilla A, Ruiz A, Marquez M, Sierra A, Matute C, Domercq M. Role of Mitochondrial Dynamics in Microglial Activation and Metabolic Switch (2021). *Immunohorizons 5:615-626.*

Montilla A, Zabala A, Matute C, Domercq M. Functional Metabolic Characterization of Microglia Culture in a Defined Medium (2020). *Frontiers in Cellular Neuroscience 14:2.*

This work was supported by:

- Spanish Ministry of Education and Science (SAF2013-45084-R and SAF2016-75292-R).
- Merck Serono (a business of Merck KGaA, Germany) - Grant for Multiple Sclerosis Innovation.
- Centro de Investigación Biomédica en Red, Enfermedades Neurodegenerativas (CIBERNED) (grant no. CB06/05/0076).
- Basque Government (IT702-13).

INDEX

LIST OF ABBREVIATIONS

ACK	Ammonium-Chloride-Potassium
AD	Alzheimer's disease
ANT	Adenine nucleotide translocase
APC	Antigen presenting cell
ATP	Adenosine triphosphate
BBB	Blood-brain barrier
BCA	Bicinchoninic acid
CAM	CNS-associated macrophages
CCL	C-C motif chemokine ligand
CCR	C-C motif chemokine receptor
CD	Cluster of differentiation
CE	Cholesterol ester
CFA	Complete Freund's adjuvant
CNS	Central nervous system
CSF	Cerebrospinal fluid
CSF	Colony stimulating factor
DAN	Diaminonaphthalene
DC	Dendritic cell
DEG	Differentially expressed gene
DMEM	Dulbecco's modified eagle medium
DMT	Disease-modifying therapy
DPI	Day post injection/immunization
EAE	Experimental autoimmune encephalomyelitis
EAE	Experimental autoimmune encephalomyelitis
EB	Evans blue
EBV	Epstein-Barr virus
ECAR	Extracellular acidification rate
ECM	Extracellular matrix
EGFP	Enhanced green fluorescent protein
FACS	Fluorescence-activated cell sorting
FBS	Fetal bovine serum

FITC	Fluorescein isotiocyanate
FoxP3	Forkhead box protein P3
GFAP	Glial fibrillary acidic protein
GM	Grey matter
GM-CSF	Granulocyte macrophage colony-stimulating factor
GO	Gene ontology
HBSS	Hanks balanced salt solution
ICC	Immunocytochemistry
IFN	Interferon
IGF	Insulin growth factor
IHC	Immunohistochemistry
IL	Interleukin
IMDM	Iscove's modified Dulbecco's medium
IMS	Imaging mass spectrometry
iNOS	Inducible nitric oxide synthase
IRF	Interferon regulatory factor
LC	Liquid chromatography
LD	Lipid droplet
LDL	Low density lipoprotein
LPC	Lysolecithin
LPS	Lipopolysaccharide
LXR	Liver X receptor
MALDI	Matrix-assisted laser desorption/ionization
MBP	Myelin basic protein
MHC	Major histocompatibility complex
MOG	Myelin oligodendrocyte glycoprotein
MRI	Magnetic resonance imaging
MS	Mass spectrometry
MS	Multiple sclerosis
NADPH	Nicotinamide adenine dinucleotide phosphate
NF-κB	Nuclear factor kappa B
NGS	Normal goat serum

NO	Nitric oxide
OCR	Oxygen consumption rate
OPC	Oligodendrocyte progenitor cell
ORO	Oil Red O
OXPHOS	Oxidative phosphorylation
PBS	Phosphate-buffered saline
PCR	Polymerase chain reaction
PE	Phycoerythrin
PER	Proton efflux rate
PFA	Paraformaldehyde
PPAR	Peroxisome proliferator-activated receptor
PPMS	Primary progressive multiple sclerosis
PPP	Pentose phosphate pathway
PRR	Pattern recognition receptor
PTX	Pertussis Toxin
RFP	Red fluorescent protein
Rh123	Rhodamine 123
ROI	Region of interest
ROR	Retinoic acid-related orphan receptor
ROS	Reactive oxygen species
RRMS	Relapsing-remitting multiple sclerosis
RT	Room temperature
SPMS	Secondary progressive multiple sclerosis
TAK	Transforming growth factor – activated kinase
TGF	Transforming growth factor
TLR	Toll-like receptor
TMM	Trimmed mean of M-values
TNF	Tumour-necrosis factor
TREM	Triggering receptor expressed on myeloid cells
WM	White matter
WT	Wild type
$\Delta\Psi m$	Mitochondrial membrane potential

INTRODUCTION

1. MULTIPLE SCLEROSIS

First described by Jean Martin Charcot in 1868 (Zalc, 2018), **multiple sclerosis** (MS) is a chronic and inflammatory disease of the central nervous system (CNS) that involves **demyelination and axonal degeneration**. MS is currently the most common cause of non-traumatic disability in young adults, as it generally manifests prior to the age of 40. The patients usually develop neurological symptoms including motor impairments such as spasticity, weakness or ataxia, sensory disturbances, bladder dysfunction and dysphagia (Dendrou et al., 2015). Nevertheless, the disease course can vary between individuals, provoking different types of lesions and diverse clinical symptomatology.

This neurodegenerative disorder affects approximately 2.5 million people worldwide, implying a substantial social and economic burden (Filippi et al., 2018). Interestingly, it is more frequent among the female population (Browne et al., 2014) and the prevalence also varies geographically (Rosati, 2001). These features suggest that MS is a highly heterogeneous disease associated with multiple **gene-environment interactions** (Fig. 1). Indeed, both kinds of risk factors have been identified. Genome-wide association studies have identified more than 200 risk *loci* associated with MS susceptibility, mostly to major histocompatibility complex (MHC), adaptive immunity and microglial function (Patsopoulos et al., 2019). Environmental factors influencing MS pathogenesis include vitamin D deficiency, smoking, adolescent obesity or infections (Thompson et al., 2018). Regarding the latter, a recent study has highlighted that Epstein-Barr virus (EBV) infection is importantly linked to a risk of subsequent MS development (Bjornevik et al., 2022).

All these genetic and environmental agents lead to aberrant inflammatory reactions against myelin components, with subsequent oligodendrocyte death, demyelination and axonal damage (Dendrou et al., 2015). Nonetheless, the specifics behind the etiology of the disorder are yet to be fully revealed.

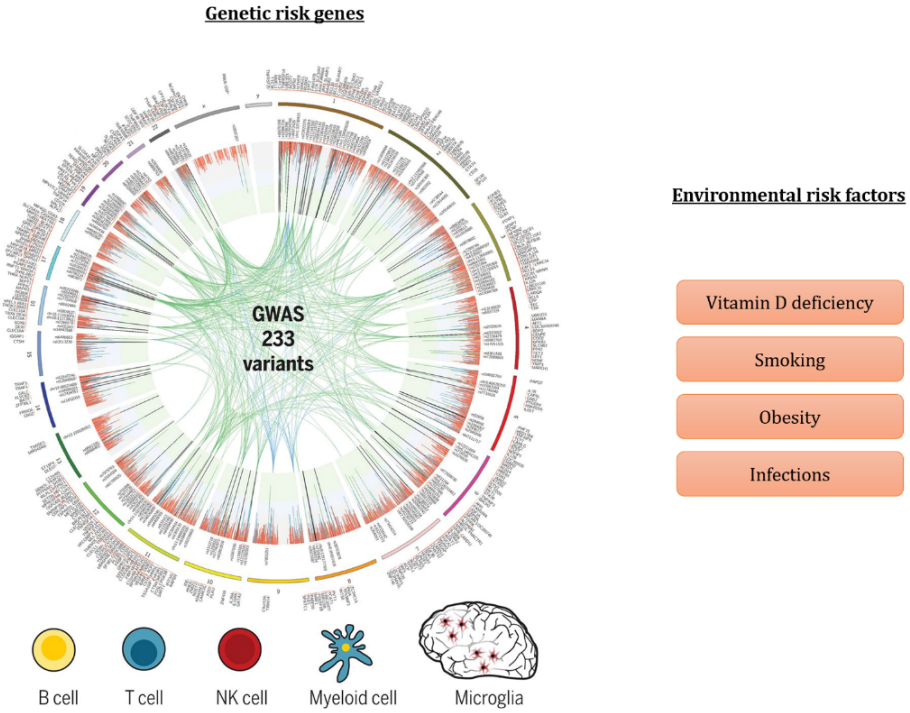

Figure 1. Gene-environment interactions behind MS complexity. (Left) Genetic map of the susceptibility genes for MS, obtained by GWAS analysis. Most associations were found in genes related to immunity. (*From Patsopoulos et al., 2019*) (Right) List of the known environmental risk factors linked to MS development.

Etiology of multiple sclerosis

Multiple sclerosis onset and progression imply complex networks of pathogenic mechanisms, involving activities of both glial and immune cells. However, it is currently unclear whether the root cause of these mechanisms is extrinsic or intrinsic.

The prevailing paradigm is known as the "**outside-in**" model, in which autoreactive T cells enter the CNS through the blood-brain barrier (BBB) and direct their action towards myelin components. These lymphocytes can damage myelin directly by releasing toxins or indirectly by inducing the activation of myeloid cells, such as microglia, and other recruited innate and adaptive immune cells. All these hallmarks lead to neuroinflammation and demyelination (Matute and Pérez-Cerdá, 2005). Some typical MS animal models, such as the experimental autoimmune encephalomyelitis (EAE), mimic the features of this model, and are based on the autoimmune attack towards myelin (Constantinescu et al., 2011).

Alternatively, the "**inside-out**" paradigm suggest that axonal damage and oligodendrocyte degeneration are the primary events triggering the development of MS. This way, infiltration of immune cells and neuroinflammation would be secondary consequences of

these features, and not the root cause of the pathology. The main evidence supporting this theory was the finding of oligodendroglial apoptosis prior to immune cell infiltration in patients who died during or shortly after the onset of a fatal relapse, at early stages of the disease (Barnett and Prineas, 2004; Matute and Pérez-Cerdá, 2005). The nature of the signals initiating oligodendrocyte apoptosis could be variable. Viral infections and the subsequent release of viral products, such as syncytin, are associated to oligodendrocyte cytotoxicity (Antony et al., 2004). Similarly, other events like glutamate or ATP-derived excitotoxicity or oxidative stress can give rise to this outcome (Matute et al., 2001; Matute and Pérez-Cerdá, 2005).

It is still a matter of debate whether demyelination is a pre-requisite for axonal injury or axonal damage can alternatively precede myelin loss. Both mechanisms can even represent independent processes in certain disease entities.

Pathophysiology of multiple sclerosis

The pathological hallmark of MS is the appearance of focal plaques, or lesions, indicative of demyelination and oligodendrocyte degeneration, in both the gray and white matter of the brain and spinal cord (Filippi et al., 2018).

As previously stated, MS pathology development is highly heterogeneous and, thus, a classification of the diverse **clinical courses** was needed. This categorization was determined in 1996 and re-examined in recent years (Lublin and Reingold, 1996; Lublin et al., 2014). MS usually presents in a relapsing-remitting pattern (RRMS), characterized by the occurrence of relapses at irregular intervals, alternating with symptom-free periods (Compston and Coles, 2008). The relapses last more than 24 hours and correspond with focal CNS inflammation and demyelination, as described by magnetic resonance imaging (MRI). RRMS accounts for almost 85% of the diagnosed patients, and most of these evolve to a progressive disease course, denominated secondary progressive MS (SPMS). SPMS is associated to irreversible neurological decline, with CNS atrophy and axonal loss, while inflammatory lesions are no longer the typical characteristic. Alternatively, a low percentage of patients (approximately 15%) experience an uninterrupted progression of the disease from the onset, without a relapsing phase; this MS subtype is called primary progressive MS (PPMS; Dendrou et al., 2015).

Neuroinflammation is found at all stages of multiple sclerosis, but it is more pronounced during the acute phases of the disease. This inflammation is caused by **infiltrating immune cells**, including CD4 and CD8 T cells, B cells and macrophages, and further exacerbated by CNS resident glial cell types (Dendrou et al., 2015; Lassmann and Bradl, 2017). Despite the CNS being considered a site of immune privilege, during MS the BBB is disrupted to favour this infiltration. The immune cells are selectively recruited by autoantigens, possibly derived from myelin proteins, such as the myelin basic protein (MBP) or the myelin oligodendrocyte glycoprotein (MOG). The specific target antigen has not been confirmed yet, due to limitations detecting them and other factors like inter-patient variation or epitope spreading (Schirmer et al., 2014; Dendrou et al., 2015).

Once in the CNS, T cells become reactivated by antigen presenting cells (APCs), such as microglia, macrophages, dendritic cells (DCs), or even oligodendrocytes themselves (Falcão et al., 2018); this is evidenced by the strong association of MHC genes and their alterations to MS (Chastain et al., 2011). Nevertheless, the main cell type involved in antigen presentation remains to be determined. $CD4^+$ T cells differentiate towards Th1 and Th17 phenotypes, both known to be involved in the pathology (Lovett-Racke et al., 2011), further promoting BBB disruption and the activation of diverse cells such as monocytes, microglia or astrocytes. These activated cells cause **myelin breakdown and axonal degeneration** by the release of pro-inflammatory mediators as well as oxygen and nitric oxide radicals (Strachan-Whaley et al., 2014) (Fig. 2).

Importantly, demyelinating lesions can undergo myelin regeneration, in a process denominated **remyelination**. This process can, at least partially, reinstate saltatory conduction and resolve functional deficits (Franklin and Ffrench-Constant, 2017), and is more efficient during the initial phases of the disease. Actually, a failure in the repairing mechanisms determines the transition from RRMS to SPMS (Dendrou et al., 2015). Remyelination is based on the generation of new myelin sheaths by newly generated oligodendrocytes. Specifically, oligodendrocyte progenitor cells (OPCs) migrate towards the lesions by chemoattractants, secreted by microglia, macrophages and astrocytes. Following recruitment, OPCs differentiate into mature and myelinating oligodendrocytes (Watanabe et al., 2002; Fancy et al., 2004), which subsequently give rise to new myelin sheaths around the demyelinated axons; nevertheless, these myelin sheaths are shorter and thinner than

the original ones. It is noteworthy to mention that efficient myelin removal by specialized phagocytes, such as resident microglia or infiltrating monocytes, is essential to facilitate this regenerative process (Neumann et al., 2009).

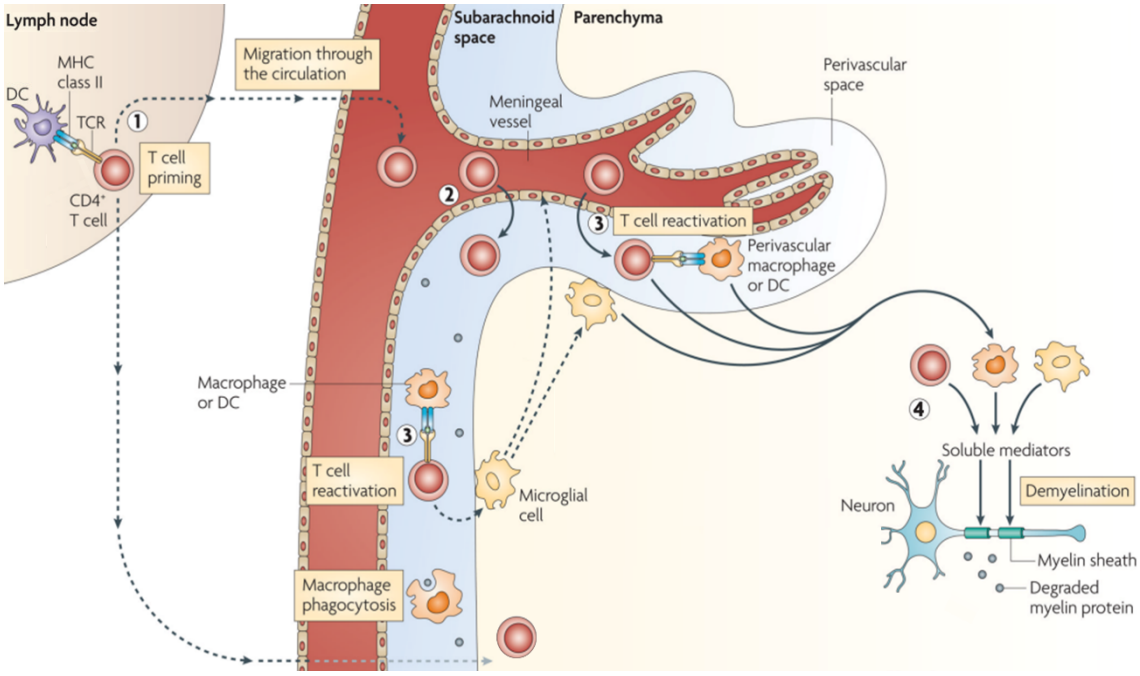

Figure 2. Proposed sequence of events promoting demyelination. (1) T cells are pre-primed in peripheral tissues by DCs presenting myelin epitopes. (2) Primed lymphocytes migrate towards CNS, crossing the blood – cerebrospinal fluid barrier. (3) Once in the CNS borders, T cells get reactivated by diverse APCs, provoking clonal expansion of these cells. (4) Reactivated T cells, along with different activated cells (microglia, infiltrating macrophages, astrocytes) provoke demyelination by releasing soluble, deleterious factors *(Adapted from Goverman et al., 2009)*.

Animal models of multiple sclerosis

Being multiple sclerosis such a heterogeneous and complex neuropathology, the development of valid animal models has been found as necessary as difficult. This far, animal models of MS are commonly used to mimic specific and limited aspects like CNS autoimmunity, acute inflammation, or demyelination/remyelination, but there are no models capturing the entire pathological spectrum of the disease (Cayre et al., 2021). In this thesis, both experimental autoimmune encephalomyelitis (EAE) and lysolecithin (LPC)-mediated demyelination were employed.

Experimental autoimmune encephalomyelitis

This is the most commonly used animal model for MS, and it reproduces the inflammatory and autoimmune aspects of the disorder. EAE is actively induced by immunization with myelin-derived peptides, mostly the MOG35-55 peptide, in addition to complete Freund's adjuvant (CFA) and pertussis toxin (PTX) to boost the immune response and overcome self-tolerance. This sensitization with myelin antigens leads to the generation of autoreactive Th1 and Th17 $CD4^+$ cells and subsequent occurrence of inflammatory and demyelinating foci. Comparably to the events taking place in MS, T cells are primed in peripheral organs, get reactivated in the CNS interfaces and parenchyma by APCs, and then clonally expand to effectively carry out their actions (Hemmer et al., 2015). Microglia and macrophage are known to participate throughout EAE development, being essential both in the onset of the symptomatology and the recovery phase.

EAE pathology is mostly confined to the spinal cord, with low affection of the forebrain or the brain stem and cerebellum, in contrast to MS common development. MOG-immunized EAE mice suffer increasing paralysis, that presents clinically in the form of a chronic progressive course; the motor disability primarily affects the tail and continues to the hind limbs, ultimately compromising the forelimbs (Palumbo and Pellegrini, 2017). Nevertheless, the clinical course can vary in relation to the immunopeptide and the animal strain used (Slavin et al., 1998); this highlights the importance of selecting the proper model in relation to the scientific question.

Lysolecithin-induced demyelination

Understanding the process of remyelination is essential for the development of new therapeutic strategies, especially for the progressive course of MS. However, the study of myelin repair cannot be addressed using EAE. Alternatively, models of demyelination induced by toxins can cover this need, as they are not as highly dependent on an adaptive immune response. The two most extensively used demyelinating agents include LPC and cuprizone, a copper chelator drug (Ransohoff, 2012; Lassmann and Bradl, 2017).

Microinjection of LPC into white matter tracts of the spinal cord causes focal demyelination due to a toxic effect on lipid membrane-rich myelin sheaths (Jeffery and Blakemore, 1995). This is a highly reproducible model, and presents the advantage of triggering the lesion at a

defined location. Demyelination, occurring during the first days after the injection, is rapidly followed by a well-defined sequence of events: 1) Myelin debris clearance by microglia and macrophages; 2) OPCs repopulation by recruitment and proliferation, starting at 2 days post-injection (dpi); 3) OPCs differentiation into mature oligodendrocytes; and 4) Remyelination (from 14 dpi to 21 dpi) (Tepavčevič et al., 2014).

Despite the fact that this model develops independently of the immune response, it involves the infiltration of T cells, B cells and monocytes; this migration is suggested to be beneficial for the remyelination process (Bieber et al., 2003). Interestingly, the degree of myelin repair is age-dependent, and may be influenced by diverse mechanisms, like the efficiency of myelin debris clearance and degradation by microglia and macrophages (Lassmann and Bradl, 2017).

Therapeutic strategies for multiple sclerosis

Thorough research on both MS post-mortem human tissue and MS-associated animal models has helped elucidate pathological mechanisms involved in the disorder; nevertheless, to date, no definitive cure for MS has been developed. The current treatments are being used to attenuate its symptoms and slow down the clinical progression. The treatments can be divided into disease-modifying therapies (DMTs), specific for this neuropathology, and symptomatic treatments, used for short-term amelioration of MS symptoms resulting from neurological dysfunction (Dobson and Giovannoni, 2019).

Among **DMTs**, most have been approved for the treatment of RRMS, and include immunosuppressant and immunomodulatory treatments that reduce the risk of disease progression. These DMTs can intervene in different pathological mechanisms, including antigen presentation, peripheral immune response or pro-inflammatory activation of microglia and macrophages (Weissert, 2013). However, current therapies fail to prevent disease worsening in patients with a progressive clinical course (Filippi et al., 2018). The major therapeutic challenges are associated to the promotion of remyelination in these patients, and this could be addressed by enhancing efficient myelin debris clearance by phagocytes, promoting OPCs differentiation, or improving the capacity of mature oligodendrocytes to enwrap naked axons.

2. MICROGLIA

Beside neurons, glial cells represent a relevant fraction of the CNS composition, being essential for healthy brain homeostasis and functioning, as well as directly involved in virtually all CNS-related disorders, including neurodegenerative diseases. They comprise microglia, astrocytes and oligodendrocytes.

First described by the Spanish researcher Pío del Río-Hortega in 1919, **microglia** are the endogenous **immune cells of the CNS** parenchyma. During this century of research, we have continuously gained comprehensive insight in microglial biology (Sierra et al., 2019). These cells constitute up to the 10% of the total cells, depending on the CNS region (Mittelbronn et al., 2001), and present unique features and origin. While they share functionalities with other tissue macrophages, microglia algo exhibit a range of CNS-specific roles (Colonna and Butovsky, 2017). The disturbance of these functions, as well as aberrant activation processes, can lead to neuroinflammation, in addition to neurodegenerative and neuropsychiatric diseases.

Microglial ontogeny and maintenance

Whereas most tissue macrophages are constantly renewed by monocytes derived from bone marrow hematopoiesis, microglia colonize the CNS early during embryonic development and are a largely self-maintaining population under homeostatic conditions.

Seminal studies strongly suggested that microglia were cells of **mesodermal origin**, and derived from embryonic hematopoietic precursors that seeded the CNS prior to the onset of bone marrow hematopoiesis. This hypothesis was only recently confirmed by *in vivo* lineage tracing studies, showing that microglia derive from primitive myeloid progenitors that arise from the yolk sac before embryonic day 8 (E8; Ginhoux et al., 2010). These progenitors colonize the neuroepithelium at E9.5, giving rise to embryonic microglia (Ginhoux et al., 2013; Ginhoux and Prinz, 2015). Moreover, recent works showed that a specific subset of microglia may also derive from progenitor cells in the fetal liver at a later timepoint (De et al., 2018; Bennett and Bennett, 2020). Although the transcriptional programme that controls the differentiation suffered by microglial lineage is only partially understood, it is known to involve the activity of transcription factors such as PU.1 and Irf8 (Kierdorf et al., 2013). Beside these transcription factors, the response to colony stimulating

factor 1 (CSF1) and the activity of matrix metalloproteinases 8 and 9 are critical during this process (Prinz and Priller, 2014). It is important to mention that the insights into the origin of microglia are mainly based on experiments conducted in mice, and it is therefore difficult to assess whether a similar ontogeny can be attributed to microglia in humans.

Alternatively, **other myeloid populations** either in the CNS, like the CNS-associated macrophages (CAMs), or in peripheral tissues show differences regarding the embryonic origin and the lineage. CAMs are found in interfaces such as the perivascular space or the meninges, and are known to also originate prenatally in the yolk sac and form stable populations, except in the case of choroid plexus macrophages (Goldmann et al., 2016; Prinz et al., 2021). The specific signals guiding them to their predefined destination in contrast to microglia, is mostly unknown. Most other tissue macrophages are derived from progenitors generated at later stages, and their development is not CSF1-dependent (Schulz et al., 2012; Hoeffel et al., 2015).

Regarding microglial population dynamics and **maintenance** in the adult CNS, Ajami and colleagues revealed that microglia renewal is dependent on resident cells under homeostatic conditions, rather than on a contribution by peripheral, infiltrating monocytes (Ajami et al., 2007). Moreover, adult microglial population can rapidly reconstitute by the proliferation of resident, surviving cells after genetic ablation (Bruttger et al., 2015) and following pharmacological depletion with PLX5622, a CSF1R specific inhibitor (Huang et al., 2018). Specifically, after this former mechanism of microglial ablation, a $Mac2^{+}$ subset of cells persists throughout the treatment and is likely to contribute to the self-renewal (Zhan et al., 2020). Even in conditions of massive monocyte infiltration, like EAE development, these peripheral population does not contribute to the resident microglial pool (Ajami et al., 2011). Interestingly, CNS environment is able to induce microglial-specific genes expression in transplanted bone-marrow macrophages in *Csf1r*$^{-/-}$ mice, although not as completely as in other yolk-sac derived myeloid cells (Bennett et al., 2018). All this information highlights the unique, non-redundant roles of microglia in relation to other myeloid populations.

Microglial functions in physiology and pathology

Research on microglia have focused on the contributions of microglia to CNS functioning, both in homeostatic and pathological conditions. These cells have been proven necessary at all stages of CNS development up to adulthood and acquire different roles depending on the developmental stage, in relation to their evolving surrounding environment (Fig. 3).

Microglia during development

Different studies have pointed out a diversity of microglial functions during the development of the CNS, acting as "architects" and coordinating the wiring of nervous tissue. Indeed, *Csf1r*-deficient mice exhibit critical abnormalities in brain development (Kierdorf and Prinz, 2017).

As professional phagocytes, microglia play a major role in **removing apoptotic neurons** from the developing CNS. In this stage, many cells undergo programmed cell death to favour the establishment of the definitive CNS architecture, in an evolutionarily conserved mechanism (Yeo and Gautier, 2004; Rogulja-Ortmann et al., 2007). Indeed, up to 50% of the newly formed neurons suffer apoptosis (Dekkers et al., 2013), and microglia are responsible for the clearance of these dead cells (Schafer and Stevens, 2015). Moreover, microglia are known to be involved in the **regulation of the correct number of neurons**, both promoting their apoptosis by themselves and their survival. On one hand, some studies suggest that microglia can induce neuronal death via the release of neurotrophins (Frade and Barde, 1998; Wakselman et al., 2008); alternatively, microglia can support the survival of developing neurons as well as neurogenesis in diverse brain regions, secreting factors like the insulin growth factor 1 (IGF-1; Ueno et al., 2013; Shigemoto-Mogami et al., 2014).

Microglia play other roles in the establishment of the CNS architecture. Importantly, they are highly implicated in the refinement of neuronal circuits by the **pruning** of unused dendritic spines (Paolicelli et al., 2011; Schafer et al., 2012), in a process probably associated to the classical complement cascade (Stephan et al., 2012). Similarly, these cells are able to engulf myelin sheaths to sculpt myelination according to axonal activity (Hughes and Appel, 2020). In addition, microglia participate in the **myelination** of the developing brain. It is suggested that they can support oligodendrogenesis in the subventricular zone of rodents (Shigemoto-Mogami et al., 2014), and a subset of $Cd11c^{+}$ microglia has been described to

regulate CNS myelinogenesis via the release of IGF-1 (Wlodarczyk et al., 2017). Microglia also participate in the proper fasciculation of axons during the *corpus callosum* formation (Pont-Lezica et al., 2014).

Lastly, development of the CNS involves **vascularization** of the distinct regions, in order to provide nutrients and oxygen to the neurons. Microglia are uniquely positioned to influence the early sprouting, anastomosis, and refinement of this growing vascular system (Arnold et al., 2013). Supporting this idea, studies depleting microglia during development found a decrease in the vascular density in diverse locations (Kubota et al., 2009).

Microglia roles in adult brain

Beside their specific, unique roles during CNS development, microglial cells play important roles in maintaining its homeostasis and integrity. Microglia are characterized by a surveillance of their environment facilitated by dynamically moving processes, which give microglia a typical homeostasis-associated ramified morphology (Glenn et al., 1992; Nimmerjahn et al., 2005). Since this scanning is constant, as well as highly sensitive and responsive towards perturbations, the notion of "resting" microglia as inactive tissue macrophages has become obsolete. In fact, physiological microglia exhibit low expression of immune-related genes while overexpressing genes mostly associated to **environmental sensing**, such as *Cx3cr1*, *P2ry12* or *Tmem119* (Hickman et al., 2013).

Microglial monitoring and phagocytosis of synaptic elements not only occurs during postnatal development and adolescence, but also in adulthood and during ageing (Wake et al., 2009; Schafer et al., 2012; Milior et al., 2016), suggesting a critical role in maintaining **synaptic plasticity** under homeostatic conditions. In fact, Tremblay and colleagues described a slower, experience-dependent remodelling of synapses in mature healthy brain (Tremblay et al., 2010). More evidence supporting this function was provided using a model of microglial depletion upon diphtheria toxin administration; specifically, this depletion provoked deficits in learning-dependent synapse formation during young adulthood (Parkhurst et al., 2013). Intriguingly, alternative microglial ablation with PLX3397 did not cause any cognitive defects in 2-month-old animals, probably suggesting that this role as modulators of network plasticity gets more limited along with ageing (Elmore et al., 2014).

Beside their importance maintaining synaptic properties, microglia serve critical functions **regulating adult neurogenesis**, through the control of neuronal progenitors density in the subventricular zona and the subgranular zone of the dentate gyrus, both considered neurogenic niches in the brain (Sierra et al., 2010; Ribeiro Xavier et al., 2015). Importantly, microglia control the size of neuronal pool by engulfing neural precursor cells, in a phagocytic process mediated by TAM receptors (Fourgeaud et al., 2016). Moreover, while ageing have a negative effect on neurogenesis, exercise and environmental enrichment physiologically prime microglia to support the generation of neurons (Vukovic et al., 2012; Gebara et al., 2013).

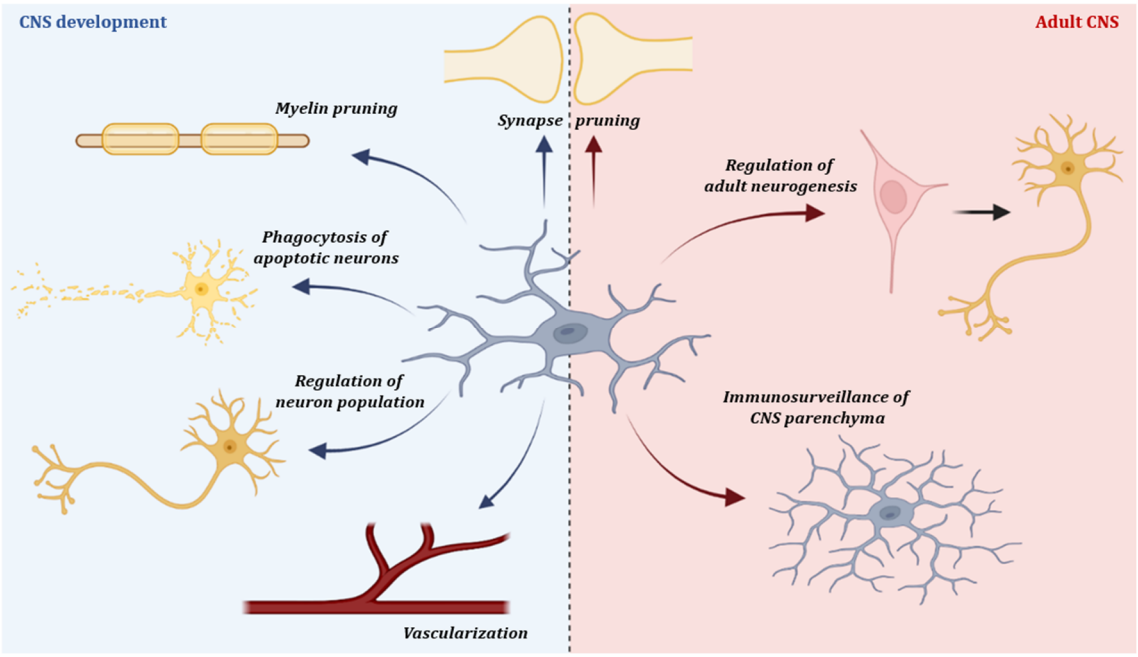

Figure 3. Homeostatic function of microglia in the developing and adult CNS. Microglia display a variety of functions to maintain tissue homeostasis. Microglia modulate the architecture of the developing CNS by controlling neuronal population, performing pruning of myelin and synapses and guiding sprouting vessels. These cells also play important roles in the healthy adult brain. Besides scanning their environment, microglia keep on modulating the plasticity of neuronal networks and regulate adult neurogenesis.

Microglia in pathology

The dysregulation of normal microglial functions leads to imbalances that can promote the generation of neurodegenerative disorders. Indeed, some genome-wide association studies have placed microglia in focus regarding some disorders like MS or Alzheimer's disease (AD), as microglial specific genes have been identified as risk factors for these pathologies (Nott et al., 2019; Patsopoulos et al., 2019). Moreover, it is increasingly appreciated that microglia are **involved in most CNS diseases**, including neurodevelopmental

abnormalities (e.g., autism), psychiatric disorders (schizophrenia or depression) as well as neuroinflammatory and neurodegenerative pathologies, like Parkinson's and Hungtinton's diseases or amyotrophic lateral sclerosis (Keren-Shaul et al., 2017; Mondelli et al., 2017; Voet et al., 2019; Masuda et al., 2020).

Microglia can rapidly respond to different stimuli, such as molecules released by surrounding cells. Actually, microglia respond to the release of adenosine triphosphate (ATP) as a consequence of focal brain injury, in a mechanism dependent on the activation of P2Y purinergic receptors (Davalos et al., 2005). Similarly, during CNS pathologies, microglial actions can be driven and regulated by molecules associated to pathogens, damage or other non-physiological conditions (Kettenmann et al., 2011; Bachiller et al., 2018). Upon all these challenges, microglia play prominent roles in the release of pro- and anti-inflammatory cytokines, the production of a wide range of factors, the presentation of antigens and in the phagocytosis of different targets, depending on the activation pattern. Indeed, specific subsets of microglia have been extensively linked to neurodegeneration (Butovsky and Weiner, 2018; Deczkowska et al., 2018).

3. MICROGLIA AND MACROPHAGES IN MULTIPLE SCLEROSIS

Immune response and neuroinflammation are key hallmarks in the development of MS and thus, assessing microglial functions during the progression of the disease is crucial to fully understand the mechanisms underneath the pathology. Indeed, pronounced microglia accumulation and activation can be observed in both the lesion areas and the normal-appearing white matter of MS patients (Lucchinetti et al., 2000), and this event is associated with neurological damage (Singh et al., 2013). Nevertheless, studying the specific contribution of this cell type remains a major challenge due to the difficulty discriminating microglia from CAMs and infiltrating monocytes-derived macrophages (Greter et al., 2015).

All these myeloid cells are known to participate in both beneficial and detrimental processes regarding MS progression, playing **dual roles** accordingly to the heterogeneity of the populations (Guerrero and Sicotte, 2020). Actually, their activation state was described to evolve throughout the course of EAE, changing the expression ratio between inducible nitric oxide synthase (iNOS) and arginase, which are typical pro- and anti-inflammatory markers,

respectively. While iNOS is predominant during the initial phases of the disease, the ratio gradually inverts during the course of the model, and microglia/macrophages show mainly anti-inflammatory phenotypes in the chronic stages of the EAE (Locatelli et al., 2018; Fig. 4). A recent study using LPC as a demyelinating agent also provides insights into the evolving and complex responses of microglia (Plemel et al., 2020).

Microglia and macrophages in demyelination

The **pro-inflammatory activation** of microglia observed during the early stages of the disease can precede and modulate peripheral cells infiltration into CNS parenchyma, as well as other neuroinflammatory, deleterious effects. One important effector function of activated microglia is the **secretion of a wide range of factors**. For example, microglia are thought to produce chemokines, like the C–C motif chemokine ligand 2 (CCL2), which would contribute to the attraction of monocytes positive for its receptor (CCR2) towards the CNS. Interestingly, CCR2-deficient mice are resistant to EAE pathology, as $CCR2^{+}$ monocytes play an essential role in disease progression (Mildner et al., 2009; Ajami et al., 2011). Beside the CCL2-dependent effect, activated microglia are known to release other cytokines that could induce neurotoxic astrocytes activation, further contributing to the inflammatory cascade (Liddelow et al., 2017). The secretion of other factors by microglia and macrophages is also responsible for promoting T cell differentiation towards Th1/Th17 phenotypes, responsible for EAE development (Dong and Yong, 2019).

Microglia and macrophages can contribute to EAE neuroinflammatory effects in other ways. Their activation can provoke **oxidative damage** by secreting reactive oxygen species (ROS) as well as nitric oxide (NO), subproducts that oxidize DNA and lipids in oligodendrocytes and myelin (Smith et al., 1999). Actually, the extent of this oxidation correlates with inflammation and injury levels (Lassmann and van Horssen, 2016; Dong et al., 2021). Interestingly, NO production is associated to the activity of iNOS, which is commonly considered as a relevant marker for pro-inflammatory macrophages. Lastly, microglia, infiltrating monocytes and CAMs can participate in **antigen presentation**, promoting T cell reactivation and clonal expansion *in situ*. Microglia and macrophages are known to alter their phenotype in active MS and EAE, losing homeostatic markers and increasing markers related to antigen presentation such as MHC or the co-stimulatory molecules CD80 and CD86 (Zrzavy et al., 2017); however, it is not entirely revealed how they contribute to this

process (Voet et al., 2019). Actually, as previously stated, DCs are the main candidates to participate in EAE progression as APCs (Jordão et al., 2019; Mundt et al., 2019).

While both microglia and macrophages show pro-inflammatory features and participate in neuroinflammation, infiltrating monocytes have been suggested to act as the primary effectors in the onset of the disease, and their accumulation correlates with the progression of symptoms (Ajami et al., 2011; Yamasaki et al., 2014). Actually, Ajami and colleagues suggested that microglia undergo apoptosis during this phase of the pathology, a process that can favour a renewal needed for regenerative processes (Ajami et al., 2011; Lloyd et al., 2019). This is in accordance to the fact that, despite the effect of these cells promoting $CCR2^{+}$ monocyte infiltration in EAE, microglia limit infiltration of macrophages towards the lesion core after LPC demyelination (Plemel et al., 2020). Moreover, sorting of the different cell types based on their Ly6C expression showed that microglia are only weakly activated, whereas infiltrated macrophages are highly immune reactive during the development of the disorder (Vainchtein et al., 2014). Nevertheless, the specific roles of microglia during the effector phase of MS in comparison to other macrophages are yet to be determined.

Microglia and macrophages in remyelination

There is evidence that the activation of microglia and macrophages not only favour deleterious effects, but can also alternatively counteract the pathological processes of MS by providing immunosuppressive factors and promoting **remyelination** (Miron and Franklin, 2014). During the chronic phase of EAE, microglia and macrophages promote myelin repair both by secreting a wide spectrum of signaling molecules and carrying out phagocytosis of myelin debris (Rawji et al., 2016; Franklin and Ffrench-Constant, 2017), as determined using models involving the depletion of both kinds of cells (Kotter et al., 2001; Miron et al., 2013). On one hand, these cells can **release anti-inflammatory cytokines** such as IL-4, IL-10, IL-33 or TGF-β, which are involved in EAE suppression or inflammation resolution (Tierney et al., 2009; Jiang et al., 2012; Psachoulia et al., 2016). In recent years, abundant macrophage-derived molecules have been identified to have direct effects on OPCs recruitment and differentiation (Patel et al., 2010; Miron et al., 2013; Madsen et al., 2016).

On the other hand, microglia and macrophages **phagocytose the myelin debris** released after demyelination; this process is essential for proper remyelination (Neumann et al., 2009). Free myelin can inhibit OPC differentiation (Plemel et al., 2013), and therefore myelin debris needs to be removed from the extracellular space not to interfere with the intrinsic mechanisms of repair, involving OPCs recruitment and maturation. Studies using cuprizone and LPC-induced demyelination have demonstrated a correlation between the abundance of debris-filled microglia/macrophages and the efficiency of remyelination. Moreover, microglial depletion emphasizes their critical role in myelin debris clearance, as it restrains remyelination capacity (Lampron et al., 2015).

Recent studies have performed in-depth assessment of this phagocytic process, due to its therapeutic potential. Specifically, this myelin phagocytosis is suggested to be mediated by the Mertk receptor, whose gene alterations are linked to MS risk (Shen et al., 2021). Triggering receptor expressed on myeloid cells 2 (TREM2), a common risk factor for many neurodegenerative disorders (Jay et al., 2017), is also essential in this clearance mechanism (Cignarella et al., 2020). Indeed, TREM2 is required for the biogenesis of lipid droplets (LDs), a common reservoir for lipids following their processing and metabolism (Gouna et al., 2021). Similarly, other studies have shown that TREM2 regulates the specific clearance of oxidized phosphatidylcholines in these lesions (Dong et al., 2021), as well as cholesterol metabolism upon myelin challenge in microglia (Nugent et al., 2020).s A recent study suggested that, in response to acute lesions, microglia can redirect captured lipids to synthetize sterols, specific species that favour inflammation resolving and remyelination by activating the liver X receptor (LXR; Berghoff et al., 2021).

Aging is one of the major impediments in adequate remyelination contributing to reduced OPCs proliferation and differentiation, as this regenerative process undergoes a progressive slowing in rate throughout adult life (Hampton et al., 2012). The ageing process affects both the intrinsic properties of OPCs and the cells that form the extrinsic environment in which remyelination takes place, including microglia. Actually, a recent study showed that aged microglia/macrophage accumulate excessive amounts of cholesterol-rich myelin debris, triggering cholesterol crystal formation. This age-associated failure in myelin degradation induces maladaptive immune response and interferes with regeneration (Cantuti-Castelvetri et al., 2018).

Microglia are more commonly associated with the regenerative effects following demyelination, as CCR2+ macrophage population importantly declines in the CNS parenchyma during the chronic phase of the EAE (Ajami et al., 2011). To sum up, microglia and macrophages display an **enormous plasticity** in their responses to injury and they are able to promote resolution of inflammation and tissue regeneration too, possibly by carrying out both specific and redundant functions. This characteristic plasticity is dependent on the signals from the environment, that model the differential activation phenotype of the cells (Fig. 4).

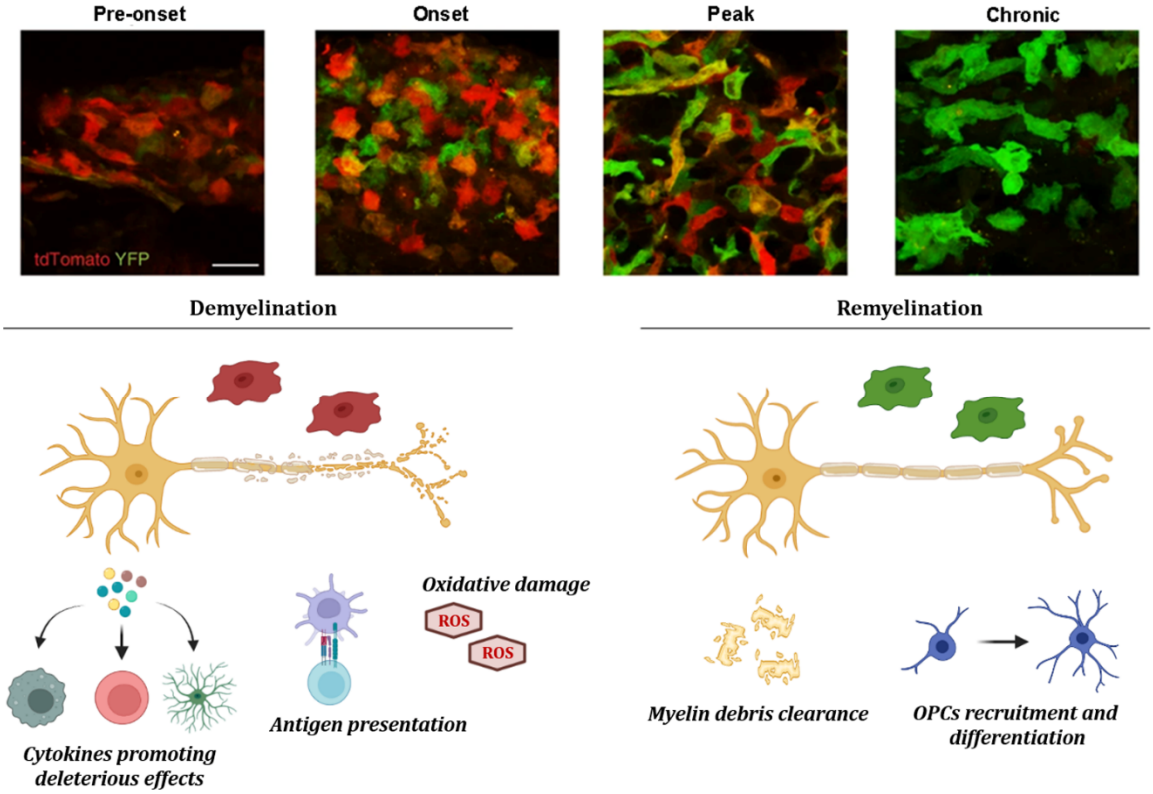

Figure 4. Dual role of microglia and macrophages in the development of MS. The upper images show the differential polarization of both type of cells represented by the expression of iNOS (tdTomato) and arginase (YFP), pro- and anti-inflammatory markers, respectively *(Adapted from Locatelli et al., 2018)*. Below, the scheme shows the dual roles of microglia and macrophages in demyelination, promoting axonal damage, and remyelination, favouring tissue repair.

4. MICROGLIAL ACTIVATION

As already described, microglial functions during the development of CNS-associated disorders like MS are accompanied by an activation process. This activation is normally linked to changes in morphology, gene expression and functional capacities, and respond to both exogenous and endogenous stimuli. Depending on the nature of the stimulus encountered, microglial activation has been traditionally oversimplified involving M1 (pro-inflammatory or classical) and M2 (anti-inflammatory or alternative) phenotypes. Nevertheless, the development of single-cell RNA sequencing and other massive analyses led to the detection of microglial subpopulation heterogeneity (Xue et al., 2014; Keren-Shaul et al., 2017), suggesting a whole **spectrum of activation states** (Ransohoff, 2016).

The factors controlling microglial activation can act through a great diversity of **signaling pathways**, involving the activity of multiple kind of receptors. Microglia can be regulated, among others, by toll-like receptors (TLRs), Fc receptors, cytokines receptors, the fractalkine receptor (CX3CR1) or receptors for specific neurotransmitters, including purinergic receptors (Lee et al., 2002; Domercq et al., 2013; Arnoux and Audinat, 2015; Fiebich et al., 2018). Downstream, intracellular pathways following the response of these receptors modulate the action of diverse **transcription factors**, which would ultimately control the molecular mechanisms behind the plethora of microglial specific functions. Interferon regulatory factor (IRF) or nuclear factor kappa B (NF-κB) are relevant examples of transcription factors families known to regulate inflammatory macrophage response (Kawai and Akira, 2009), mainly in response to TLR activation.

Emerging strategies to drive microglia toward beneficial activation are appearing in recent years, and a variety of approaches has been proposed. These range from treatments with pharmacological agents, lipid messengers or microRNAs, to nutritional approaches or therapies with immunomodulatory cells (Fumagalli et al., 2018). Reprograming microglia toward advantageous functions may provide new therapeutic opportunities to prevent the deleterious effects of inflammatory microglia and to control excessive inflammation in brain disorders. In relation to this, several signaling pathways and specific molecular mechanisms in microglia stand out as potential targets and fields of interest.

Interferon Regulatory Factor 5 signaling

Microglia express high levels of toll-like receptors (TLRs), which are considered as pattern recognition receptors, being an important part of the general innate immune response. Their activation can trigger the action of IRF transcription factors, implicated in a variety of functions such as apoptosis, cell cycle, cell development and even oncogenesis (Tamura et al., 2008). Among the IRF family, that comprises nine members (IRFs 1-9), IRF5 plays a **major role in inflammation**. It mediates the induction of pro-inflammatory cytokines such as IL-6, IL-12, IL-23 and tumour-necrosis factor-alpha (TNF-α), and is a key factor defining the inflammatory macrophage phenotype interacting with other proteins like RelA (Takaoka et al., 2005; Krausgruber et al., 2011; Saliba et al., 2014). *Irf5* expression is highly associated WITH immune cells and, in microglia/macrophages, it is upregulated in response to an inflammatory environment, and in particular to stimulation with granulocyte macrophage colony-stimulating factor (GM-CSF) and interferon gamma (IFN-γ; Krausgruber et al., 2011; Weiss et al., 2013), in a process specifically dependent on TLR7/9 activation and associated to the myeloid differentiation primary response 88 protein (MyD88) signaling pathway (Honda and Taniguchi, 2006) (Fig. 5).

Irf5 gene has been proposed as a **risk factor** in several inflammatory, autoimmune disorders. Actually, polymorphisms in this transcription factor were originally linked to systemic lupus erythematosus (Sigurdsson et al., 2005), but later associated with the inflammatory bowel disease, Sjögren's syndrome and rheumatoid arthritis (Dideberg et al., 2007; Nordmark et al., 2009; Shimane et al., 2009). Regarding the latter, Weiss and colleagues observed an increase in the *Irf5* transcript levels in a mouse model of arthritis, denominated antigen-induced arthritis (Weiss et al., 2013). Moreover, in the CNS, the role of IRF5 in different paradigms of neuroinflammation has been highlighted in the last few years. It has been highly associated with microglial activation and the subsequent inflammation occurring after cerebral ischemia, along with IRF4 (Al Mamun et al., 2020) and, similarly, it was observed to mediate the inflammation caused by intracerebroventricular injection of LPS (Fan et al., 2020). IRF5 is hence pointed out as an attractive therapeutic strategy for many inflammation-mediated alterations (Almuttaqi and Udalova, 2019).

In accordance with these observations, two SNPs (rs4728142 and rs3807306) and an insertion-deletion polymorphism reached significant association to **MS development** in three independent cohorts (Kristjansdottir et al., 2008), a finding validated shortly afterwards (Vandenbroeck et al., 2011). Regarding this disorder, the purinergic receptor P2X4 has recently been identified by our group as a possible new target to control microglial activation as well as to potentiate myelin phagocytosis and remyelination in the EAE mouse model (Zabala et al., 2018). Importantly, P2X4R$^+$ reactive microglia was suggested to be driven and controlled by the IRF8-IRF5 transcriptional axis; in fact, mice lacking *Irf5* could not upregulate spinal cord P2X4 after peripheral nerve injury, a model in which that purinergic receptor is particularly implicated in the generation of neuropathic pain (Masuda et al., 2014).

The importance of the IRF5 transcription factor in the promotion of inflammatory responses has been extensively assessed using a myriad of *in vitro* and *in vivo* models, including some associated with MS. However, the particular roles of IRF5 in the development of MS and the different animal models of this disorder are yet to be determined.

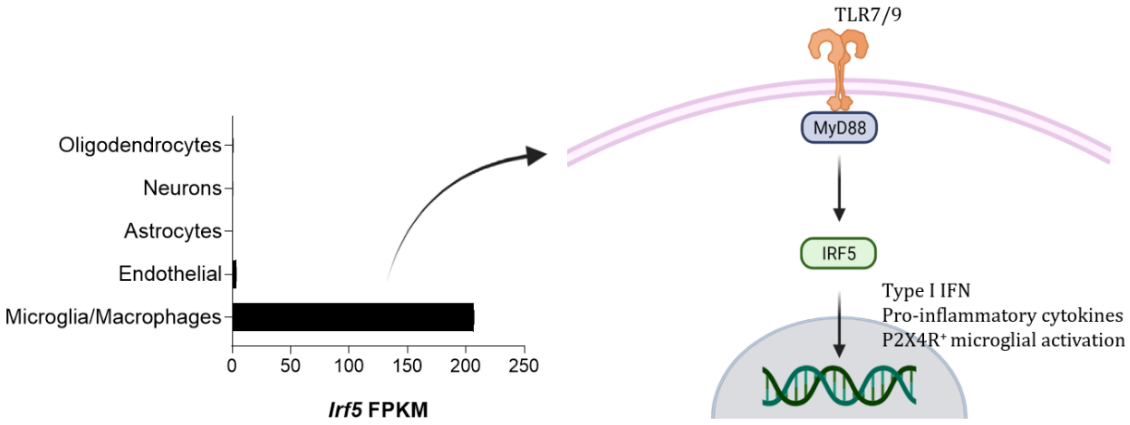

Figure 5. IRF5 expression and signaling pathway. IRF5 expression in CNS is limited to microglia and macrophages (*From Zhang et al., 2014*). In these cells, activation of IRF5 is dependent on the response by TLR7/9 and the MyD88 intracellular mediator; this activation provokes the expression of inflammation-related genes, and promotes the P2X4R$^+$ microglial state.

Microglial metabolic reprogramming

Most of the mechanisms governing microglial phenotypes, functions and environmental response dynamics remain largely unexplored. Nevertheless, it is well established how these cells can undergo distinctly programmed metabolic changes in response to diverse stresses. This process is denominated metabolic reprogramming, and shows similarities to the Warburg effect suffered by cancer cells, which present high and efficient energy demand (Herst et al., 2018). Metabolic reprogramming is also shared with multiple cells participating in the immune response, such as macrophages, T cells or DCs (Kelly and O'Neill, 2015; Andrejeva and Rathmell, 2017; Stienstra et al., 2017). In microglia, metabolic flexibility is suggested to support the differential activation patterns as well as their main functions, including the continuous immune surveillance of the brain (Bernier et al., 2020). Microglia can express the full set of genes required for both glycolytic and oxidative energy metabolism (Zhang et al., 2014); nevertheless, homeostatic microglia seems to primarily rely their basal energy needs in the oxidative phosphorylation (OXPHOS) pathway (Ghosh et al., 2018).

Upon activation, alternatively, microglia as well as other immune cells drastically increase their demand for nutrients to mount an effective immune response. Specifically, as a response to **pro-inflammatory stimuli**, microglia switch their metabolism and increase their reliance on the **glycolytic pathway**. This allows for microglia to produce ATP rapidly, despite being comparatively less efficient (Schuster et al., 2015). As an example, treatment with LPS on BV-2 microglial cells increased lactate production and reduced the mitochondrial oxygen consumption (Volobоueva et al., 2013). Similarly, pro-inflammatory IFN-γ induces glycolysis in microglia (Holland et al., 2018). Moreover, the same effect was observed with both factors in combination with Aβ (Rubio-Araiz et al., 2018; McIntosh et al., 2019). Glycolytic microglia generate high levels of glucose-6-phosphate, promoting the pentose phosphate pathway (PPP) and the production of nicotinamide adenine dinucleotide phosphate (NADPH). NADPH can, in turn, contribute to the synthesis of ROS and fatty acids, eventually favouring the inflammation process (Van den Bossche et al., 2017; Yang et al., 2021). NO is also synthesized through oxidation of L-arginine by iNOS using the electrons supplied by NADPH (Orihuela et al., 2016) (Fig. 6). Lastly, the involvement of mitochondria and their dynamics has been recently assessed, as blockade of mitochondrial fission with

the mitochondrial division inhibitor 1 (Mdivi-1) was able to revert metabolic reprogramming (Nair et al., 2019).

While pro-inflammatory responses are associated to high glycolytic levels and disruption of OXPHOS, microglia stimulated with **anti-inflammatory** factors such as IL-4 and IL-13 maintain and even enhance their **OXPHOS activity**. Actually, BV-2 microglia downregulate lactate production, an indicator of anaerobic glycolysis, under this condition (Gimeno-Bayón et al., 2014). Besides, macrophages facing this kind of stimuli activate carbohydrate kinase-like protein, lowering the PPP flux and reducing the NADPH-related inflammatory effects (Haschemi et al., 2012). Anti-inflammatory microglia are also associated with high rates of fatty acid oxidation and mitochondrial biogenesis (Vats et al., 2006), as well as elevated levels of arginase-mediated arginine metabolism to ornithine (Rath et al., 2014c) . All these changes can ultimately contribute to their neuroprotective properties (Fig. 6).

Despite the fact that the field of immunometabolism is rapidly improving our understanding of immune responses, as well as the importance of the metabolic pathways in inflammatory diseases such as MS (van der Poel et al., 2019), the entirety of mechanisms regulating this metabolic flexibility is yet to be described. More in depth comprehension of the processes involved can offer a series of potential and promising therapeutical targets.

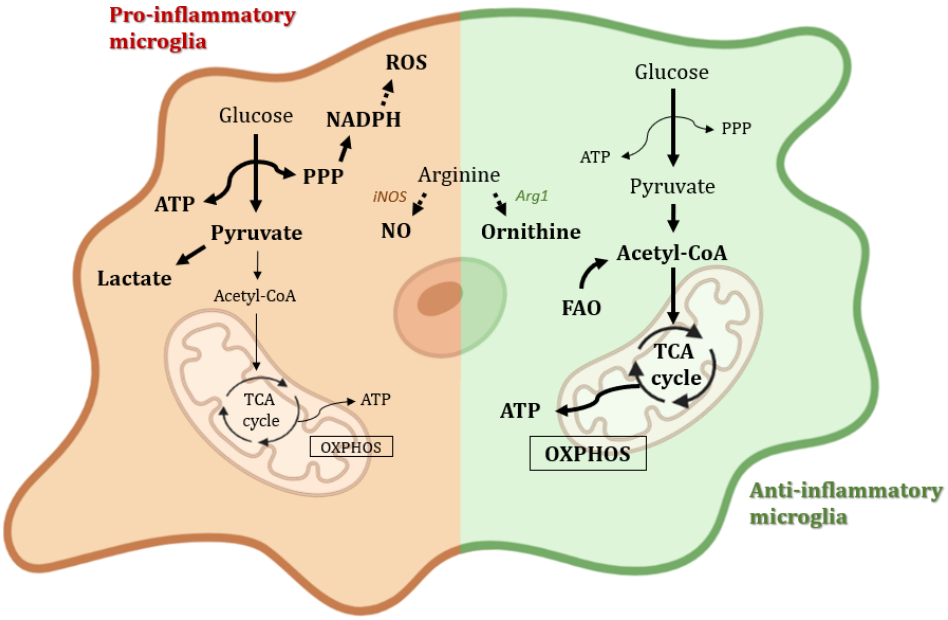

Figure 6. Metabolic reprogramming in microglia. Similarly to other immune cells, microglia can adapt their intracellular metabolism in response to the environmental stimuli. Pro-inflammatory microglia relies their metabolism on anaerobic glycolisis and PPP, while anti-inflammatory microglia carry out OXPHOS and fatty acid oxidation. Arginine is also differentially metabolized.

Lipid uptake and metabolism

Lipid metabolism is key controlling the activation of microglia, this being a reciprocal effect, as action of these cells can involve the efficient uptake/phagocytosis of lipids. Several studies have highlighted the need for increased expression of genes associated with lipid metabolism (e.g., TREM2 and ApoE) during damage and disease (Keren-Shaul et al., 2017; Krasemann et al., 2017). Moreover, during MS, proper myelin debris clearance is necessary to promote remyelinating responses, and this process comprises the correct uptake of the debris and its subsequent processing (Fig. 7).

Regarding the **uptake**, microglia express a large repertoire of receptors that can modulate the translocation of diverse type of lipid species inside the cell. CD36, a type B scavenger receptor that recognizes low-density lipoproteins (LDL) and oxidized phospholipids, is crucial for this process (Chausse et al., 2021); moreover, microglia present a broad variety of LDL receptors (LDLRs), that mediate lipid uptake and regulate the subsequent intracellular signaling (Pocivavsek et al., 2009). In the particular case of myelin debris clearance, it is a process mediated by receptors such as TREM2, Fc or complement receptors, which normally cluster in clathrin-coated pits distributed along the extracellular membrane (Grajchen et al., 2018).

Internalized lipids can serve as products for membrane composition, similarly to what occurs to the lipids synthetized independently and matured in the endoplasmic reticulum and peroxisomes. For this to happen, uptake of lipid debris needs to be followed by its **processing**. Lipids are the principal constituents of transport vesicles and, thus, their processing involves a complex machinery of intracellular trafficking. Indeed, cell compartments carrying central function in lipid processing interact via contact sites (Jain and Holthuis, 2017), and disturbances in this trafficking can lead to alterations in tissue homeostasis. Regarding myelin, its degradation in lysosomes following the uptake of the debris give rise to free lipid species, such as diverse types of fatty acids and cholesterol (Chausse et al., 2021). The final destination of all these lipids is variable: they can be added to membranes, exported via efflux systems in the form of lipoproteins or stored in LDs to serve as energy reservoirs. In the case of cholesterol, it has to be previously esterified and form **cholesterol esters** (CE) in order to be accumulated in LDs (Maxfield and Tabas, 2005).

In normal conditions, myelin-derived lipids can regulate microglial function and activation. In fact, some of these lipids such as sterols regulate the phagocytic activation of microglia and macrophages, by activating the LXR signaling (Bogie et al., 2012). This activation promotes further uptake of myelin debris and polarize microglia towards an anti-inflammatory phenotype (Mailleux et al., 2018), in an effect also associated with the peroxisome proliferator-activated receptor (PPAR) pathways (Bogie et al., 2014). Nevertheless, during demyelinating disorders and ageing, myelin deposition in the CNS parenchyma exceeds the capacity of these mechanisms and generates **imbalances in lipid processing** (Cantuti-Castelvetri et al., 2018; Gabandé-Rodríguez et al., 2019). Aged microglia, for instance, accumulate excessive amounts of cholesterol triggering the formation of dense structures, denominated cholesterol crystals, in the lysosomes. These cholesterol crystals are thought to destabilize the lysosome, resulting in the induction of an inflammatory activity through the stimulation of the inflammasome complex (Cantuti-Castelvetri et al., 2018). The same group described that cholesterol esterification is required for LD formation as a response to demyelination, and that defectiveness in LD biogenesis can lead to failures in the repair mechanisms (Gouna et al., 2021). Similarly to this latter observation, a recent study highlighted that LD-accumulating microglia represent a dysfunctional state in the aging brain (Marschallinger et al., 2020). Interestingly, while the work from Gouna and colleagues suggests TREM2 as mediator for LD formation, another study showed that TREM2$^{-/-}$ microglia abnormally enhances the production of CE and its accumulation in LDs upon excessive myelin challenge (Nugent et al., 2020).

When microglia are exposed to external stimuli such as apoptotic cells or myelin debris, lipids can function as signaling molecules for phagocytosis and activation (Nadjar, 2018), and abnormalities in lipid metabolism can be related to disorders. During MS development, lipid intermediates accumulate in patients' blood plasma and cerebrospinal fluid (Villoslada et al., 2017). In light of the above, lipid metabolism is deemed to be a key regulator in the metabolic and functional alterations of microglia.

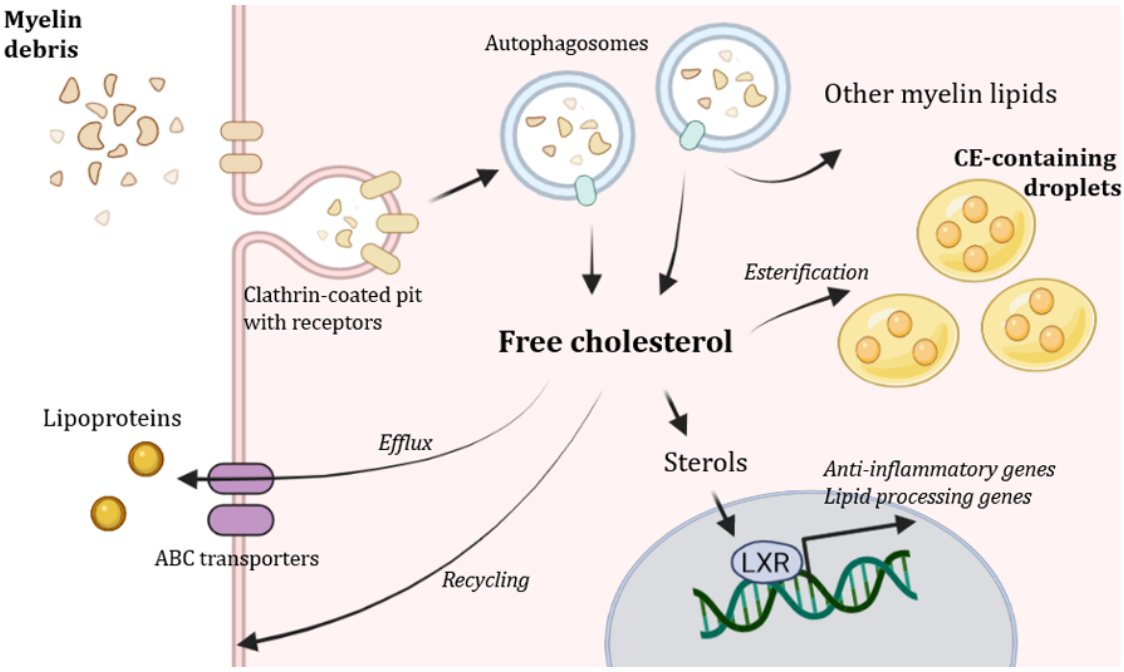

Figure 7. Myelin uptake and processing by microglia. After phagocytosis of debris, components are degraded and redirected. Free cholesterol can be recycled to be part of biological membranes, be released to the extracellular medium by efflux systems, or be esterified and storaged in lipid droplets. Moreover, cholesterol can be metabolized into different sterols, that activate the LXR receptor and can modulate the anti-inflammatory activation of microglia.

HYPOTHESIS AND OBJECTIVES

Microglia are the resident immune cells of the central nervous system, and are crucially involved in the pathogenesis of most neurodegenerative disorders, including MS. These cells participate in neuroinflammatory events and contribute both to demyelination and subsequent myelin regeneration. Nevertheless, the specific implications of microglia in comparison to infiltrating macrophages and other CAMs in the development of MS are still poorly understood. Similarly, the determinants of microglial dichotomy behavior are yet to be fully described. In-depth knowledge of the mechanisms and intracellular pathways controlling the differential microglial activation would shed light on possible therapeutic targets aiming to reprogram these cells and promote beneficial functions. Activation of microglia involves the action of diverse transcription factors, like IRF5, that modulate the production of cytokines and other factors. Moreover, microglial cells are known to undergo complex adaptations in their metabolic phenotypes, in order to properly respond to the environment and promote actions accordingly.

In light of the above, the global objective of this Doctoral Thesis is to **characterize the role of microglia and its activation in the development of demyelinating disorders.** The detailed aims are as follows:

Objective 1. To assess the specific roles of microglia in the development of MS, in comparison to other macrophagic populations. We evaluated microglial function in the different stages of the EAE by selectively depleting microglial population using the CSF1R inhibitor PLX5622.

Objective 2. To evaluate the role of IRF5 in microglial activation and function in demyelination and remyelination. We analyzed the involvement of IRF5 transcription factor in the development of EAE and in response to acute demyelination by LPC injections using *Irf5*$^{-/-}$ mice.

Objective 3. To characterize the mechanisms modulating microglial metabolic reprogramming and evaluate this process throughout the development of EAE. We analyzed mitochondrial integrity and implication of mitochondrial dynamics in microglial metabolic switch; moreover, we developed a model to metabolically characterize microglia isolated from adult mice.

MATERIALS AND METHODS

ANIMALS

All experiments were performed according to the procedures approved by the Ethics Committee of the University of the Basque Country (UPV/EHU), following the European Directive 2010/63/EU, and animals were handled in accordance with the European Communities Council Directive. Animals were kept under conventional housing conditions (22 ± 2°C, 55 ± 10% humidity, 12-hour day/night cycle and with *ad libitum* access to food and water) at the University of the Basque Country animal unit. All possible efforts were made to minimize animal suffering and the number of animals used.

Experiments included C57BL/6 wild-type (WT) mice, *Irf5*$^{-/-}$ C57BL/6 mice and CCR2-RFP/fms-EGFP mice. The two latter were kindly provided by Dr. Irina Udalova, from the Kennedy Institute of Rheumatology (Oxford, UK) and by Dr. Amanda Sierra, from the Achucarro Basque Center for Neuroscience (Leioa, Spain), respectively. To generate the CCR2-RFP/fms-EGFP mice double transgenic mice, Ccr2$^{RFP/RFP}$ and fms$^{EGFP/EGFP}$ mice were crossed and first-generation littermates were used. Both transgenic lines are on a C57BL/6 genetic background.

IN VIVO MODELS

Experimental autoimmune encephalomyelitis induction

EAE was induced in 8- to 10-week-old male or female C57BL/6, *Irf5*$^{-/-}$ and CCR2-RFP/fms-EGFP mice. Mice were immunized with 200 µg of myelin oligodendrocyte glycoprotein 35-55 ($MOG_{35–55}$; MEVGWYRPFSRVVHLYRNGK) in incomplete Freund´s adjuvant (IFA; Sigma) supplemented with 8 mg/mL *Mycobacterium tuberculosis* H37Ra (Fisher). Pertussis toxin (500 ng; Sigma) was injected intraperitoneally on the day of immunization and 2 days later, to facilitate the development of the disease model.

In this model, mice present the onset of motor symptoms at around 10-12 days post-immunization (dpi). The motor deficits increase with time reaching a maximum peak at around 20 dpi, followed by a partial and slow recovery, denominated chronic phase. Motor symptoms were recorded daily and scored from 0 to 8 as follows: 0, no detectable changes in motor behavior; 1, weakness of the tail; 2, paralyzed tail; 3, impairment or weakness in

hindlimbs; 4, hemiparalysis of hindlimbs; 5, complete hindlimb paralysis; 6, hindlimb paralysis and loss rigidity in forelimbs; 7, tetraplegia; and 8, moribund. Mice were euthanized at different phases of the disease (pre-onset, onset or chronic phase) in accordance to the experimental question addressed.

After EAE, mice were euthanized and the tissues were removed and differentially processed in accordance to the subsequent experimental procedure. For immunohistochemistry, the lumbar region of the spinal cord, where lesions typically accumulate, was fixed by immersion for 4 hours in 4% paraformaldehyde (PFA), dissolved in 0.1 M phosphate buffer (PB, pH = 7.4), rinsed in phosphate-buffered saline (PBS) and then transferred to 15% sucrose in 0.1 M PB for at least 2 days for cryoprotection. Next, tissue was frozen in 15% sucrose - 7% gelatine solution in PBS, and cut in a Leica CM3050 S cryostat to obtained 12-µm coronal sections. For real-time quantitative polymerase chain reaction (qPCR), the cervical and thoracic regions were flash frozen in dry ice; the same procedure was performed with peripheral immune-related organs, such as spleen or lymph nodes. All the fluorescence-activated cell sorting (FACS) experiments performed after EAE included the isolation of the whole spinal cord. Nevertheless, flow cytometry of control and PLX5622-treated C57BL/6 mice also included the isolation of spleen and peripheral blood. The latter was extracted from the heart right ventricle after the euthanasia and collected in lithium-heparin tubes to avoid coagulation.

Lysolecithin-induced demyelination

To analyze remyelination in *Irf5*$^{-/-}$ mice, we performed LPC-induced demyelination in the spinal cord of both WT and *knock-out* 14-week-old male mice. Briefly, the lesions were induced by stereotaxic injection of 0.5µl of 1% LPC (Sigma) in saline solution, as previously described (Tepavčevič et al., 2014). Prior to the surgery, animals were anesthetized by intraperitoneal injection of a solution of ketamine (100 mg/kg) and xylazine (10 mg/kg). The tissue covering the vertebral column was removed taking advantage of two longitudinal incisions into the *longissimus dorsi*, and the intravertebral space of the 13th thoracic vertebra was exposed by removing the connective tissue after fixing the animal in the stereotaxic frame. Dura mater was then pierced using a 30G needle, and LPC was injected via a Hamilton syringe attached to a glass micropipette using a stereotaxic micromanipulator

The lesion specific site was marked with sterile charcoal so that the area of tissue at the center of the lesions could be unambiguously identified afterwards. Following LPC injection, the wound was sutured and mice were allowed to recover. Buprenorphine (0.1 mg/kg) was administered by subcutaneous injection as postoperative analgesic treatment. Mice were euthanized 4 and 14 days after surgery, in order to assess the response to demyelination.

After LPC-induced demyelination, mice were perfused with 2% PFA for 15-20 minutes and spinal cords were post-fixed in 2% PFA for another 30 minutes. Tissue was then processed the same way as the EAE lumbar spinal cords.

Microglial depletion

To deplete microglia *in vivo*, both C57BL/6 and CCR2-RFP/fms-EGFP mice were fed with 1200 ppm PLX5622 (Plexxikon Inc.) *ad libitum*. Respective control animals received standard chow instead, also acquired from the same supplier. Mice were fed for 21 days prior to further experimental procedures to ensure maximal microglial depletion.

***IN VITRO* MODELS**

Primary microglia culture

Primary mixed glial cultures were prepared from the cerebral cortex of neonatal rats and both WT and Irf5$^{-/-}$ mice (P0-P5). After 10-15 days in flask culture with Iscove's modified Dulbecco's medium (IMDM), microglia were isolated by mechanical shaking (400 rpm, 1h) and purified by plating the floating cells on non-coated bacterial grade Petri dishes (Thermo Fisher), as previously described (Domercq et al., 2007). These cells were maintained in these Petri dishes with Dulbecco's modified eagle medium (DMEM; Gibco) supplemented with 10% fetal bovine serum (FBS; Gibco) for 48 hours. Afterwards, microglial cells obtained with this procedure were tripsinized and seeded in poly-D-lysine (PDL)-coated coverslips in DMEM + 10% FBS at variable cellular density, in relation with the subsequent biochemical analysis (20.000 cells/wells for immunocytochemistry, 100.000 cells/wells for qPCR experiments, 200.000 cells/wells for myelin phagocytosis experiments, or 1.000.000 cells/well for liquid chromatography experiments). Microglia were seeded in 35 mm, glass-bottom dishes (Ibidi) for specific experiments, like the wound-healing assay or the

mitochondrial measurements, or in Seahorse manufacturer's plates (Agilent) for metabolism experiments. During all the steps of the protocol, cells were maintained at 37ºC in a humidified incubator with 5% of CO_2.

Microglial cells were polarized with specific stimuli in FBS-supplemented DMEM. To generate an anti-inflammatory phenotype in these cells, they were treated for 24 hours with IL-4 (20 ng/ml; Peprotech) and IL-13 (50 ng/ml; Peprotech). On the other hand, pro-inflammatory microglia were generated with a treatment of both LPS (10 ng/mL; Sigma) and IFN-γ (20 ng/ml; Peprotech) for 24 hours. To assess the inflammatory activation time course and the IRF5 translocation to the nucleus, the LPS+IFN-γ treatment was maintained for a variable number of hours prior to the analysis.

TECHNIQUES

Immunofluorescence analysis

Coronal sections of tissues coming from healthy mice, EAE mice and mice with LPC demyelinating lesions were analyzed by immunohistochemistry (IHC). First, sections were permeabilized and blocked with 0.1% Triton X-100 (Sigma), 4% normal goat serum (NGS; Palex), 0.02% azide (Sigma) in 0.1 M PBS for 1 h at room temperature (RT). Of note, spinal cord MBP staining required a 10 minutes step of permeabilization with 100% ethanol at -20ºC and subsequent washes in PBS preceding this blocking. Next, the tissue was incubated with specific primary antibodies overnight at 4ºC. Following this incubation, the sections were washed three times in PBS, and subsequently incubated with fluorochrome-conjugated secondary antibodies and DAPI (4 µg/mL) in blocking solution, at RT for 1 h. Last, the washings were repeated and the tissue was mounted under coverslips using Glycergel mounting medium (Dako). Similarly, several immunofluorescence assays were performed on the primary microglial cells coming from WT and *Irf5*$^{-/-}$ C57BL/6 mice. After experimental procedures and treatment, seeded cells were fixed in 4% PFA for 20 minutes, and processed for immunocytochemistry (ICC), in a similar protocol to the one followed for IHC. Specific primary and secondary antibodies used for all the immunofluorescence analyses are listed in the **Table 1**.

Images of the **IHC** were acquired using a Leica TCS STED SP8 confocal microscope, a Zeiss LSM800 confocal microscope, a Leica LCS SP2-AOBS confocal microscope or a Pannoramic MIDI II slide scanner (3DHistech), maintaining the same settings for all samples within one experimental group. All the image analysis was performed with the ImageJ software (National Institutes of Health; NIH).

To determine the effect of microglial depletion with PLX5622, healthy spinal cords were processed as described previously, and the number of microglial cells was determined based on Iba1 staining. Images were acquired using a LEICA TCS STED SP8 confocal microscope, with a 40x amplification. The number of cells in PLX5622-treated mice was normalized to the numbers in the control mice, to determine the percentage of cells depleted with the treatment. In EAE, we used CCR2-RFP/fms-EGFP mice to determine the ratio between the microglial cells and infiltrating monocytes in control and PLX5622-treated animals. 40x amplification images were obtained from tissues of 4 different animals for each experimental group, with the same confocal microscope, and both the lesions and the gray matter (GM) were analyzed. Cells positive for EGFP (CSF1R) and negative for RFP (CCR2) were defined as microglia, while cells positive for RFP were designated as peripheral monocytes.

For further histological analysis of EAE lesions**,** images of the whole section were obtained using Pannoramic MIDI II slide scanner. The lesion area was defined as the lack of MBP staining along with accumulation of myelin debris (identified by an increase in MBP fluorescence), and normalized in relation to the area of the entire white matter (WM) of each section. Infiltration of immune cells towards the EAE lesions was defined as the area occupied by the different markers (CD3, B220 or Ly6G), again normalized to the WM area of each section. The different regions of interest (ROIs) were defined in ImageJ. Representative images were acquired using a Leica TCS STED SP8 confocal microscope, using a 40x objective and generating z-stack projections. In the same tissues, astrogliosis was determined by the fluorescence intensity of glial fibrillary acidic protein (GFAP) in the lesion, the peri-lesion (defined as the rest of the WM) and the GM, in images obtained with the same confocal microscope and objective as before.

To analyze the BBB permeabilization in the differential experimental groups of the EAE, animals were injected intraperitoneally with 2% Evans blue (EB; Sigma) in saline solution (200 μL), and let it spread throughout the body for 1 hour. Lumbar spinal cord tissue was processed as described above and EB staining in blood vessels was evaluated by immunohistochemistry. The analysis was performed using three biological replicates for each experimental group.

To histologically assess LPC-induced demyelination, the extent of the lesion was determined by the absence of MBP staining in all individual animals (n = 5 WT mice, 6 *Irf5*$^{-/-}$ mice in the case of 14 dpi tissues, n = 4 WT mice, 5 *Irf5*$^{-/-}$ mice in the case of 4 dpi). The number of T cells and different oligodendrocyte populations were normalized to the area of the lesion in each case. To quantify axonal damage SMI-32 immunoreactivity was calculated in the lesion ROI. For these quantifications, images are 20x, z-stack projections acquired with a Leica TCS STED SP8 confocal microscope.

To assess lipid metabolism in EAE and LPC-induced lesions, tissues were stained with Oil Red O (BioVision), following manufacturer's instructions. Briefly, tissues were incubated in 60% isopropanol for 5 minutes, and then stained with Oil Red in a 60% isopropanol – 40% distilled water solution for 15 minutes, with gently shaking. Finally, the sections were washed three times in distilled water. Images of the stained neutral lipids were acquired with a Zeiss LSM800 confocal microscope. Restrained to the lesion areas, the size and number of individual lipid bodies were quantified by thresholding the immunofluorescence signal with ImageJ. Cholesterol crystals images were obtained using a Leica LCS SP2-AOBS confocal microscope, taking advantage of reflection microscopy. The reflectivity of the crystals allowed us to quantify the accumulation of this lipid, in relation to the LPC-induced lesion area. Lastly, the accumulation of particles of oxidized lipids was defined on the basis of E06 staining, and normalized to the lesion area.

Images of **ICC** were acquired using a Zeiss LSM800 confocal microscope, maintaining the same settings for all samples within one experimental group. All the image analysis was performed with the ImageJ software (NIH).

The morphology of microglial cells after Mdivi-1 treatment was analyzed using the Iba1 immunofluorescence, as the whole soma was stained with this marker. Specifically, the circularity of these cells was calculated as defined in ImageJ; a circular shape would approach a value of 1. Immunoreactivity of the different markers after pro-inflammatory, anti-inflammatory and/or Mdivi-1 treatments was calculated as the fluorescence intensity normalized to the number of cells in the selected field of view. All these experiments included multiple independent experiments performed in duplicates.

To study the effect of LPS treatment on IRF5 translocation to the nucleus to promote a response in microglia, the ratio between the cytoplasmic and nuclear IRF5 fluorescence intensity mean was calculated at different time points (2 to 24 hours). The compartments were designated by ROIs in ImageJ, using Iba1 to define the soma of the cell and DAPI staining to properly delimitate the nuclei.

Flow cytometry analysis of PLX5622-treated mice

For the analysis of microglial population in the chronic EAE after PLX5622 treatment, both microglial and macrophage populations were analyzed by FACS from the whole spinal cord. Spinal cords were enzymatically and mechanically digested to obtain single cell suspensions, and erythrocytes were lysed using an Ammonium-Chloride-Potassium (ACK) lysis buffer (155 mM NH_4Cl, 10 mM $KHCO_3$, 0.1 mM EDTA, pH 7.2). A Percoll gradient was performed to remove the myelin from the samples. After blocking the suspensions with anti-mouse CD16/32 antibody (TruStain FcX™, BioLegend) for 15 minutes, cells were stained with fluorochrome-conjugated monoclonal antibodies in FACS buffer, containing 1 mM EDTA (Sigma) and 0.1 % bovine serum albumin (Sigma). For this analysis, we used CD11b-FITC (1:200; BioLegend) and CD45-PE (1:100; BioLegend) as antibodies, identifying microglia as the $CD11b^+/CD45^{low}$ population, and infiltrating monocytes as the $CD11b^+/CD45^{hi}$ population. This experiment was performed using a BD FACSJazz cell sorter and analyser.

To assess the immune populations in the pre-onset and the onset of EAE development after PLX5622 treatment, cells from spleen, spinal cord and peripheral blood were analyzed. Spleens were mashed through 70 µm cell strainers using a syringe piston, and the blood was

extracted as explained above. Spinal cords were processed as in the previous analysis. In all cases, erythrocytes were lysed with an ACK lysis buffer. The specific antibodies used for this analysis are listed in **Table 2**. This experiment was performed using a BD FACSCelesta cell analyser, in the University Medical Center Hamburg-Eppendorf (Hamburg, Germany), and all the data was analyzed with FlowJo software (BD Bioscience).

Serum cytokines quantification

Using part of the blood serum from control and PLX5622-treated mice, the levels of different pro- and anti-inflammatory cytokines were measured. Specifically, the levels of IFN-γ, TNF-α, IL-2, IL-6, IL-17A and IL-22 were measured using a LEGENDplex™ Mouse Th Cytokine Panel (BioLegend), according to the manufacturer's instructions. The analysis was performed using 7 biological replicates for each experimental group.

Quantitative RT-PCR

Total RNA from EAE lumbar spinal cords, spleens and lymph nodes was isolated using TRIzol (Invitrogen) according to the manufacturer's instructions. Afterwards, 2 μg of this RNA was used to perform a retrotranscription protocol, using SuperScript III Reverse Transcriptase (200 U/μL; Invitrogen) and random hexamers as primers (Promega).

qPCRs were conducted in a Bio-Rad Laboratories CFX96 real-time PCR detection system, as previously described (Domercq et al., 2016). The reactions were performed using SYBR Green as the DNA-binding dye and specific primers for different T cell subtypes. The primers were designed using Primer Express Software (Applied Biosystems) at exon junctions to avoid genomic DNA amplification. The cycling conditions comprised 3 min of polymerase activation at 95°C and 40 cycles consisting of 10 s at 95°C and 30 s at 60°C. The amount of cDNA was quantified using a standard curve from a pool of cDNA obtained from the different conditions of the experiment. Finally, the results were normalized using a normalization factor based on the geometric mean of housekeeping genes obtained for each condition using the geNorm v3.5 software (Vandesompele et al., 2002).

Similarly, total RNA from microglial cells cultures treated with LPS + IFN-γ, Mdivi-1 or a combination of both was also extracted using TRIzol (Invitrogen). Afterwards, 1 μg of this

RNA was used for the retrotranscription process, and the qPCR was carried out similarly to what is described in the previous paragraph, using primers for pro- and anti-inflammatory canonical genes. The primers used for qPCRs of tissues and primary microglia are listed in **Table 3**.

Bulk RNA sequencing

In order to assess the transcriptomic profiles of WT and *Irf5*$^{-/-}$ microglia and macrophages, we performed RNA-sequencing experiments in the isolated populations of both cell types from control and EAE animals' spinal cords.

In order to isolate the cells while maintaining their specific activation state, all the steps in the sorting were performed at 4ºC. Spinal cords were only mechanically dissociated, avoiding enzyme-including steps to avoid overactivation of microglia. Percoll concentration for this protocol was of 24.4%. Cells were stained with CD11b-FITC, CD45-PE, Ly6C-PE/Cy7 (1:300; BioLegend) and SYTOX AADvanced™ Ready Flow™ (Thermo Fisher), a marker for dead cells. We isolated microglia identifying them as SYTOX^{-}/CD11b^{+}/CD45^{low}/Ly6C^{-} cells, and infiltrating macrophages identifying them as the SYTOX^{-}/CD11b^{+}/CD45^{hi}/Ly6C^{+} population. The cells were collected in RNAprotect Cell Reagent (Qiagen), to favour the stability of their RNA, and stored at -80ºC until further experimentation. Specifically, we isolated microglia and macrophages from 5 WT and *Irf5*$^{-/-}$ mice at the chronic phase of the EAE. In the control mice, we only isolated microglia (there was no infiltration of macrophages in healthy conditions) from 4 WT and 3 *Irf5*$^{-/-}$ mice.

Total RNA from these populations was extracted using the RNeasy Plus Micro kit (Qiagen), according to the manufacturer's protocol. RNA integrity number (RIN), indicative of its quality, as well as RNA quantity were determined using a high sensitivity RNA ScreenTape assay on a 4200 TapeStation system (Agilent), in the Research Sequencing Facility of the University Medical Center of Groningen (Groningen, The Netherlands). Subsequently, all 27 RNA samples were sent for processing with RNA-sequencing in GenomeScan (Leiden, The Netherlands), a specialized service for next-generation sequencing. Briefly, RNA-sequencing in GenomeScan involved a first step to assess the quality of the samples, determining their concentration with a Fragment Analyzer. Then, NEBNext Low Input RNA

Library Prep Kit for Illumina was used to process the sample; cDNA was synthesized and amplified from poly-A tailed mRNA. Clustering and DNA sequencing using the NovaSeq6000 was performed according to manufacturer's protocols; for this last step, a concentration of 1.1 nM of DNA was used. Lastly, primary data processing was done in the service, including quality checks, reads trimming and alignment to the most recent mouse genome.

All downstream bioinformatics analyses were performed with a variety of available packages in RStudio (v2021.09.0). First, for the differential gene expression analysis, low and non-expressed genes were excluded. The bioconductor package edgeR (v3.34.1; Robinson et al., 2009) was used for normalization using the timed mean of M-values (TMM) method, and for identification of the differentially expressed genes (DEGs) between the different experimental groups, by fitting a generalized linear model. DEGs were identified as those with an adjusted p-value < 0.05 and a log (Fold Change) > 1. Gene ontology (GO) analysis of the recognized DEGs for every comparison was performed using the DAVID (Huang et al., 2009) and Metascape (Zhou et al., 2019) web resources. These analyses were mostly performed in the University Medical Center of Groningen (Groningen, The Netherlands).

MALDI-IMS

In order to evaluate the changes in the lipidomic signatures in the context of LPC-induced demyelination, 12 µm-thick coronal sections were obtained from WT and *Irf5*$^{-/-}$ mice spinal cords at 14 dpi. The tissues were scanned using matrix-assisted laser desorption/ionization - imaging mass spectrometry (MALDI-IMS), in the Spectroscopy Unit of the University of the Basque Country. Specifically, the samples were scanned in a MALDI-LTQ-Orbitrap XL (Thermo Fisher), using the negative-ion mode for the m/z region where the most relevant lipid species appear (650-1200 Da). The sections were covered with a 1,5-diaminonaphtalene (DAN) matrix (Thomas et al., 2012), using an in-house designed sublimator that offers an optimized sample preparation, and introduced in the MALDI source. Data acquisition was performed with a spatial resolution of 100 µm/pixel and 60.000 at m/z = 400 mass resolution.

For the processing of the lipid signatures obtained from the MALDI analysis, the multiple spectra obtained were processed using a software developed in MatLab (MathWorks). Briefly, the peaks obtained were identified and filtered. Then, the different lipid signatures related to the diverse regions of the spinal cord were segmented using a *k*-means clustering method. The lipidomic profile of the LPC-induced lesion, as well as the peri-lesion area and the healthy white matter of 5 WT and 5 *Irf5*$^{-/-}$ injected mice were extracted and subsequently compared.

Myelin phagocytosis assay

Mouse myelin was isolated as previously described (Norton and Poduslo, 1973). Briefly, spinal cord was mechanically homogenized in 0.32 M sucrose and subjected to repeated sucrose gradient centrifugation and osmotic shocks to separate myelin from other cellular components. Myelin concentration was measured with Bradford assay and adjusted to 1 mg/mL. Then myelin was labelled with Alexa488-NHS dye (A2000 Life Technologies) for 1 hour at RT in PBS (pH 8). Dyed myelin was dialyzed for removing dye excess, resuspended in PBS (pH 7.4) and frozen until further use. For the assay of phagocytosis, myelin was thawed, vortexed for 60 seconds in order to fragment it in homogeneous size aggregates, and added to microglia culture medium (1:200 dilution). To evaluate myelin endocytosis, WT and *Irf5*$^{-/-}$ primary microglia were incubated with Alexa488-NHS-labeled myelin for 1 hour at 37ºC, rinsed and fixed with 4% PFA for 20 minutes. To evaluate myelin degradation, microglial cells were incubated with this myelin for 1 hour, and fixed 24 hours later. Images were taken with a Zeiss LSM800 confocal microscope, and fluorescence intensity as well as area of the intracellular myelin per cell were quantified with ImageJ.

Lipid extraction and quantification

In order to assess lipid metabolism of WT and *Irf5*$^{-/-}$ microglia, we challenged these primary cells with 25 µg/mL purified myelin for 48 hours; after treatment, excess of myelin was washed with PBS, and cells were subsequently scrapped and repeatedly centrifuged. Cell pellets were stored at -80ºC until further experimentation.

Cell pellets were resuspended in PBS and sonicated in 2 cycles of 10 seconds, with an interval of 10 seconds between cycles and an amplitude of 25%, maintaining the samples in

ice to avoid excessive heat interfering with their integrity. For lipid extraction, a commonly used method was carried out (Bligh and Dyer, 1959). Briefly, 2 mL of chloroform and 4 mL of methanol were added to 40 µg of protein from the cell homogenates, obtained after quantification using the bicinchoninic acid (BCA) assay. Importantly, this initial volume also includes a mixture of standards, like Splash Lipidomix® (Avanti Polar Lipids). Tubes were vigorously shaken for 2 minutes, and 2 mL of chloroform were then added to the mixture. After shaking for another minute, 3.2 mL of distilled water was added to the tubes, and another 1-minute vortex step was performed. This mixture was centrifuged at 1500 g for 10 minutes, at 4ºC, to allow the separation of the aqueous and organic phases. The lower, organic phases containing the lipids were transferred to clean tubes, and the lipids retained in the upper, aqueous phase were re-extracted by adding a mixture of chloroform, methanol and distilled water and repeating the shaking and centrifuge steps. The new organic phase was combined with the previously obtained one. Last, the solvent was evaporated using a Thermo Savant SC250 EXP SpeedVac vacuum concentrator to obtain the final lipid extract; this extract was stored at -80ºC under N_2 atmosphere.

For the analysis of the lipid extract, the samples were analyzed using UltiMate 3000 ultrafast liquid chromatography system (UHPLC; Thermo Scientific) coupled to a QExactive™ HF-X Hybrid Quadrupole-Orbitrap mass spectrometer (MS), in the University of the Basque Country lipidomic facilities. The lipid extract was resuspended in 90 µL of 9:1 methanol:toluene mixture, and 7 µL of the resulting supernatant was injected into the HPLC--MS system. Electrospray ionization was performed in either positive or negative ion mode.

Lipid species predicted by the quantification of the HLPC-MS results were filtered to remove the low reliability data as well as the repeated lipids, were classified into lipid families and were finally quantified in accordance to the standard signals and their concentrations. This experiment was performed on 4 WT and 4 *Irf5*$^{-/-}$ cultures, and the data represent the mean quantity (µg) of each species in a lipid class, normalized to the quantity of initial protein from each sample.

Wound healing assay

In order to assess migratory capacity on WT and *Irf5*$^{-/-}$ microglia, cells were seeded in DMEM+10%FBS in glass-bottom dishes (Ibidi), generating a confluent monolayer. The monolayer was scratched in a straight line using a sterile 200 mL pipette tip. To follow the migration of microglia towards the scratched area, we performed a 24-hour time-lapse of the cells using a BioStation IM-Q microscope (Nikon), maintaining the dishes at 37ºC and 5% CO_2 during the whole extent of the experiment. The number of microglia migrated towards the scratched area, as well as the percentage of the area occupied by these cells, were quantified in the initial image, as well as in images after 12 and 24 hours.

Cell viability assay

Microglial viability was assessed using the calcein-AM dye (Invitrogen). The data from this assay was obtained using the Gen5 software (Bio-Tek).

For the performance of the calcein assay, cells were incubated with 0.5 μM of the dye for 30 minutes at 37º C. The wells were then washed with PBS and the number of viable cells were calculated with a Synergy HT fluorimeter/spectrophotometer reader (Bio-Tek) with 485 nm excitation and at 528 nm of emission wavelengths. A well with PBS was also measured in each experiment to subtract its values as a background control. The results are expressed as the relative percentage of cellular death with respect to non-treated microglial cells.

Reactive oxygen species analysis

The production of ROS by WT control and LPS + IFN-γ-treated microglia was measured using the CM-H_2DCFDA dye (Invitrogen). Specifically, cells were incubated with the dye for 30 minutes. The wells were then washed with PBS and the ROS signal was calculated using the same fluorimeter as described above, with 485 nm excitation and at 528 nm of emission wavelengths, following the guidelines of the manufacturer. ROS signal was normalized to the calcein levels measured in each well.

Mitochondrial membrane potential and mitochondrial calcium measurements

For the quantification of mitochondrial membrane potential (ΔΨm), we used Rhodamine 123 dye (Rh123) a reliable dye for confocal microscopy analysis of ΔΨm (Hardingham et al., 2002; Yan et al., 2020), under quenching concentrations (Corona and Duchen, 2014). Microglial cells were loaded with Rh123 (10 µM) for 15 min in Hanks balanced salt solution (HBSS) without phenol red, to avoid interferences. After loading, microglia were washed for 10 minutes in the same medium. Living cell imaging was then performed with a 63x objective in an inverted Leica LCS SP2-AOBS confocal microscope at an acquisition rate of 1 frame every 15 seconds for 5 min. In this short-term protocol, no cell toxicity was detected with Rh123. After obtaining some basal images, FCCP (1 µM), an uncoupler of the mitochondrial oxidative phosphorylation, was added to the plates and the increase in the Rh123 fluorescence level was measured to determine the membrane potential. For each plate, a homogenous population of approximately 20 cells was selected in the field of view, and the background fluorescence signal was subtracted from the individual values. For the experiments involving tetramethylrhodamine ethyl ester (TMRE), the protocol was slightly different. Microglia were loaded with TMRE (100 nM) for 15 minutes. After some basal images, oligomycin (2 µM) was added to the medium, and FCCP was incorporated in the last minute of recording to provoke an acute, complete depolarization.

Regarding the measurement of the mitochondrial calcium content, time-lapse images were acquired using a 63X objective in a Leica TCS STED CW SP8 confocal microscope, at an acquisition rate of 1 frame every 15 seconds for 5 min. Cells were loaded with 1 µM Fluo-4 (Thermo Fisher) in HBSS (Ca^{2+} and Mg^{2+} free) with 0.5 µM EGTA for 30 minutes at 37ºC. Microglial cells were subsequently washed and, after obtaining some basal images, 1 µM FCCP was added to depolarize the mitochondrial membrane and force the release of Ca^{2+} from mitochondrial matrix to the cytosol. The choosing of the field of view was determined as in the ΔΨm measurement experiments.

Mitochondrial morphology analysis

For the quantification of mitochondrial length, living cell imaging was performed on microglial cells, loaded with 50 µM Rh123 for 20 min. Mitochondrial images were taken

using a Zeiss LSM800 confocal microscope at 40X magnification, and analyzed using the Object Analyzer tool of Huygens image analysis software (Scientific Volume Imaging, B.V, version 20.10). First, background noise was removed using the maximum fluorescence intensity value of Rh123 in the nuclear region. Afterwards, a size filter was applied to remove objects smaller than mitochondria (38 voxels = 0.06 μm^3; Freya and Mannellab, 2000). A watershed segmentation was then performed using a sigma value of 0.2 to separate objects that were not discriminated in the raw images due to the inherent resolution limit of confocal microscopy. After all these pre-processing steps, the average length of each mitochondrial object per cell was calculated.

OXPHOS and glycolysis analysis

Real time measurements of oxygen consumption rate (OCR), extracellular acidification rate (ECAR) and glycolytic proton efflux rate (glycoPER) were performed using a Seahorse XFe96 Extracellular Flux Analyzer (Agilent), following manufacturer's instructions to carry out both the XF Cell Mito Stress Test Kit or the XF Glycolytic Rate Assay Kit (Agilent). Microglia cells were seeded as a monolayer in the Agilent XF96 microplate. Before the assay, cells were washed and equilibrated in the XF Assay modified DMEM medium during 30 minutes at 37ºC.

For the performance of the XF Cell Mito Stress Test Kit, the levels of OCR were determined in response to the sequential addition of oligomycin (2 μM), FCCP (1 μM) and rotenone/antimycin A (0.5 μM). The parameters obtained through this experiment were defined following manufacturer's guidelines. Basal mitochondrial respiration was calculated subtracting final OCR from the basal levels. The spare respiratory capacity was obtained by subtracting the basal respiration level from the maximum rate measurement reached after addition of FCCP to the medium. ATP-linked OCR was determined by subtracting oligomycin-induced OCR from basal OCR. For the acute treatment with LPS + IFN-γ, these factors were added to the cells after the basal measurement of OCR, and prior to the addition of oligomycin. For the measurement of the basal glycoPER, the XF Glycolytic Rate Assay Kit was carried out. This test includes the sequential addition of rotenone/antimycin A (0.5 μM), and 2-deoxyglucose (2-DG; 50 mM). The glycoPER

corresponds to the proton efflux rate derived from glycolysis (discounting the effect of CO2-dependent acidification, included in the ECAR measurement) (Fig. 8).

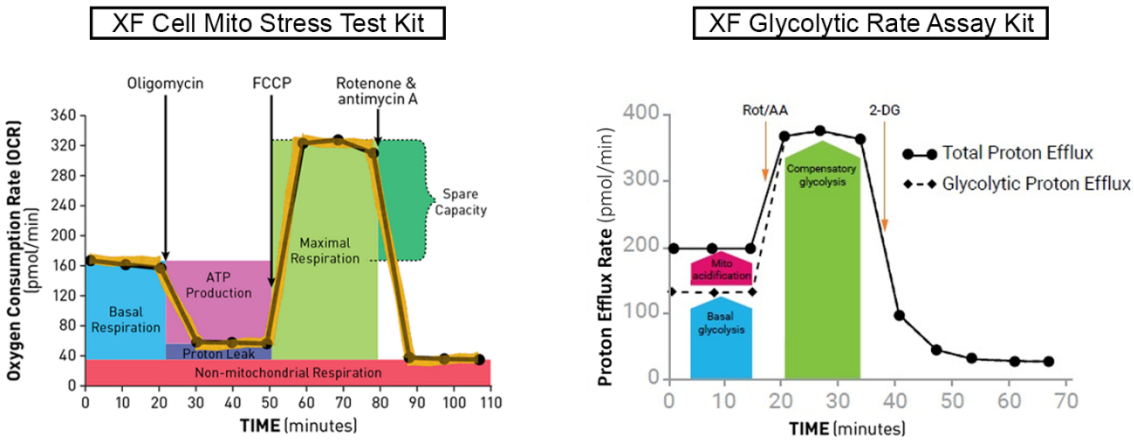

Figure 8. Schematic profiles of Seahorse metabolic assays. Profiles showing the sequence of microinjections and the different parameters that can be obtained performing the Agilent Seahorse XF Cell Mito Stress Test Kit (left) and XF Glycolytic rate assay (right).

All the parameters analyzed in these experiments were obtained using the report generator for the specific used kit (Agilent). For each single experiment, eight replicates were performed per experimental condition.

Statistical analysis

Data are presented as mean ± standard error of mean (SEM) and n represents the number of animals, cultures or cells analyzed; this is specificized in figure legends. Statistical analyses were performed using GraphPad Prism 8 (GraphPad Software Inc), applying the corresponding statistical treatment for each experiment. Unless otherwise stated, comparisons between two groups were analysed using paired Student's two-tailed t-test for data coming from *in vitro* experiments and unpaired Student's two-tailed test for data coming from *in vivo* experiments. Comparisons among multiple groups were analysed by one-way ANOVA followed by Bonferroni post-hoc analysis. In all instances, p values < 0.05 were considered statistically significant.

Table 1. Antibodies used for immunohistochemistry and immunocytochemistry

Antibody	Host	Concentration	Company
Primary antibodies			
CC1	Mouse	1:200	Calbiochem
CD3	Rat	1:50	Bio-Rad
CD31	Mouse	1:100	Santa Cruz
CD45R	Rat	1:200	BD Bioscience
E06	Mouse	1:200	Avanti
GFAP	Mouse	1:40	Millipore
GFP	Rat	1:1000	Nacalai
Iba1	Rabbit	1:500	Wako
Iba1	Guinea Pig	1:500	Synaptic Systems
iNOS	Mouse	1:500	BD Bioscience
IRF5	Rabbit	1:500	Abcam
Ki67	Rabbit	1:500	Vector
Ly6G	Rat	1:100	BioLegend
MBP	Mouse	1:1000	Covance
MBP	Rabbit	1:200	Millipore
MRC1	Rabbit	1:200	Abcam
Olig2	Mouse	1:1000	Invitrogen
SMI-32	Mouse	1:1000	Covance
Secondary antibodies			
IgG Rabbit-Alexa 488	Goat	1:400	Invitrogen
IgG Rabbit-Alexa 594	Goat	1:400	Invitrogen
IgG Mouse-Alexa 488	Goat	1:400	Invitrogen
IgG Mouse-Alexa 594	Goat	1:400	Invitrogen
IgG Rat-Alexa 488	Goat	1:400	Invitrogen
IgG Rat-Alexa 594	Goat	1:400	Invitrogen
IgG Guinea Pig-Alexa 488	Goat	1:400	Invitrogen

Table 2. Antibodies used for FACS analysis of immune populations

Marker	Fluorochrome	Concentration	Company
CD11b	Bv510	1:100	BioLegend
CD11c	Bv605	1:100	BioLegend
CD3	PE/Cy7	1:100	BioLegend
CD4	Bv785	1:100	BioLegend
CD45	APC/Cy7	1:100	BioLegend
CD8	Bv650	1:100	BioLegend
CD80	PE	1:100	BioLegend
CD86	Bv421	1:100	BioLegend
Ly6G	AF700	1:100	BioLegend
MHC-II	FITC	1:100	BioLegend
P2Y12	APC	1:100	BioLegend
TCRgd	PerCP/Cy5.5	1:100	BioLegend

Table 3. Sequences for mouse and rat primers used for qPCRs

Target gene	**Forward** sequence **(5'->3')**	**Reverse** sequence **(5'->3')**
Rat target genes		
Arg1	GGATTGGCAAGGTGATGGAA	CGACATCAAAGCTCAGGTGAA
Ccl2	AGCAGCAGGTGTCCCAAA	TTCTTGGGGTCAGCACAGAC
Il1b	TGGCAACTGTTCCTGAACTCA	GGGTCCGTCAACTTCAAAGAAC
Nos2	GAGGAGCAGGTGGAAGACTA	GGAAAAGACTGCACCGAAGATA
Mouse target genes		
Ror	ACTGAAAGCAGGAGCAATGGAAG	TTCAAAAAAGACTGTGTGGTTGTTG
FoxP3	ACCACACTTCATGCATCAGCTC	GGCTGGGTTGTCCAGTGGAC
Ifnγ	TAACTATTTTAACTCAAGTGGCATAGATGTG	GCCAGTTCCTCCAGATATCCAAG
CD4	GGCATGGGAGAAAGGATCG	TACCCGGACTGAAGGTCACTT
CD8	GTGCCAGTCCTTCAGAAAGTGA	GGCGAAGTCCAATCCGGT

Housekeeping genes	**Forward** sequence **(5'->3')**	**Reverse** sequence **(5'->3')**
Rat housekeeping genes		
Hprt2	CAGTACAGCCCCAAAATGGTTA	AGTCTGGCCTGTATCCAACA
Ppia	AGGGTTCCTCCTTTCACAGAA	TGCCGCCAGTGCCATTA
Mouse housekeeping genes		
B2m	ACTGACCGGCCTGTATGCTA	ATGTTCGGCTTCCCATTCTCC
Gapdh	AGACGGCCGCATCTTCTT	TTCACACCGACCTTCACCAT

RESULTS

Part I. Specific role of microglia in experimental autoimmune encephalomyelitis development

Neuroinflammation is a complex system orchestrated by the response of many cell types. The different macrophages that can found in this condition, involving resident microglia, CAMs and infiltrating monocyte-derived macrophages, are key promoting the inflammatory environment, and are suggested to play non-redundant functions. However, the specific role of microglia during EAE in comparison to the rest of myeloid populations is not entirely elucidated. Here, we assessed the effect of microglial depletion in EAE development, and we analyzed the possible role behind the alterations observed.

Microglial depletion causes a delay in EAE onset and massive infiltration of macrophages

In both MS and EAE animal model, CNS-resident microglia and invading macrophages are thought to contribute to the pathogenesis of the disease, participating both in the progression and the recovery of the disease (Prinz et al., 2021). In order to address the particular role of microglial cells in all EAE stages, we used the CSF-1R specific inhibitor PLX5622 (administered at 1200 ppm in chow, *ad libitum*) to deplete microglial population from the CNS.

Animals were treated with this compound for 21 days, prior to further experimental procedures (see scheme in Fig. 9A). In basal conditions, this treatment was enough to deplete 90% of the microglial population throughout the lumbar spinal cord, in a similar proportion of that achieved in other studies (Elmore et al., 2018; Spangenberg et al., 2019) (Fig. 9A). To analyze the relevance of microglia in the development of EAE, we induced this MS model in control mice as well as in PLX5622-treated mice. Microglial depletion provoked a consistent and significant delay in the onset of EAE symptoms, even though no more differences were found in the course of the disease (Fig. 9B). We did not observe differences in the maximal neurological score reached at the peak of the disease, nor in the recovery capacity during the chronic phase of EAE (Fig. 9B).

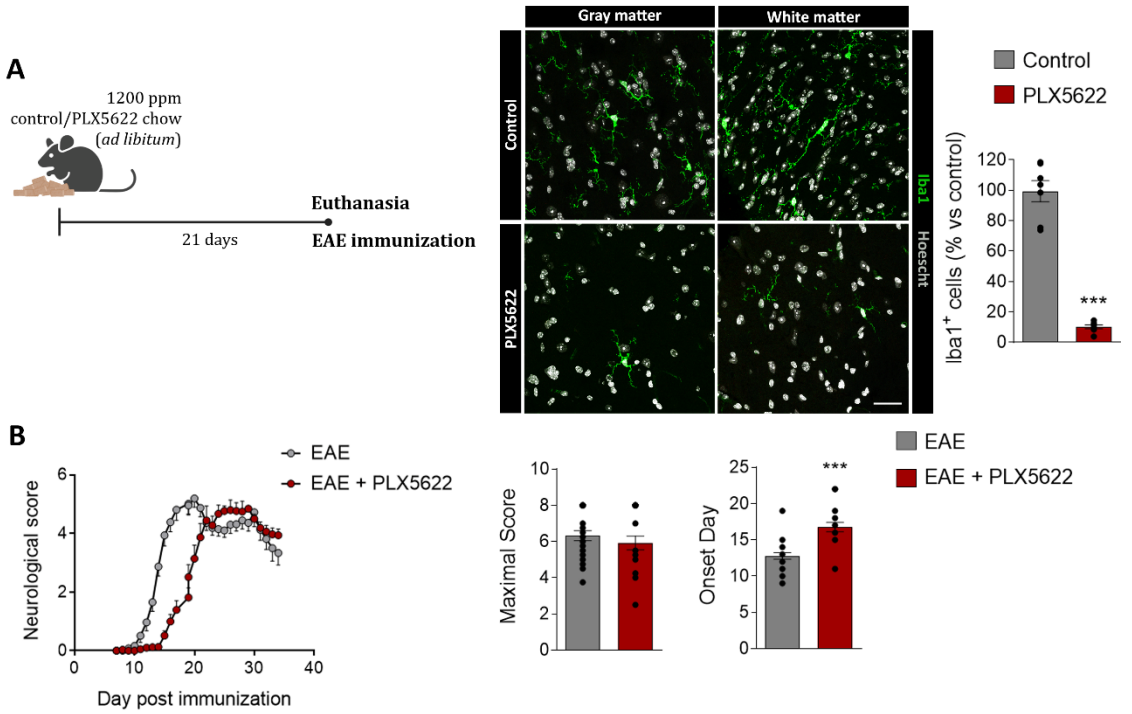

Figure 9. PLX5622 microglial depletion provokes a delay in the onset of EAE and massive infiltration of macrophages. ***(A)*** (Left) Scheme showing the paradigm of microglial depletion with PLX5622. (Right) Representative images showing microglial (Iba1⁺ cells) depletion in both the white and gray matter of healthy spinal cord. Histogram shows the loss of microglia after PLX5622 treatment, in comparison to control mice. Scale bar = 25 µm. ***(B)*** (Left) Neurological score of control and PLX5622-treated mice, (n = 20-25 mice from 3 independent EAE experiments). (Right) Histograms showing the maximal score reached by every animal, as well as the onset day of clinical signs. Data are presented as means ± SEM. ***p < 0.001

Then, we assessed the populations of microglia (CD11b⁺ CD45^{low}) and invading macrophages (CD11b⁺ CD45^{hi}) at the end of the disease by FACS, and we observed that the ablation of microglia was maintained throughout EAE development (Fig. 10A). As flow cytometry dot plot pointed out to an increase in the total number of macrophages after the treatment, we repeated EAE in control and PLX5622-treated CCR2-RFP/fms-EGFP mice (kindly provided by Dr. Amanda Sierra). These mice allowed us to distinguish resident microglia (*Ccr2*$^{-}$ *fms*$^{+}$) from infiltrating macrophages (*Ccr2*$^{+}$ *fms*$^{-}$) on spinal cord sections. Of note, CNS-infiltrated macrophages (*Ccr2*$^{+}$) started to express fms once in the CNS parenchyma, so we also considered *Ccr2*$^{+}$ *fms*$^{+}$ cells as infiltrating macrophages. We observed a higher accumulation of peripheral macrophages into demyelinated lesions in PLX562-treated mice (Fig. 10B). In addition, macrophages penetrated into the non-damage white matter and even into the gray matter in PLX562-treated mice (Fig. 10B). This result demonstrates that resident microglia limit the massive entry of macrophages and its dispersion through the CNS parenchyma in response to pathological conditions.

Interestingly, despite the massive infiltration of macrophages, microglial depletion did not trigger an exacerbated progression of EAE, nor did it cause a failure in the recovery phase, as described earlier (Ajami et al., 2011).

Together, these results indicate that microglial ablation provokes a compensatory mechanism based on a robust peripheral macrophages infiltration. On the other hand, depletion of microglia seems to have a specific effect on the triggering of the symptomatology, as it delayed the disease onset.

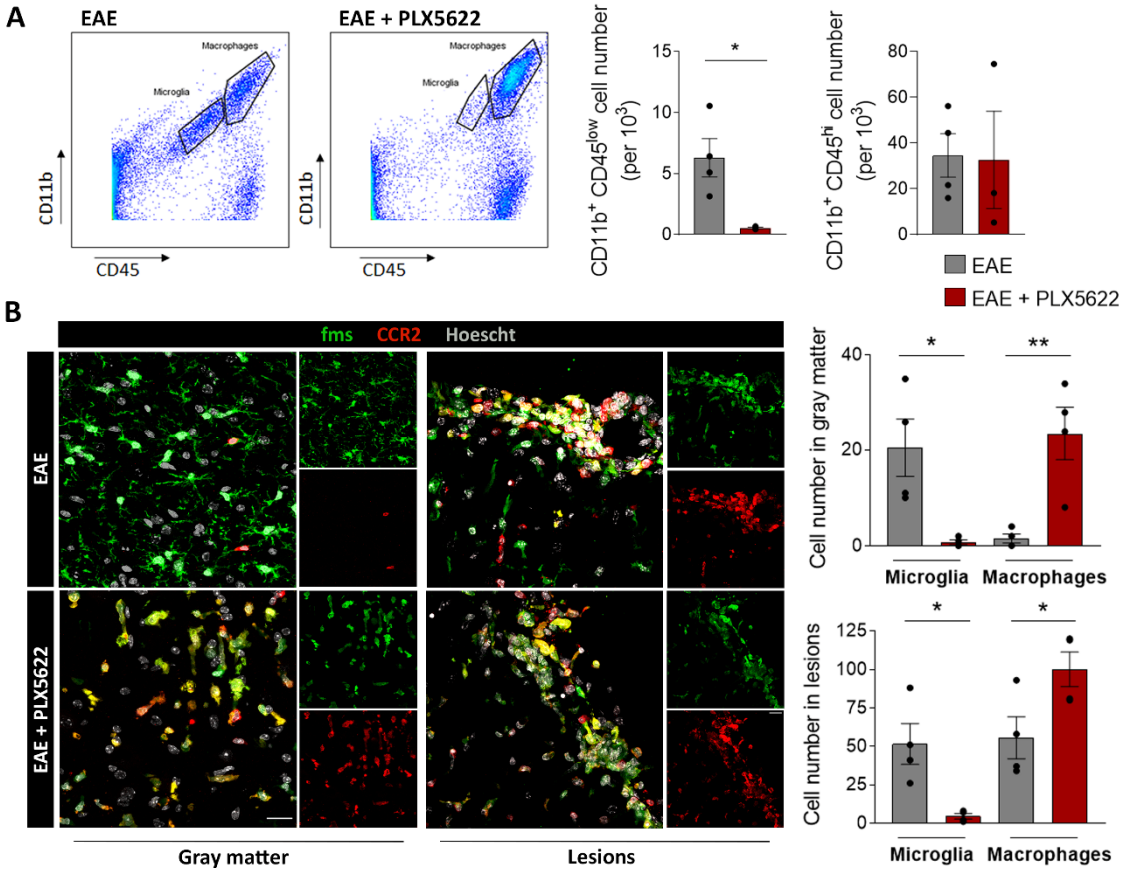

Figure 10. Microglial depletion by PLX5622 favours a massive infiltration of macrophages intro CNS parenchyma. ***(A)*** Plots depicting the strategy to distinguish resident microglia ($CD11b^+/CD45^{low}$) from invading macrophages ($CD11b^+/CD45^{hi}$) in EAE spinal cords from control and PLX5622-treated mice. Histograms show the quantification of both populations, in relation to the total number of analyzed cells in the samples (n = 4 mice per group). ***(B)*** Representative images of *fms*$^+$ microglia and *Ccr2*$^+$ macrophages in the gray and white matter of control and PLX5622-treated CCR2-RFP/fms-EGFP mice at EAE chronic phase. Histograms at the right show the quantification of microglia (fms^+ $CCR2^-$ cells) and macrophages ($CCR2^+$ cells) in each region (n = 3). Scale bar = 20 µm. Data are presented as means ± SEM. *p < 0.05, ***p < 0.001

Microglial depletion does not alter EAE chronic symptoms

Microglial function during EAE is commonly associated to its capacity to phagocytose the released myelin debris, promoting recovery and regeneration in the chronic phase of the disease. We further assessed whether the depletion of microglia affects neuroinflammation and demyelinated lesions on histological levels at this stage, using immunohistochemistry (Fig. 9B).

We performed histopathological assessment of demyelination and inflammatory cell infiltration. Regarding the lesions, we observed no differences in the total white matter area affected by EAE model, comparing control and PLX5622-treated mice (Fig. 11A). The lesioned area was determined by the accumulation of infiltrating cells, as well as by the loss or damage of myelin (characterized by high MBP immunoreactivity). Since demyelination in EAE is mediated by an immune response, mainly based on T cell activity but also on B cells infiltration (Bakhuraysah et al., 2021), we analyzed the presence of both populations in the lesions. No differences were found in meningeal and infiltrating accumulation of both kind of cells in the lesion sites (Fig. 11B). Lastly, we observed no alteration in astrogliosis neither in the lesions nor in the surrounding parenchyma (Fig. 11B).

In sum, these findings show that the course of the chronic phase of EAE was not altered in mice with depleted microglia. As we detected similar partial remission of the symptoms in both experimental groups, this suggests that microglial cells are not necessary for a EAE better outcome or a more efficient remyelinating process during the disease, pointing out to a compensatory mechanisms by other infiltrating myeloid cells.

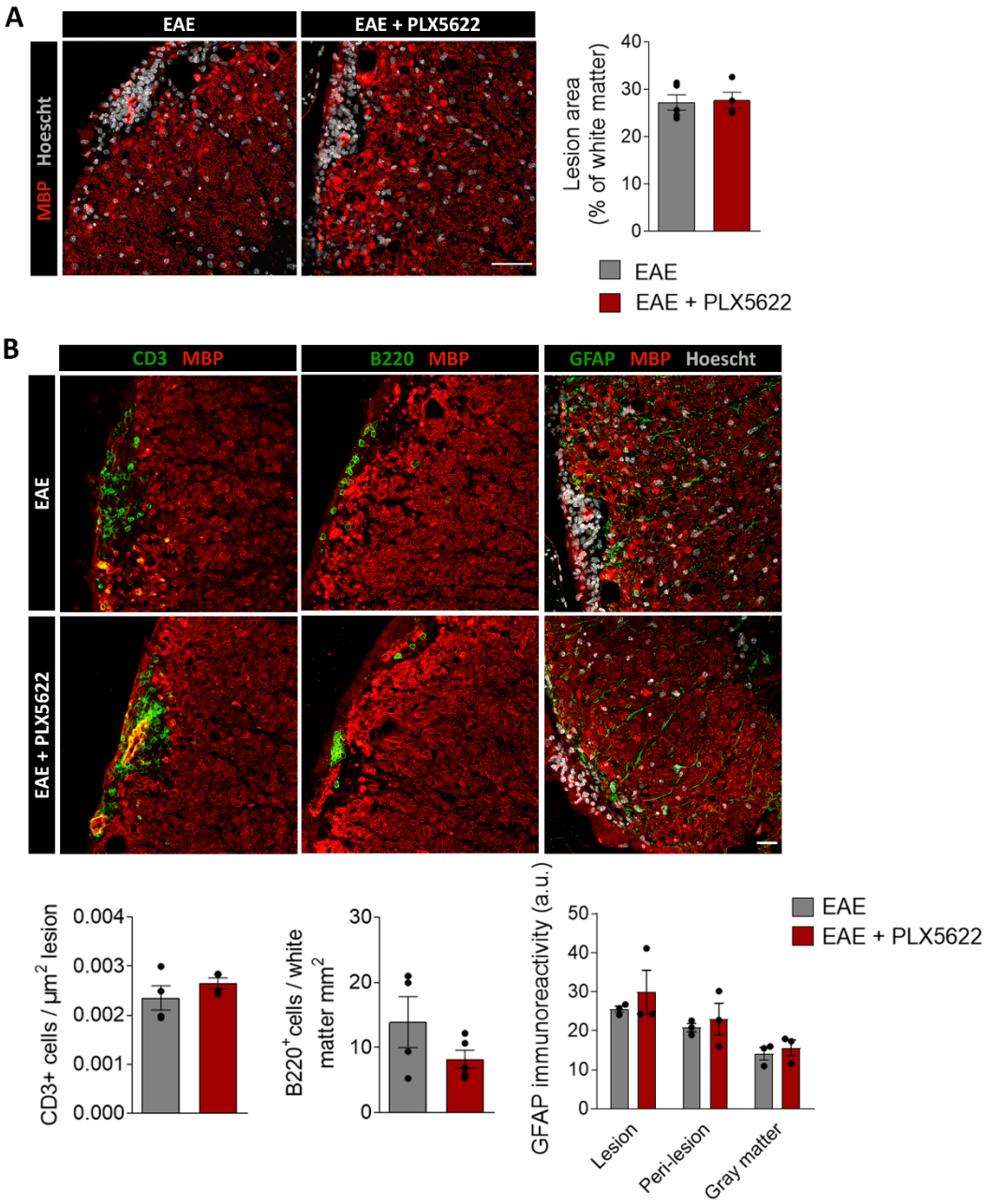

Figure 11. PLX5622 microglial depletion did not alter the EAE chronic phase. ***(A)*** Representative images of EAE lesions in the lumbar spinal cord of control and PLX5622-treated mice, at 35 days post-immunization. Histogram shows the percentage of lesioned white matter versus total white matter (n = 5). Scale bar = 50 µm. ***(B)*** Representative images showing the accumulation of $CD3^+$ T cells and $B220^+$ B cells in EAE lesions as well as the astrogliosis in control and PLX5622-treated at EAE chronic phase. Scale bar = 25 µm. Histogram shows the number of cells normalized to lesion area or total white matter for T and B cells, respectively (n = 5), and astrocyte immunoreactivity, indicative of astrogliosis (n = 3). Data are presented as means ± SEM.

Peripheral immune priming is not altered in EAE after microglial depletion with PLX5622

As previously described, EAE initial stages primarily imply T cell activation in peripheral lymphoid organs, such as the spleen or lymph nodes, against myelin-specific peptides (Prinz and Priller, 2017). Since microglial ablation delayed EAE onset, we hypothesyzed that microglia could modulate immune priming or immune infiltration. In order to corroborate these hypotheses, we first assessed whether microglia could influence peripheral early responses right after immunization, and prior to the appearance of first motor deficits.

We immunized mice and euthanized them at the pre-onset phase of EAE (dpi 8-9; no clinical signs). At this timepoint, we performed flow cytometry analysis of the immune cell populations in spleen and peripheral blood. (FACS gating specified in Fig. 12A). Microglial depletion by inhibition of CSF-1R did not alter the proportion of any immune population ($CD4^+$ T cells, $CD8^+$ T cells, γδ T cells, neutrophils and macrophages) neither in the spleen nor in the blood at EAE pre-onset stage (Fig. 12B, C)

Taking advantage of the blood sampling, we analyzed the concentration of pro- and anti-inflammatory cytokines in the serum of both animal groups, using a bead-based immunoassay. Specifically, we measured the levels of innate and adaptive immune cytokines such as IL-2, IL-6, IL-17, IL-22, IFNγ and TNFα, all associated with EAE pathology (Jahan-Abad et al., 2020). Microglial ablation did not lead to any difference in the cytokine profiles in the serum at EAE pre-onset (Fig. 12D). Moreover, as EAE model is based predominantly in a $CD4^+$ T cell response, we assessed their phenotypes by qPCR analysis in spleen and lymph nodes, both tissues where T cells are early activated. We measured the levels of mRNA expression for forkhead box protein P3 (*FoxP3*), retinoic acid-related orphan receptor (*Ror*), transcription factors specifying Treg and Th17 activity respectively, as well as *Ifnγ*, signature cytokine for Th1 cells. We did not find differences in the expression of these markers between control and PLX5622-treated mice at EAE pre-onset (Fig. 12E).

All these results suggest that microglial ablation does not provoke important alterations in the primary, peripheral immune priming after EAE induction. Thus, the delay in the onset of the symptoms might be associated with an effect of PLX5622 in the CNS environment.

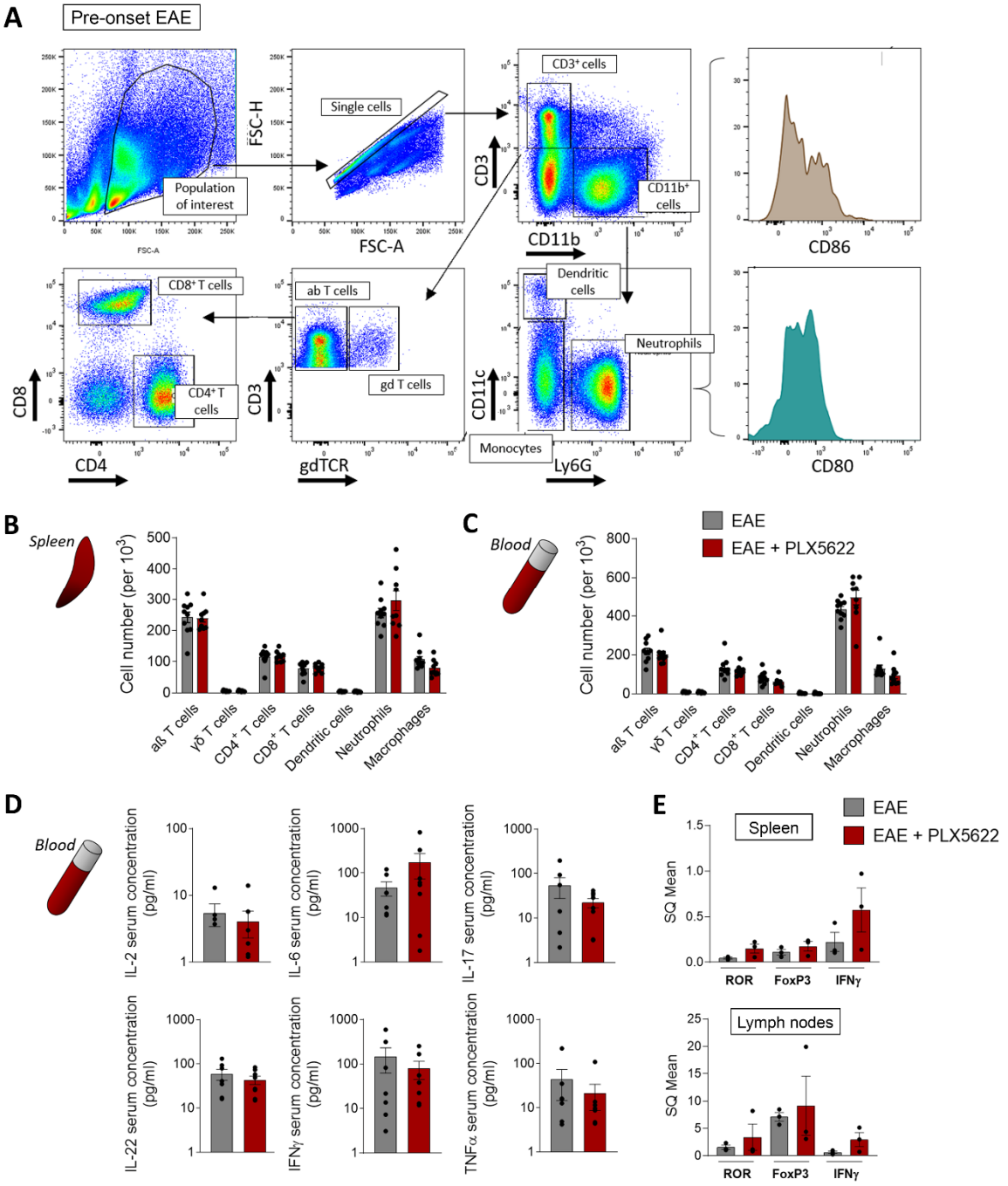

Figure 12. PLX5622 did not alter peripheral immune priming after immunization. ***(A)*** Flow cytometry gating strategy for analysis of immune populations in the spleen and peripheral blood of mice at EAE pre-onset (dpi 8-9). ***(B, C)*** Quantification of αβ T cells ($CD3^+$ $\gamma\delta TCR^-$), γδ T cells ($CD3^+$ $\gamma\delta TCR^+$), CD4 T cells ($CD3^+$ $CD4^+$) CD8 T cells ($CD3^+$ $CD8^+$), dendritic cells ($CD11b^+$ $CD11c^+$), neutrophils ($CD11b^+$ Ly6G+), and macrophages ($CD11b^+$ $CD11c^-$ $Ly6G^-$) populations in spleen (B) and blood (C), in relation to the total $CD45^+$ single cells analyzed at this stage (n = 10). ***(D)*** Concentration of cytokines in blood serum from control and PLX5622-treated mice at EAE pre-onset stage (n = 7). ***(E)*** Relative mRNA expression of *Ror*, *Foxp3* and *Ifnγ* in spleen and lymph nodes of both mice groups, at EAE pre-onset stage (n = 3). Data are presented as means ± SEM.

Spinal cord early EAE affection is not altered in microglial depletion conditions

As peripheral response was not altered in microglia-depleted mice, we next analyzed the spinal cord of both control and PLX5622-treated mice at the pre-onset stage of EAE, in order to look for early signs of alteration that would lead to the delay in the symptomatology.

We assessed immune cell infiltration towards the spinal cord by flow cytometry profiling at EAE pre-onset (gating strategy specified in Fig. 13A). Aside from the expected significant reduction in the number of microglial cells in the PLX5622-treated animals, we did not identify any other differences in immune populations (Fig. 13B). Moreover, analysis of first-arriving $CD4^+$ T cells' profiles in spinal cord by qPCR did not show any differences between both experimental groups (Fig. 13C). Since alterations in BBB permeability are a key initiating factor promoting the infiltration of myeloid and lymphoid cells to the CNS parenchyma in MS and EAE (Bennett et al., 2010), we subsequently analyzed the state of BBB integrity by histological analysis of EB in spinal cord vascularity. No differences were observed in the extravasation of EB between control and PLX5622-treated mice at EAE pre-onset, with all the staining remaining inside the $CD31^+$ blood vessels in both groups (Fig. 13D).

These results highlight that CSF-1R inhibition does not significantly alter primary immune response at the pre-onset stage of the disease. Thus, delayed symptomatology is probably linked to a later alteration, most likely affecting events occuring in the CNS.

Microglia is key in the immune response in the CNS parenchyma

The efficient activation of T lymphocytes after arriving to the CNS parenchyma is a critical requirement for the induction of CNS inflammation and associated EAE pathology. Because of this, and given the delay in the appearance of the motor alterions in microglial-depleted mice, we next analyzed whether immune ablation altered the immune response at EAE onset in the CNS parenchyma. We induced EAE in control and PLX5622-treated mice and euthanized them at dpi 12-14, a common timepoint for the study of the symptomatology onset.

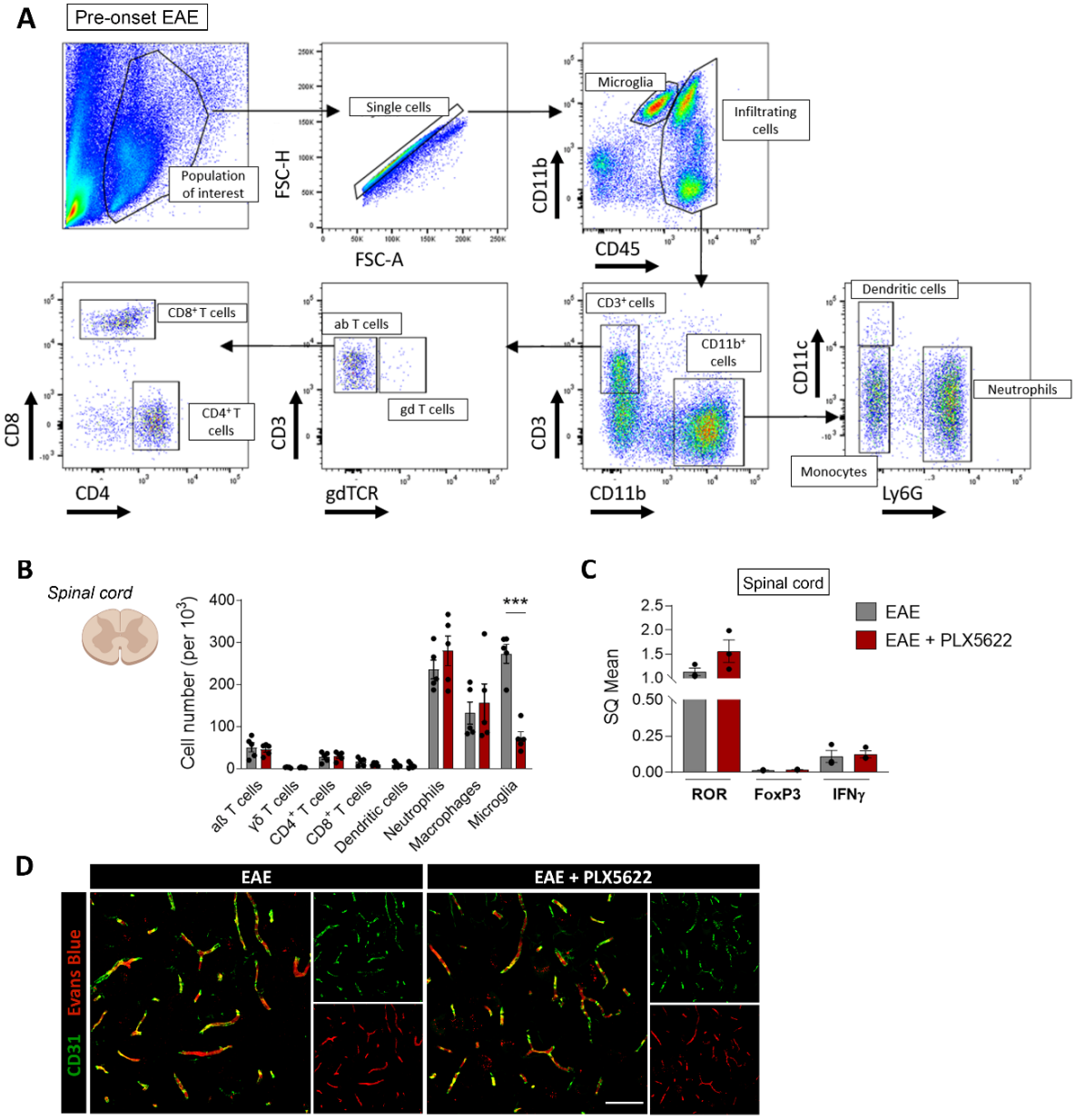

Figure 13. PLX5622 did not alter early, CNS-related events at the pre-onset EAE. ***(A)*** Flow cytometry gating strategy for analysis of immune populations from the spinal cord of mice at EAE pre-onset (dpi 8-9). ***(B)*** Quantification of the same populations as in the previous figure plus microglia ($CD11b^{+}$ $CD45^{low}$) in spinal cord, in relation to the total number of analyzed cells, at this stage (n = 5). ***(C)*** Relative mRNA expression of *Ror*, *Foxp3* and *Ifng* in the spinal cord of both mice groups, at EAE pre-onset stage (n = 3). ***(D)*** Representative images showing Evans Blue staining restricted to $CD31^{+}$ blood vessels, showing a lack of BBB disruption in the spinal cord of both control and PLX5622-treated mice. Scale bar = 50 µm. Data are presented as means ± SEM. *p < 0.05.

At this timepoint, we observed a consistent difference in the degree of pathology development (Fig. 14A). Indeed, control mice were starting to show the first motor deficiencies while PLX5622-treated mice presented absent or low clinical signs. We performed flow cytometry analysis of the immune cell populations in peripheral tissues (spleen and blood); the gating strategy was carried out as previously described (Fig. 12A). These FACS experiments allowed us to observe that microglial depletion, again, was not causing an alteration in the immune cell populations in spleen and blood (Fig. 14B). However, FACS analysis of the spinal cord immune populations, also following the previously described gating strategy (Fig. 13A), showed an increase proportion of neutrophils as well as lesser percentages of macrophages and $CD4^+$ T cells in PLX5622-treated animals (Fig. 14C).

Although the proportion of the major immune populations was not affected in microglia depleted mice, the total number of immune cells infiltrated into the CNS parenchima was massively reduced in PLX5622-treated mice, as revealed by immunohistochemistry (Fig. 14D). Indeed, control mice presented high levels of infiltration of T cells, B cells and neutrophils, as assessed by immunostaining of CD3, B220 and Ly6G respectively, in correlation with the neurological score (Fig. 14D). Alternatively, PLX5622-treated mice showed very limited infiltration of these cells, and mostly restricted to the meninges and blood vessels (Fig. 14D).

These results suggest that microglia depletion somehow provokes a delay in the accumulation of immune cells in the CNS parenchyma, and this effect is directly linked to the delay in the appearance of the motor deficits.

Microglia elimination reduces antigen presentation and T cell reactivation in EAE onset

The accumulation of T cells in the CNS tissue during neuroinflammation is commonly preceded by a reactivation step carried out by APCs. As we observed an alteration in this agreggation, we assessed the antigen presentation process both at the pre-onset and onset stages of EAE, by FACS analysis. Specifically, we measured the expression of the B7 co-stimulatory molecules (CD80 and CD86), which are known to participate along with MHC-II in this mechanism (Shemer and Jung, 2015), in diverse APCs.

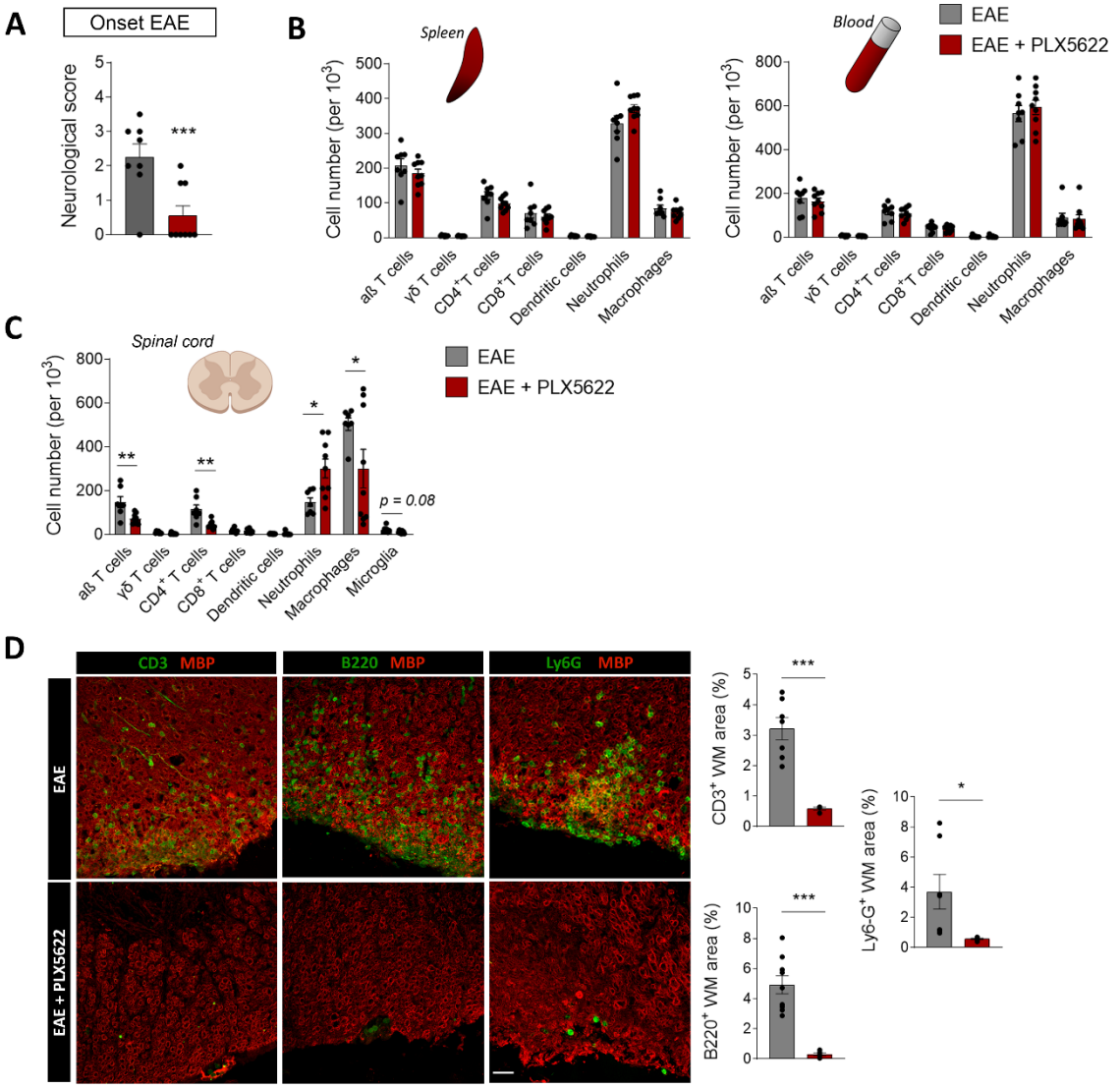

Figure 14. PLX5622 provoked a delay in the infiltration of immune cells towards CNS parenchyma ***(A)*** Histogram showing the neurological score reached by control and PLX5622-treated mice when euthanized at 12-14dpi. ***(B)*** Quantification of immune populations in spleen and peripheral blood, in relation to the total number of analyzed cells, at this timepoint (n = 10). Gating strategy is specified in Fig. 11A. ***(C)*** (Left) Representative images of CD3⁺, B220⁺ and Ly6G⁺ cells infiltration into spinal cord parenchyma. (Right) Histograms show the area occupied by these cells, in relation to the whole white matter area, in control and PLX5622-treated animals. Scale bar = 30 µm. ***(D)*** Quantification of immune populations in spinal cord, in relation to the total number of analyzed cells, at EAE onset (n = 10). Gating strategy is specified in Fig. 12A. Data are presented as means ± SEM. *p < 0.05, **p<0.005, ***p < 0.001.

At the pre-onset phase of EAE (dpi 8-9), we hardly found any significant differences regarding CD80 and CD86 intensity in the cell types analyzed (microglia, DCs and macrophages) in microglial-depleted mice (Fig. 15A), except for a decrease in CD86 intensity in spleen macrophages. However, at EAE onset we detected that the expression of these co-stimulatory molecules was altered in the spinal cord, but not in spleen or blood

(dpi 12-14). Specifically, the expression of CD80 was decreased in DCs and infiltrating macrophages in PLX5622-treated mice (Fig. 15B). Likewise, CD86 intensity was also reduced in macrophages of these PLX5622-treated mice (Fig. 15B). This finding suggests a role of microglia in modulating antigen presentation, not only as an intrinsic mechanism , but also affecting other APC cells and their function.

As these observations suggest that antigen presentation is altered in spinal cord after microglial depletion, and this process is needed for T clonal expansion in CNS parenchyma, we assessed whether the proliferation rate of these cells was differential between control and PLX5622-treated mice. Control EAE mice showed a massive proliferation of immune cells inside the lesions, whereas proliferaton was limited in PLX5622-treated mice at EAE onset (dpi 12-14; Fig. 15C). In particular, the number of $Ki67^{+}$ $CD3^{+}$ T cells was significantly reduced, suggesting that T cell proliferation and therefore their clonal expansion was delayed in microglia-depleted mice (Fig. 15C). Of note, this effect is also observed in the first T cells arriving to the CNS after preipheral priming (Fig. 15D).

Taken together, the results described in this section showed that microglia is determinant to limit the dispersion of CNS-infiltrated macrophages into the CNS parenchyma. In their absence, macrophages are able to colonize this parenchyma and contribute to both EAE development as well as the recovery/remyelinating mechanisms occuring in the chronic phase. On the other hand, we concluded that microglia are important to EAE development. Actually, their deletion delayed the immune cell activation responsible for the onset of the disease, by altering the antigen presentation in the brain.

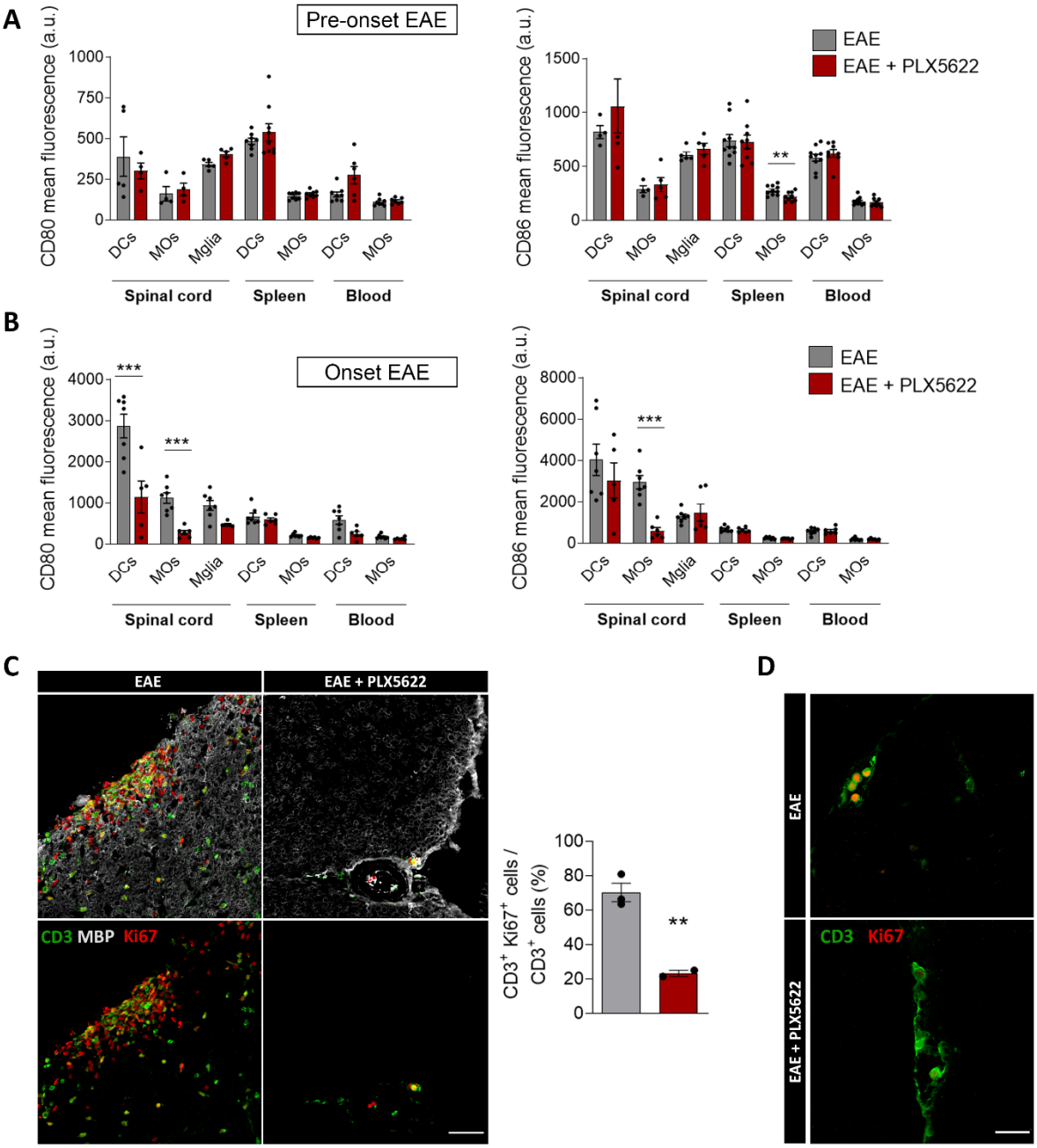

Figure 15. Microglial depletion with PLX5622 alters antigen presentation and T cell reactivation in the spinal cord ***(A, B)*** Histograms showing CD80 and CD86 fluorescence intensity in different APCs (dendritic cells, macrophages and microglia) and in diverse tissues, as analyzed by FACS, at the pre-onset stage of EAE (A; dpi 8-9) (n = 5 spinal cord samples, n = 10 spleen and blood samples), and ***(B)*** at the onset stage of EAE (B; dpi 12-14) (n = 10). ***(C)*** Representative images showing $CD3^+$ lymphocytes and Ki67 proliferative-associated expression in spinal cord, at dpi 10-12 12 after EAE immunization in control and PLX5622-treated mice. Histogram show the proportion of $Ki67^+$ $CD3^+$ T cells in relation to the total number of $CD3^+$ T cells (n = 3). Scale bar = 25 µm. ***(D)*** Representative images showing the Ki67 profile of the first infiltration $CD3^+$ lymphocytes spinal cord, at EAE onset (dpi 10). Scale bar = 30 µm. Data are presented as means ± SEM. ***p < 0.001.

Part II. Role of microglial IRF5 transcription factor in demyelinating disorders

Due to the dichotomic role of microglia and macrophages in neuroinflammatory events, it could be pivotal to find targets to modulate their activation, in order to eliminate their deleterious effects and promote a pro-regenerative state. Importantly, the IRF5 transcription factor drives inflammatory responses in diverse immune cells, including microglia, and is a risk factor for several autoimmune disorders. Of note, two *Irf5* SNPs are associated with MS (Kristjansdottir et al., 2008). However, the role of IRF5 in microglia and in this pathology remains unknown. In this section, we have assessed the role of IRF5 in different models of MS, including processes of both demyelination and remyelination.

IRF5 relevance in microglia and MS

Initially, we analyzed the expression of IRF5 transcription factor in total RNA from post-mortem optic nerve samples of control and MS patients (Matute et al., 2007). We did not observe any increase in the expression of *Irf5* in MS tissue (Fig. 16A), suggesting that this gene is not upregulated during the development or at late stages of the disease. Then, we performed *in silico* analysis based on published data obtained by single-cell RNA sequencing, in cells isolated from healthy human tissue and from early active multiple sclerosis patients (Masuda et al., 2019). We found that *Irf5* is downregulated, although not significantly, in microglial cells in the pathology ($p=0.08$; Fig. 16B).

Given the decrease in *Irf5* expression in microglia, we analyzed its role in these cells. We set up an *in vitro* pro-inflammatory paradigm in which primary microglia were treated with inflammation-associated factors (10 ng/mL LPS + 20 ng/mL IFN-γ), and assessed whether this transcription factor was translocated to the nucleus to promote its functions. Indeed, we observed an increase in the nuclear/cytosolic ratio regarding IRF5 expression after 8 hours of treatment (Fig. 16C), in comparison to control microglia. This outcome highlights the relevance of IRF5 in microglial-mediated inflammatory responses.

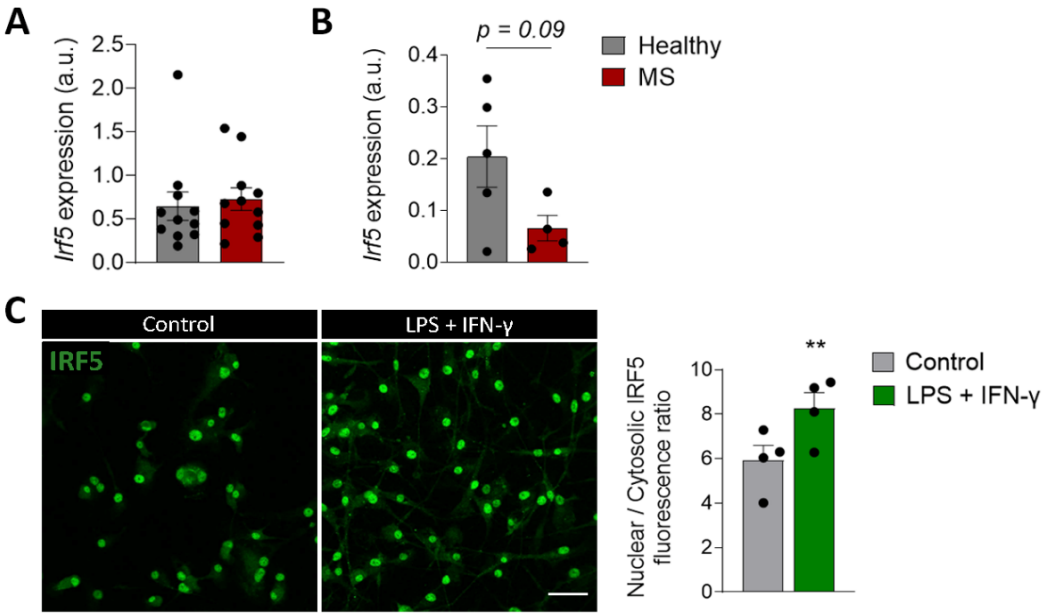

Figure 16. Expression and function of *Irf5* in MS microglia *(A)* Relative mRNA expression of *Irf5* in total RNA from human optic nerve samples of control and MS patients (n = 10). ***(B)*** Relative mRNA expression of *Irf5* in microglia; data obtained by *in silico* analysis of published data obtained by single-cell RNA sequencing, in microglial cells isolated from healthy human tissue and from early active multiple sclerosis patients (*Masuda et al., 2019*). ***(C)*** Analysis of IRF5 nuclear translocation upon pro-inflammatory stimulation of primary microglia. Histogram shows the ratio between the nuclear and cytosolic fluorescence of IRF5 in control microglia and microglia treated with LPS + IFN-γ for 8 hours. (n = 3 independent experiments). Scale bar = 20 µm. Data are presented as means ± SEM. **p < 0.005.

Irf5 deletion delays EAE onset and exacerbates damage at EAE chronic phase

We then addressed the specific role of the IRF5 transcription factor in the development of EAE using *Irf5*$^{-/-}$ mice. Previously, we characterized whether the deletion of this gene could alter the microglial population in the healthy CNS, and we did not find any differences in the number of microglial cells in the spinal cord of two-months-old *Irf5*$^{-/-}$ mice (Fig. 17A).

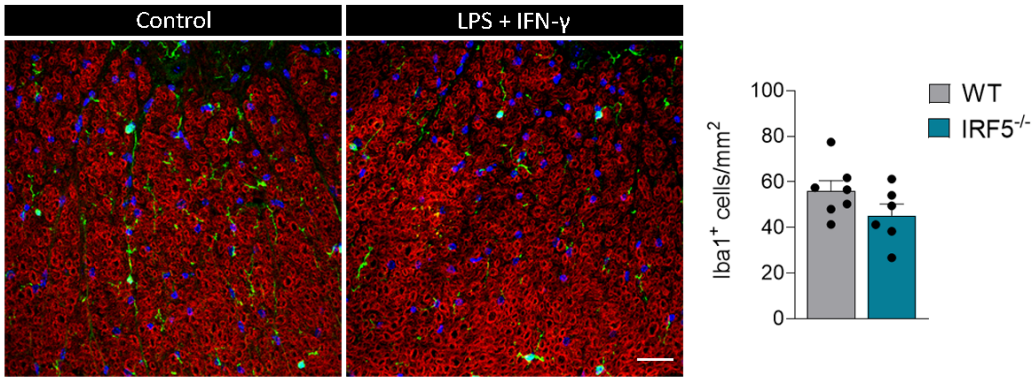

Figure 17. Homeostatic microglia in *Irf5*$^{-/-}$ *mice.* (Left) Representative image of Iba1^{+} microglia in spinal cord from control *Irf5*$^{-/-}$ mice. (Right) Histogram shows the number of Iba1^{+} cells per mm^{2} in this tissue (n = 7). Scale bar = 30 µm. Data is presented as mean ± SEM.

Then, we compared the neurological score of WT and *Irf5*$^{-/-}$ MOG-immunized mice. We observed a significant delay in the onset of motor disabilities in the mice lacking IRF5 (Fig. 18A), suggesting a role of this transcription factor in immune priming as previously demonstrated for other transcription factors of the same family, such as IRF8 (Yoshida et al., 2014). However, *Irf5*$^{-/-}$ mice showed an exacerbation of the clinical signs at the chronic phase of EAE (Fig. 18A), this result being indicative of either an aggravated demyelination or a failure in the remyelinating processes.

We next assessed whether this difference at the chronic phase of EAE could be associated with alterations at histological level. We performed immunohistochemistry analyses of the lumbar spinal cords of both WT and *Irf5*$^{-/-}$ mice. Demyelinated lesions, defined by the absence of MBP staining, tended to be larger in *Irf5*$^{-/-}$ mice, although the difference between groups was not statistically significant ($p = 0.07$; Fig. 18B). In addition, *Irf5*$^{-/-}$ mice presented significant increase in myelin debris deposition, which can be identified by higher MBP immunostaining due to the unmasking of protein epitopes (Fig. 18B). *Irf5*$^{-/-}$ mice also showed an increase in axonal damage, as assessed with IHC for SMI32 (Fig. 18B). Finally, these mice showed more accumulation of microglia and macrophages in the lesions, determined by Iba1 immunostaining (data not shown). Thus, *Irf5* deletion led to an exacerbation of tissue damage at the chronic phase of EAE, which again can be associated with a decrease in remyelination and recovery.

Since myelin clearance is necessary for remyelination and recovery (Kotter et al., 2006; Neumann et al., 2009), and we observed a higher accumulation of myelin debris in *Irf5*$^{-/-}$ mice, we challenged the hypothesis that these features could be the consequence of a failure on microglia/macrophage-mediated phagocytosis. With this in mind, we next analyzed the phagocytic capacity of *Irf5*$^{-/-}$ microglia and macrophages in EAE lesions. Briefly, phagocytosis was quantified at EAE chronic phase of WT and *Irf5*$^{-/-}$ mice, assessing the colocalization of Iba1 and MBP immunostaining. Myelin debris size was bigger and located preferentially in the phagocytic processes of *Irf5*$^{-/-}$ Iba1^{+} cells (Fig. 19A). In contrast, WT mice presented more abundance of partially degraded myelin in the cytoplasm of microglia/macrophages (Fig. 19A). This outcome could further support the idea of an impaired phagocytic capacity in cells lacking IRF5.

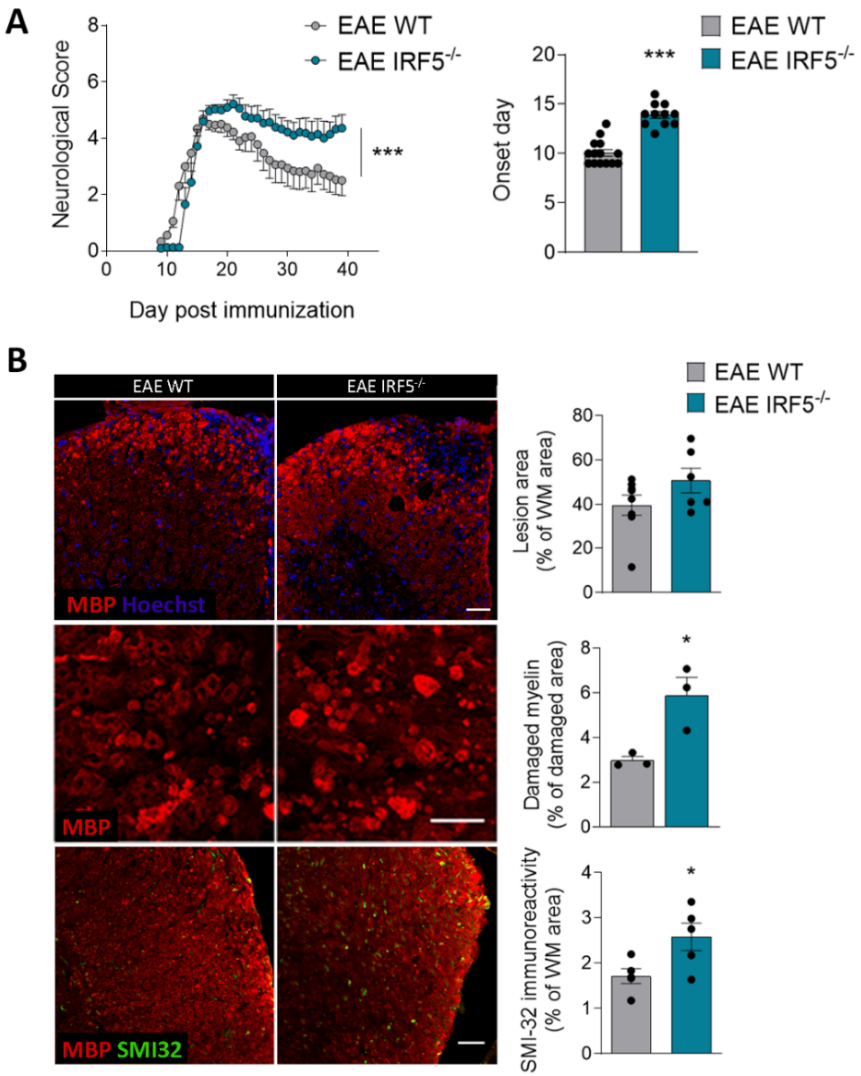

Figure 18. *Irf5* deletion exacerbates chronic phase of EAE. ***(A)*** Neurological score of WT and *Irf5*$^{-/-}$ mice after EAE. Histogram shows the day of appearance of the first motor symptoms induction (n = 12-15 mice from 2 independent EAE experiments). ***(B)*** Histological assessment of demyelinated lesion area, MBP^{+} myelin debris accumulation and axonal damage (SMI32) in WT and *Irf5*$^{-/-}$ mice at EAE chronic phase. Scale bar = 50 µm. Data are presented as means ± SEM. *p < 0.05, ***p < 0.001.

To further check the impact of *Irf5* deletion in microglial phagocytosis, we assessed the phagocytic and degradatory capacity of WT and *Irf5*$^{-/-}$ microglia *in vitro*. Specifically, cells were treated for 1 hour with myelin conjugated with an Alexa Fluor 488 fluorescent dye for the assessment of phagocytosis; then, myelin debris was removed from the medium and the cells were allowed to deliver the myelin to lysosomes and degrade the phagocytosed lipids for subsequent 23 hours. We observed a significant decrease in myelin phagocytosis in *Irf5*$^{-/-}$ microglia at 1h (Fig. 19B). Moreover, while WT microglia showed a higher capacity to degrade the internalized myelin after 24 hours, *Irf5*$^{-/-}$ microglia showed a failure in the myelin degradatory process (Fig. 19B). These results corroborate that *Irf5*$^{-/-}$ microglia

present an alteration in myelin phagocytosis and degradation, which could be responsible for the regeneration failure in IRF5-deficient mice.

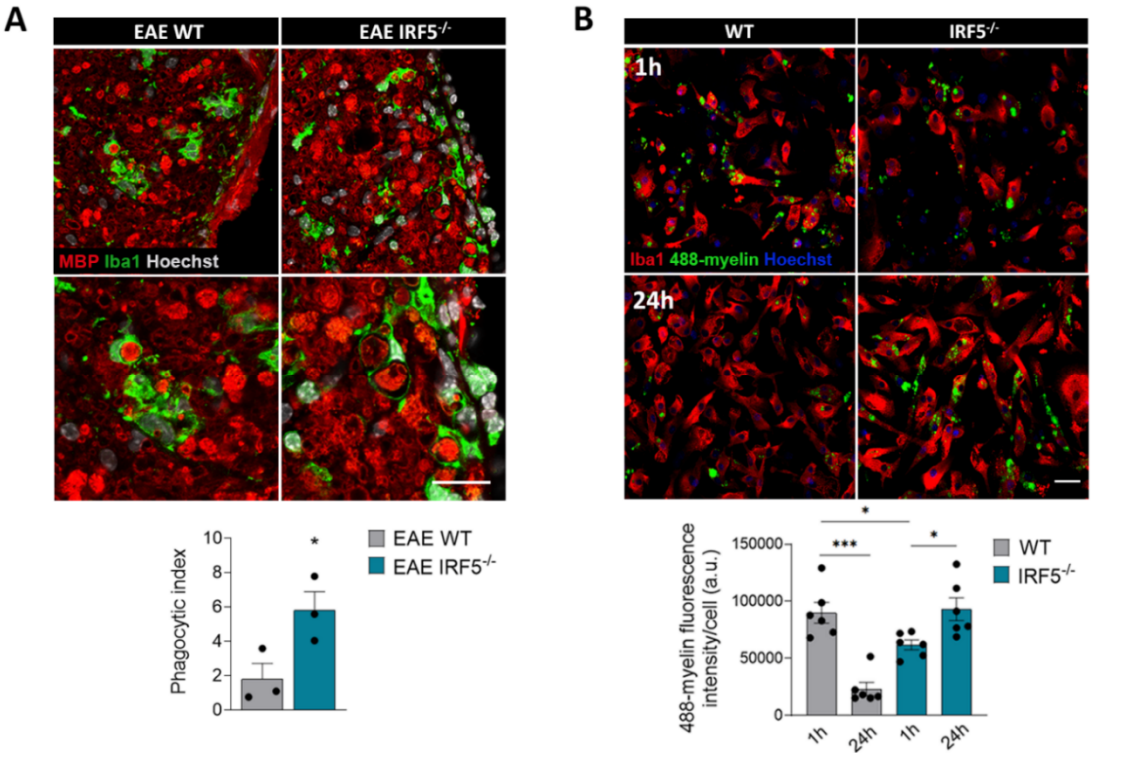

Figure 19. Myelin phagocytosis is altered in *Irf5*$^{-/-}$ microglia *in vivo* and *in vitro*. *(A)* Representative images of MBP and Iba1 immunostaining in spinal cord sections of WT and *Irf5*$^{-/-}$ mice at EAE chronic phase. Histogram shows the phagocytic index (detailed in methods) of microglia/macrophages in these conditions (n = 3 per group). Scale bar = 20 µm. ***(B)*** Representative images showing phagocytosis (1h) and degradation (24h) of Alexa-488 labelled-myelin by WT and *Irf5*$^{-/-}$ microglia *in vitro.* Scale bar = 30 µm. Histogram shows the fluorescence of 488-myelin in the cells, defined as ROIs using Iba1 staining (n = 6). Data are presented as means ± SEM. *p < 0.05, ***p < 0.001.

Exacerbated demyelination in *Irf5*$^{-/-}$ mice after LPC-induced demyelination

EAE model is commonly used to analyze the inflammatory events leading to demyelination, but not so much to assess the remyelinating capacity. To determine whether IRF5 is involved in remyelination, we used a specific MS model for remyelination analysis, in which demyelination is induced chemically and independently of an immune reaction. We provoked focal demyelinating lesions injecting lysolecithin (LPC) in the spinal cord of WT and knock *Irf5*$^{-/-}$ mice, and the lesions were histologically assessed after 14 days (Fig. 20A). At this timepoint, OPCs have been recruited into the lesions, have differentiated into mature oligodendrocytes and the remyelinating processes are expected to be already initiated (Tepavčevič et al., 2014).

In accordance with the data obtained in the EAE model, we observed that *Irf5*$^{-/-}$ mice presented larger lesions upon LPC injection than WT mice (Fig. 20B), although these mice did not show increased axonal damage (Fig. 20C). Higher lesions in *Irf5*$^{-/-}$ mice could mean a failure the remyelinating process; because of that, we quantified the oligodendroglial populations in these tissues. Interestingly, IRF5 deficiency was associated with a decreased number of total oligodendrocytes as well as mature oligodendrocytes in the lesions, as determined by the staining of Olig2 and CC1, respectively (Fig. 20D). However, we found no difference in the proportion of mature oligodendrocytes in relation to the total number of Olig2^{+} cells in these LPC-induced lesions (Fig. 20D). This outcome points out to a failure in OPCs recruitment towards the lesions as the reason behind the larger extent of lesions in *Irf5*$^{-/-}$ animals, rather than an alteration in the differentiation of these oligodendrocytes.

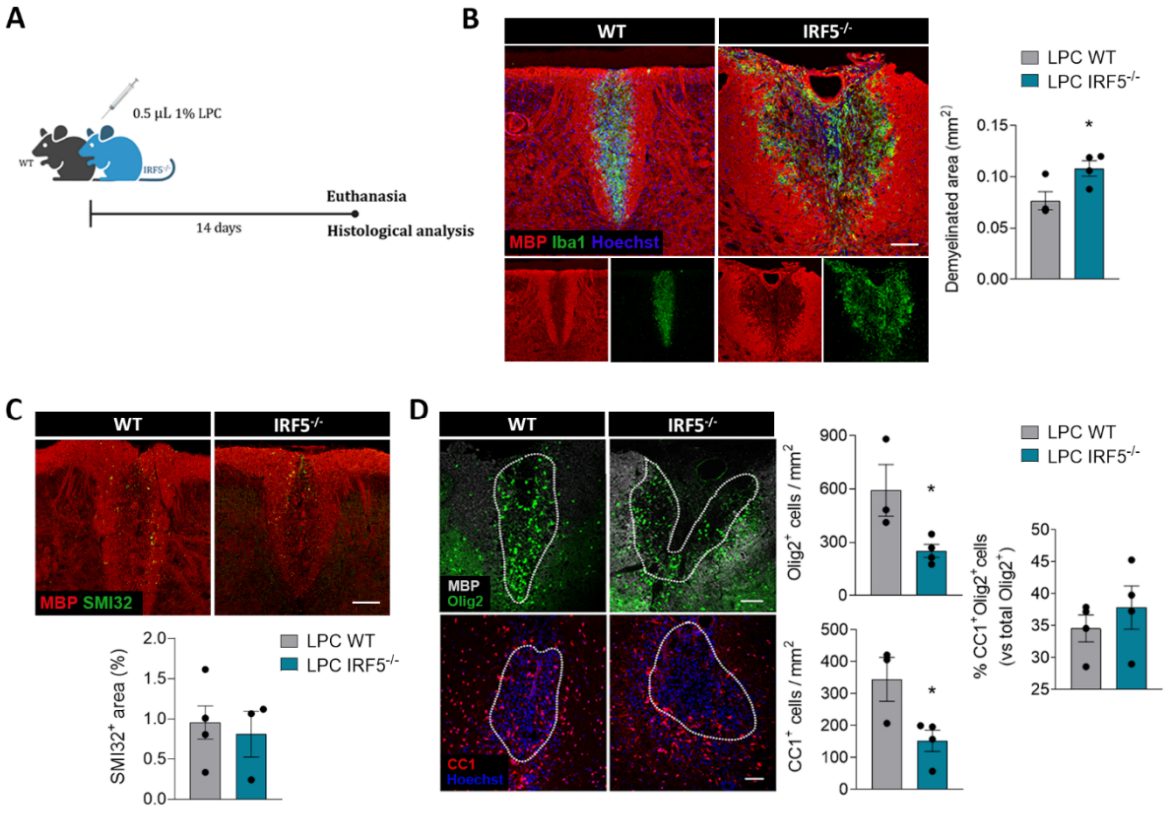

Figure 20. IRF5 deficiency alters remyelinating capacity. ***(A)*** Scheme showing the experimental design for the analysis of remyelination after LPC-induced demyelination, both in WT and *Irf5*$^{-/-}$ mice. ***(B)*** Extent of the demyelinating lesions and the accumulation of Iba1^{+} cells in LPC-induced lesions in WT and *Irf5*$^{-/-}$ mice, 14 days after the injection. Scale bar = 100 µm. Histogram shows the area of demyelinated WM in these animals. ***(C)*** Analysis of SMI32 in LPC-induced lesions in WT and *Irf5*$^{-/-}$ mice. The histogram shows the area positive for this marker in the lesions of both groups of mice. Scale bar = 100 µm. ***(D)*** Assessment of total (Olig2) and mature (CC1) oligodendrocyte populations in LPC-induced lesions in WT and *Irf5*$^{-/-}$ mice. Scale bar = 50 µm. Histograms show the number of both populations in the lesions, as well as the proportion of mature oligodendrocytes in relation to the total Olig2^{+} cells. Data are presented as means ± SEM. n = 4 WT and 5 *Irf5*$^{-/-}$ mice. *p < 0.05.

To further check oligodendrocyte migration, we analyzed the distribution of these cells in the LPC-induced demyelinating lesions. For that, we quantified the lineal distribution pattern of Olig2 and MBP immunoreactivity from the center of the lesion towards an equal distance in the perilesional, non-damaged tissue (Fig. 21A). The graphs show the distribution of the fluorescence signals throughout the lesion and the non-lesioned white matter. Lesion area and border (dash line) were defined by the drop in MBP immunoreactivity (Fig. 21C). Interestingly, $Olig2^{+}$ cells were located in the lesion core in WT mice, while oligodendrocytes remained at the rim of the lesion and did not migrate into the lesion core in *Irf5*$^{-/-}$ mice (Fig. 21C). Similarly, reactive astrocytes and hyaluronic acid (HA) forming the glial scar accumulated at the lesion border in *Irf5*$^{-/-}$ mice, but not inside the lesion as in WT mice (Fig. 21B, C), a fact that could be determinant for the observed failure in OPC migration. The glial scar could potentially act as a physical barrier for proper cell motility.

Altogether, the data obtained in both models (EAE and LPC-induced demyelinating lesions), demonstrated that *Irf5* has an essential role in remyelination and point to a deficit in myelin phagocytosis or degradation as one of the mechanisms for the exacerbated damage observed in IRF5-deficient mice.

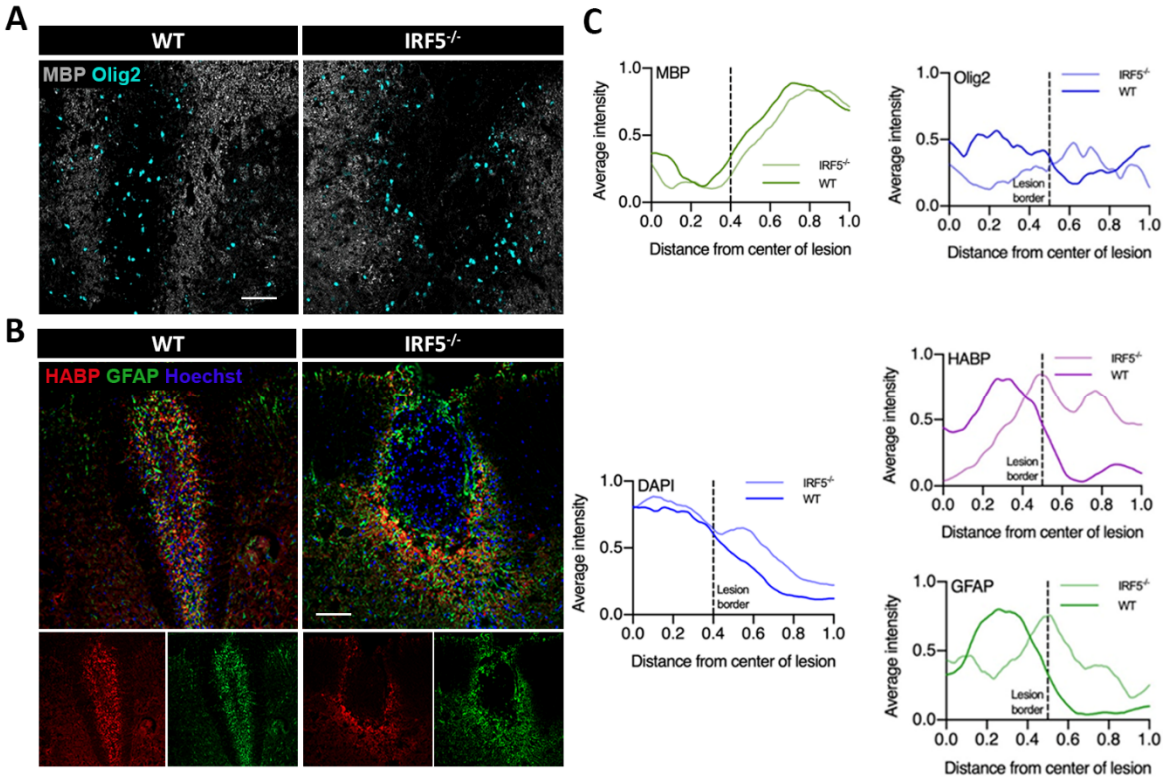

Figure 21. Histological analysis of LPC-induced lesions' components, at 14 dpi. ***(A)*** Representative confocal images showing Olig2 (oligodendroglial lineage) and MBP (myelin) stainings, the latter delineating the lesion. Note that oligodendrocytes are successfully recruited into the lesion core only in WT mice. ***(B)*** Representative images showing GFAP (astrocytes) and HABP (hyaluronic acid) staining in in LPC-induced lesions, at 14 dpi. ***(C)*** Graphs representing the distribution of MBP and Olig2 fluorescence intensity (top) as well as DAPI, GFAP and HABP (bottom), in an area comprising both lesioned and non-lesioned WM. Quantification of fluorescence intensity along radial profiles obtained from images as in left panel. Fluorescence intensity was averaged between profiles and normalized to allow comparisons. Distance was normalized likewise. After manual ROI creation to delineate the lesions, profiles were automatically drawn with a fixed width (250 px) and length (1 diameter of lesion ROI). Scale bars = 75 µm.

IRF5 deficiency leads to alterations in microglial transcriptome

In order to study the specific processes that are altered in *Irf5*$^{-/-}$ microglia leading to impaired phagocytosis, we performed bulk RNA-sequencing in FACS-sorted microglia, isolated from the spinal cord of control WT and *Irf5*$^{-/-}$ mice, as well as of mice at EAE chronic phase (Fig. 22A). Microglia were identified as the Cd11b^{+} CD45^{low} Ly6C^{-} population (see gating strategy in Fig. 22B).

As expected, EAE induction resulted in huge differences in gene expressions in comparison to control conditions, both in WT and *Irf5*$^{-/-}$ mice (Fig. 22C). Interestingly, only half of the differentially expressed genes (DEGs) for control – EAE comparisons were shared between

the different genotypes, while a part of the responses to EAE immunization was specific of each genotype (Fig. 22C). However, until now, we have not detected clear pathways differentially regulated in EAE in WT vs *Irf5*$^{-/-}$ mice. Moreover, we found a myriad of DEGs in control conditions between both genotypes (Fig. 22C, D). These contradictory results are probably due to a masking effect of the animal model, whose strong inflammatory responses can vastly alter the mice transcriptome. Nevertheless, we first decided to focus on control conditions, given the substantial amount of identified DEGs.

The specific DEGs between control experimental groups were clustered in a genotype-dependent way (Fig. 22E). A gene ontology (GO) enrichment analysis was performed on these conditions, and this GO analysis revealed that *Irf5*$^{-/-}$ microglia upregulated genes associated with specific immune responses (e.g., "Metal sequestration by antimicrobial proteins", "Viral process") as well as to DNA damage and related mechanisms ("Regulation of DNA damage", "Cell cycle" or "Response to ionizing radiation") (Fig. 22F; red annotations). While the former enriched GO could be expected with regard to the known role of IRF5 in immunity, the latter is probably related to the DNA alteration suffered by *Irf5*$^{-/-}$ cells due to the knock-out machinery. Conversely, microglia with IRF5 deficiency strongly downregulated genes associated with GTPases signaling ("Small GTPase mediated signaling", "CDC42 GTPase"), as well as other genes linked to immune responses ("Insulin signaling pathway"), lipid metabolism ("Phosphatidylinositol biosynthesis, "Lipoprotein metabolism" or "LDL clearance", among others), phagocytic capacity ("Endocytosis" or "Fc-gamma R-mediated phagocytosis", not shown) and other metabolic processes (Fig. 22F; green annotations). These data suggest a role of the IRF5 transcription factor in modulating not only immune inflammatory responses, but also intracellular metabolism and signaling in microglia, with a possible impact on myelin clearance, a fact that could have potential influence on demyelination resolution.

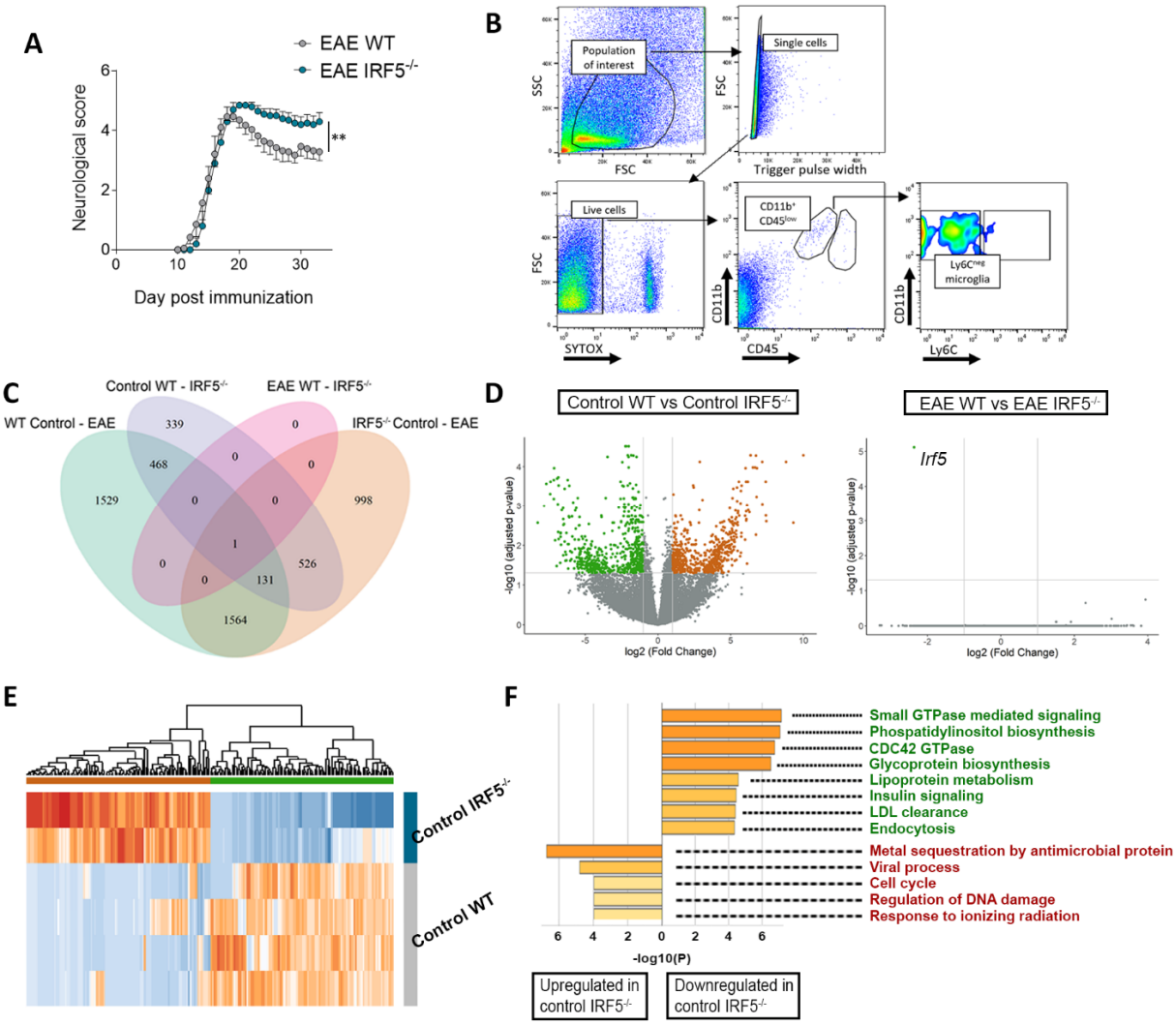

Figure 22. Transcriptomic analysis of WT and *Irf5*$^{-/-}$ microglia in control and EAE conditions. ***(A)*** Neurological score of WT and *Irf5*$^{-/-}$ mice until the point of euthanasia for subsequent RNA-sequencing analysis of microglial transcriptome (n = 5 per experimental group). ***(B)*** Flow cytometry gating strategy for isolation of microglia from the spinal cord of WT and *Irf5*$^{-/-}$ mice. ***(C)*** Venn diagram showing the DEGs for every comparison and their overlapping. ***(D)*** Volcano plots depicting gene expression comparisons between control WT and control *Irf5*$^{-/-}$ microglia (left) and between EAE WT and EAE *Irf5*$^{-/-}$ microglia (right). Each dot represents an individual gene. Non-significant genes are marked in gray while significant ones are marked in color. ***(E)*** Heatmap of DEGs between control WT and control *Irf5*$^{-/-}$ microglia, showing in green and orange the main clustering identified between the conditions. ***(F)*** GO enrichment analysis of the DEGs between control WT and control *Irf5*$^{-/-}$ microglia, showing the top GOs enriched in both conditions. Green annotations are downregulated in control *Irf5*$^{-/-}$ microglia in comparison to WT microglia, and red annotations are upregulated in *Irf5*$^{-/-}$ microglia.

Irf5$^{-/-}$ microglia show impair motility *in vitro* but does not affect response to demyelination

Next, we decided to validate signaling pathways altered in *Irf5*$^{-/-}$ microglia. With regard to the GTPase signaling, the Rho family of small GTPases (including Rho, Rac and Cdc42) critically regulates the dynamic organization of actin cytoskeleton and subsequently, cell motility. Indeed, microglial Cdc42 is critical for microglial migration (Barcia et al., 2012). Although no previous data have linked IRF5 to microglia motility, IRF8 is necessary for microglia migration towards the epicenter of traumatic spinal cord lesions (Kobayakawa et al., 2019) and its deficit exacerbates axonal damage and prevents remyelination after SCI. We then tested whether, similarly, IRF5 deficiency could affect microglia migratory capacity. We performed wound healing assays with WT and *Irf5*$^{-/-}$ microglia *in vitro*, and observed that, after 24 hours, IRF5-deficient microglia repopulated the scratched area less than WT microglia (Fig. 23A), suggesting that alterations in Cdc42 GTPases signaling in *Irf5*$^{-/-}$ microglia actually lead to abnormal microglial motility.

To further check the impact of IRF5 deficiency in microglial migration into lesions, we analyzed LPC-induced demyelination lesions at 4 days post-injection, a timepoint coincident with microglia/macrophage migration towards the lesions (Fig. 23B). At this stage, we did not detect differences in the extent of demyelinated area between WT and *Irf5*$^{-/-}$ mice (Fig. 23C), but we did observe non-significantly higher myelin debris accumulation in *Irf5*$^{-/-}$ mice in comparison to WT mice, which were practically devoid of this debris (Fig. 23C). This latter result is in accordance with the observations previously described in EAE lesions. Therefore, at 4 dpi *Irf5*$^{-/-}$ animals already showed some signs pointing out to a failure in myelin clearance and subsequent remyelination. Regarding microglia migration, we did not observe an affection in Iba1^{+} cells number into the lesions of *Irf5*$^{-/-}$ mice, as assessed by IHC. Indeed, *Irf5*$^{-/-}$ mice showed more Iba1 immunoreactivity inside the lesion than WT mice (Fig. 23C). In accordance, we did not detect any failure of microglia/macrophage migration into EAE lesions Altogether, these data suggest that, although *Irf5*$^{-/-}$ microglia showed some impairments in motility *in vitro*, this deficit does not seem to be responsible for the failure in remyelination in EAE and LPC lesions.

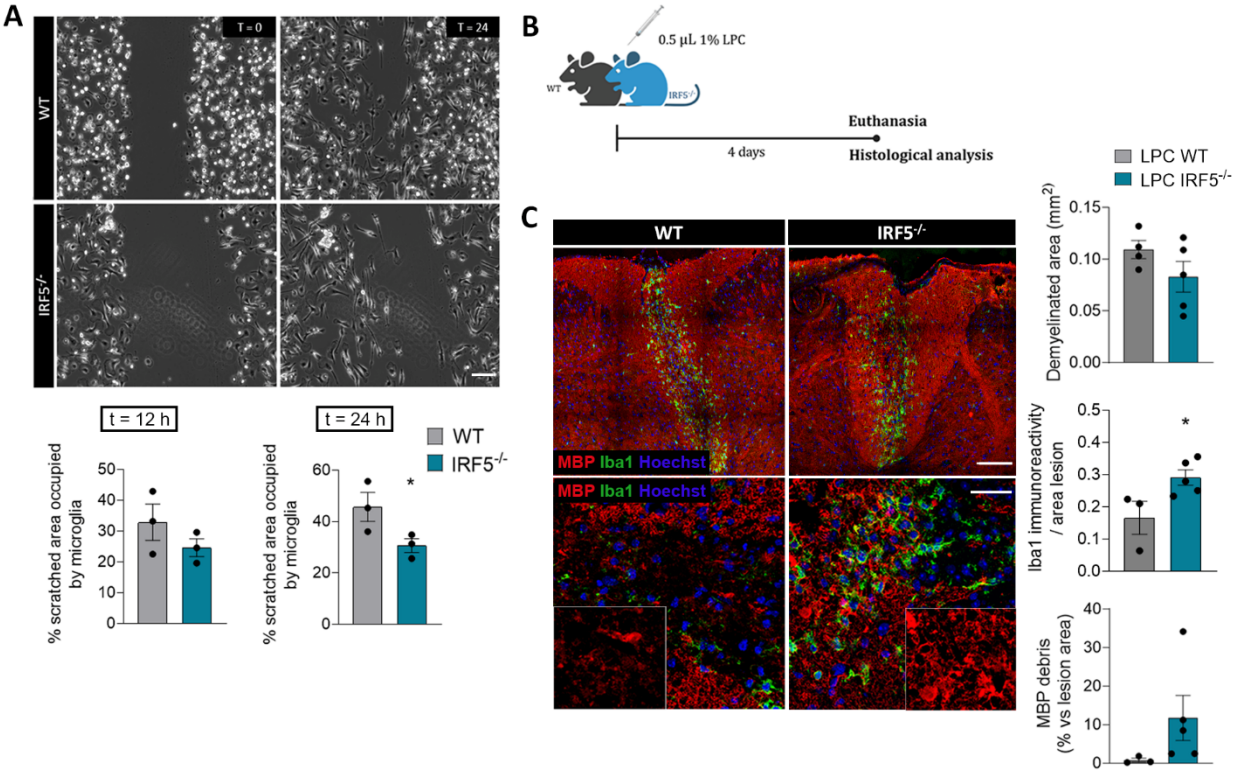

Figure 23. *Irf5*$^{-/-}$ microglia showed altered motility *in vitro* but not after demyelination. ***(A)*** Representative images of wound healing assay on WT and *Irf5*$^{-/-}$ microglia. Scratch was made on plate bottom with a 200 µL pipette tip. Scale bar = 10 µm. Histograms show the % of the initially empty scratched area occupied by microglial cells after 12 and 24 hours. ***(B)*** Scheme showing the experimental design for the analysis of remyelination after LPC-induced demyelination, both in WT and *Irf5*$^{-/-}$ mice, at 4 dpi. ***(C)*** (Top) Representative images of Iba1 and MBP immunostaining in LPC-induced lesions at 4 dpi, in WT and *Irf5*$^{-/-}$ mice. Histograms show the extent of the lesions, defined by both the absence of MBP staining and accumulation of myelin debris, as well as Iba1 immunoreactivity inside the lesion, normalized to injured area. Scale bar =100 µm. (Bottom) Detailed view of myelin debris accumulation in these lesions. Histogram shows the percentage of lesion occupied by myelin debris. Scale bar = 30 µm. Data are presented as means ± SEM. *p < 0.05.

IRF5 deficiency provokes impaired lipid homeostasis in microglia

Other pathways downregulated in *Irf5*$^{-/-}$ microglia involved lipid metabolism, endocytosis and LDL clearance. In particular, regarding the latter, we detected several *Irf5*-dependent genes involved in different stages of lipid uptake and processing: lipid endocytosis (*Ldlr*), egress of cholesterol from lysosomes (*Npc1*) and efflux of cholesterol out of the cell, in order to eliminate the intracellular excess (*Hdlbp*). Moreover, genes implicated in the regulation of cellular lipid homeostasis were also downregulated (*Srebf1* and *Srebf2*). These latter genes encode transcription factors that regulate lipid homeostasis (Rong et al., 2017) and favour the generation of sterols that serve as LXR ligand and promote regenerative actions

(for more details, see scheme and table in Fig. 24A). Thus, intracellular transport and processing of cholesterol, a main component of myelin, could be defective in *Irf5*$^{-/-}$ microglia.

In order to test the hypothesis that lipid degradation is impaired in IRF5-deficient cells, we challenged both WT and *Irf5*$^{-/-}$ microglia with an excess of myelin (25 μg/mL) and let the cells metabolize the lipids for 48 hours. Of note, myelin was not removed during this timelapse. Cells were collected through scraping, and lipids were isolated from the samples using a common method (Bligh and Dyer, 1959) and analyzed by HPLC-MS (Fig. 24B). We detected clear differences in the processing of myelin between WT and *Irf5*$^{-/-}$ microglia; for instance, we observed a decrease in the concentration of diverse phospholipid families like plasmalogens or phosphatidylinositols in IRF5-deficient microglia (PIs; Fig. 24C). On the other hand, we found a significant increase in the concentration of all the cholesterol ester (CE) species detected in *Irf5*$^{-/-}$ microglia in comparison to WT cells (Fig. 24D). In contrast, no change was observed in total free cholesterol between WT and *Irf5*$^{-/-}$ microglia (data not shown). All these results suggest that IRF5 deficiency provokes impair lipid processing in microglia, and this lipid dysregulation could be behind the failure in remyelination.

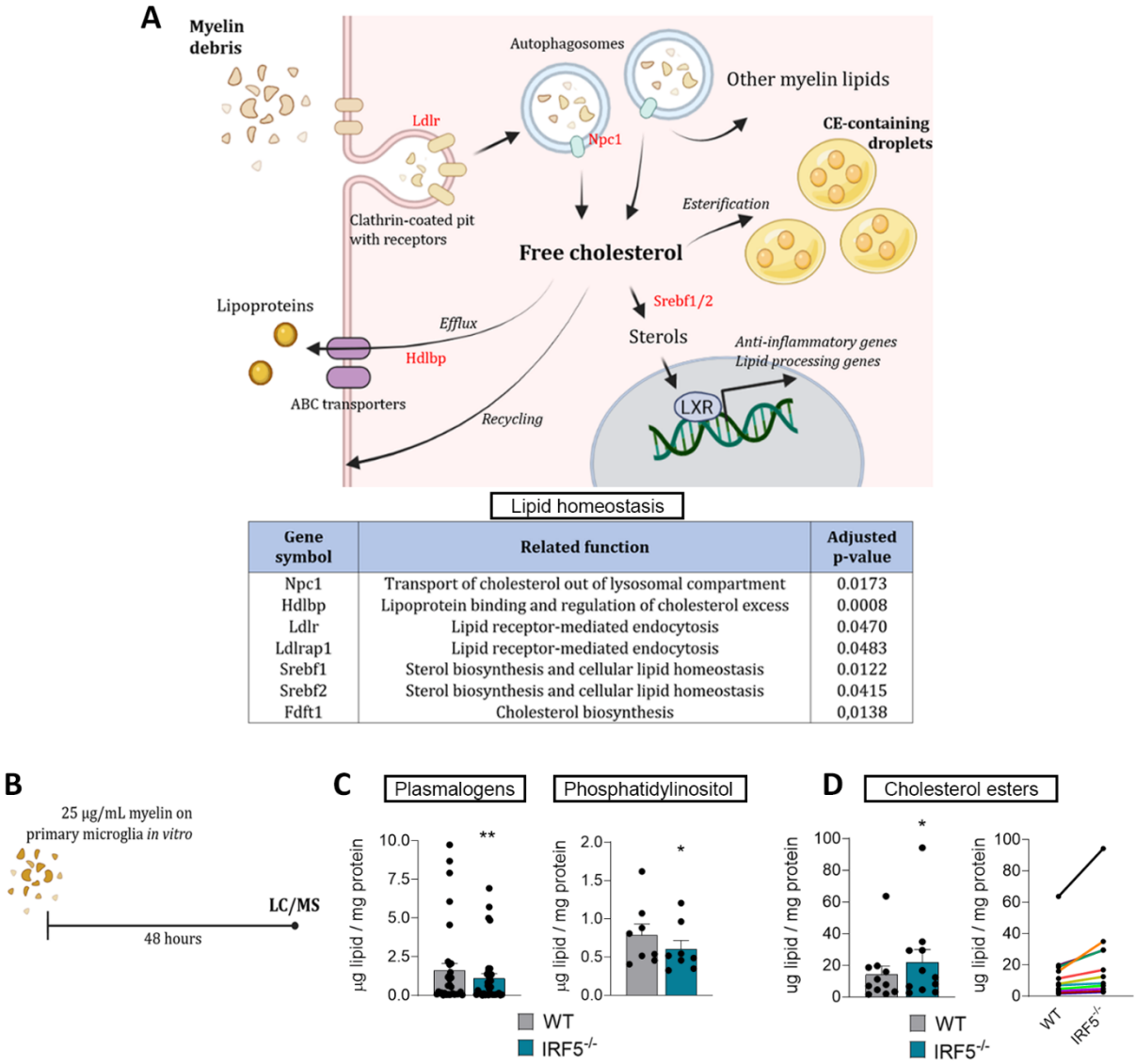

Lipid homeostasis

Gene symbol	Related function	Adjusted p-value
Npc1	Transport of cholesterol out of lysosomal compartment	0.0173
Hdlbp	Lipoprotein binding and regulation of cholesterol excess	0.0008
Ldlr	Lipid receptor-mediated endocytosis	0.0470
Ldlrap1	Lipid receptor-mediated endocytosis	0.0483
Srebf1	Sterol biosynthesis and cellular lipid homeostasis	0.0122
Srebf2	Sterol biosynthesis and cellular lipid homeostasis	0.0415
Fdft1	Cholesterol biosynthesis	0,0138

Figure 24. Altered lipid homeostasis and metabolism in *Irf5*$^{-/-}$ microglia. ***(A)*** Scheme showing normal lipid processing after myelin debris clearance. In red, genes downregulated in *Irf5*$^{-/-}$ microglia in comparison to WT microglia, as identified by bulk RNA-sequencing, placed near to their related mechanisms. The table at the bottom specifies these genes, as well as their attributed function and the adjusted p-value obtained through statistics. ***(B)*** Experimental strategy for LC/MS analysis of lipid processing in WT and *Irf5*$^{-/-}$ microglia *in vitro*, after challenge with 25 µg/mL myelin for 48 hours. ***(C)*** Histograms showing the concentration of different plasmalogens (left) and PIs (right) in WT and *Irf5*$^{-/-}$ microglia after 48 hours of myelin challenge. ***(D)*** Histograms showing the concentration of different cholesterol esters in WT and *Irf5*$^{-/-}$ microglia after 48 hours of myelin challenge. Each point in these graphs represent a single lipid species analyzed by HPLC-MS. Data are presented as means for every lipid species from 4 different experiments. *p < 0.05, ** p < 0.01.

IRF5 deficiency leads to altered lipid clearance and metabolism after demyelination

Toxic overload of cholesterol drives the formation of foamy macrophages and maladaptive immune response in arteriosclerosis (Chistiakov et al., 2016). Similarly, myelin debris accumulation within lysosomes induces lipid droplets and needle-shaped cholesterol crystals formation in aged microglia, typical hallmarks of a toxic cholesterol overloading that would in turn limit the remyelinating, pro-regenerative processes (Cantuti-Castelvetri et al., 2018). We next performed matrix-assisted laser desorption/ionization (MALDI)-imaging mass spectrometry as well as immunohistochemistry to characterize lipid processing *in vivo* in LPC lesions.

Mass spectrometry imaging is a method that combines microscopic imaging analysis to mass spectrometry to interrogate surfaces, thereby obtaining spatial distributions, of lipids in our case, by mass-to-charge (m/z) ratios. After MALDI imaging, tissue was immunolabeled using antibodies to MBP, Iba1 and iNOS to delineate demyelinated lesions and define pro-inflammatory microglia/macrophages. The MALDI spectra and their associated lipid signatures related to the diverse regions of the spinal cord were segmented using a *k*-means clustering method (Fig. 25A). Of note, the uninjured tissue displayed a very different segmentation pattern between the white and gray matter. Within this segmentation model, we also clearly identified distinct clustering patterns inside the demyelinated lesions. MBP immunostaining absence inside the lesion showed a clear correlation with MALDI segmentation profiles, demonstrating that demyelinated lesions present a different lipid signature from non-damaged white matter (Fig. 25A). Importantly, lipid clustering also identified another region with a characteristic lipid signature in the rim of the lesion (peri-lesion). This cluster overlapped with $iNOS^+$ $Iba1^+$ microglia/macrophages, as revealed by immunohistochemistry, and with the presence of signs of myelin damage, probably indicative of active process of demyelination. Both MALDI imaging and immunohistochemistry analysis showed a higher area corresponding to this lipid cluster and a higher accumulation of $iNOS^+$ $Iba1^+$ microglia/macrophages in the periphery of the lesions in *Irf5*$^{-/-}$ mice (Fig. 25A).

Therefore, we performed the comparison of lipid signatures between WT and *Irf5*$^{-/-}$ mice in the clusters identified as lesion core, peri-lesion and normal white matter. A clear and

significant decrease of the major ceramides and plasmalogen PE species was consistently observed inside the lesion core in comparison to the normal white matter, both in WT and *Irf5*$^{-/-}$ mice (Fig. 25B). Aside from cholesterol, that could not be detected by our MALDI setup, ceramides and plasmalogens are highly enriched in myelin (Poitelon et al., 2020). Galactosylceramides (cerebrosides) represent bona fide myelin signature lipids. In fact, the concentration of cerebroside in the brain has been shown to be directly proportional to the amount of myelin present (Norton and Poduslo, 1973). Moreover, myelin is characterized by a high content of plasmalogen PE containing dominant oleic acid (Aggarwal et al., 2011). With this in mind, the reduction of these myelin signature lipids in the lesion core could be explained by the process of demyelination. In the lesion core, we only detected small changes in lipid composition between WT and *Irf5*$^{-/-}$ mice (data not shown). However, when we compared the lipid signature in the peri-lesions, we detected a significant reduction of plasmalogens in *Irf5*$^{-/-}$ mice (Fig. 25C). This is accordance to the significant reduction of these lipids detected in *Irf5*$^{-/-}$ microglia *in vitro* upon exposure to myelin challenge (Fig. 24C). Further experiments are needed to understand the reason and the meaning of plasmalogen PE species alteration in *Irf5*$^{-/-}$ mice.

We further analyzed lipids distribution in LPC lesions using Oil Red O^{+} (ORO) particles. ORO stains neutral lipids, normally associated with lipid droplets. We observed an increase in the number and size of ORO^{+} particles accumulated in the lesions of *Irf5*$^{-/-}$ mice (Fig. 26A), which might be associated with the previously described alteration of myelin intracellular processing. As CEs are normally the form in which cholesterol is stored in LD, this result is in line with our previous finding showing an increase in CE in *Irf5*$^{-/-}$ microglia, after maintained myelin challenge (Fig. 24D). Given that accumulation of intracellular cholesterol, the main constituent of myelin (Poitelon et al., 2020), is linked to an abnormal, pathogenic formation of cholesterol crystals in microglia, we then analyzed whether the accumulation of ORO^{+} particles could be accompanied by an increase of these crystals. Taking advantage of reflection microscopy, we observed an increase in the crystals' deposition in *Irf5*$^{-/-}$ lesions (Fig. 26B). This aberrant aggregation of cholesterol is a probable consequence of the alteration in lipid homeostasis in IRF5-deficient microglia, and can provoke further defects in myelin phagocytosis, as previously stated.

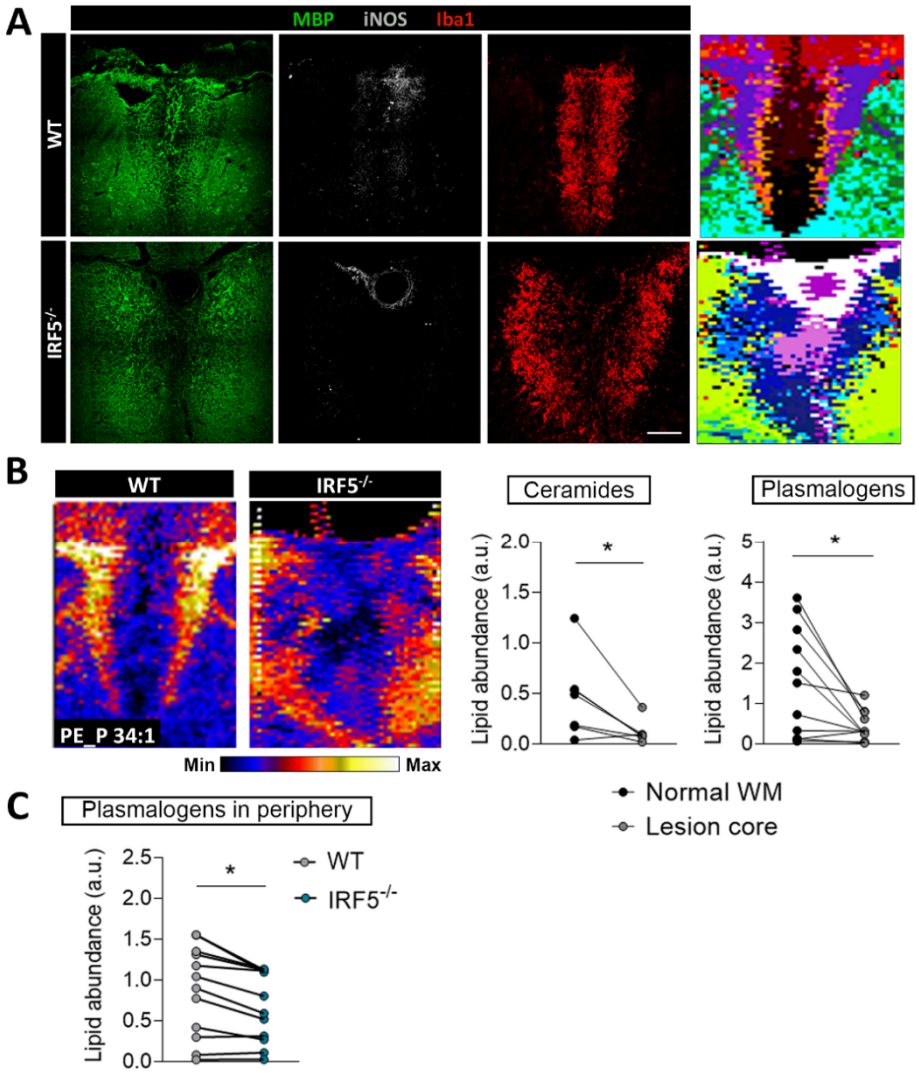

Figure 25. MALDI-IMS profiling of lipids in LPC-induced demyelination. ***(A)*** (Left) Representative immunohistochemical images of LPC-induced lesions at 14 dpi, in WT and *Irf5*$^{-/-}$ mice, showing MBP staining as well as Iba1^{+} and iNOS^{+} microglia/macrophages. (Right) Representative lipid segmentation obtained of these lesions, following *k*-means clustering method. Of note, there are different lipid profiles corresponding to the lesion core, the peri-lesion and the normal WM. ***(B)*** Representative MALDI mass spectrometry imaging (MSI) maps of a major plasmalogen (PE plasmalogen 34:1), in LPC-induced lesions at 14 dpi, both in WT and *Irf5*$^{-/-}$ mice. Histograms shows the difference of abundance of different ceramides and plasmalogens in the normal WM and the lesion core. ***(C)*** Abundance of different plasmalogens in the peri-lesion of WT and *Irf5*$^{-/-}$ mice, in LPC lesions at 14 dpi. Each point in the graphs represent a single lipid species analyzed by MALDI. Data are presented as means for every lipid species from 5 different mice. *p < 0.05

Lastly, we aimed to quantify the accumulation of oxidized phosphatidylcholines in these lesions, as these lipid species have been identified as potential mediators of the neurodegeneration happening in MS (Dong et al., 2021b). However, we did not observe significant differences in the number of E06^{+} particles in the lesions, being E06 a specific marker for these species (Fig. 26C). All these results suggest that IRF5 can have a role

modulating myelin clearance and subsequent cholesterol metabolism after demyelination, and its deficiency leads to accumulation of extracellular debris as well as intracellular LDs and cholesterol crystals. The results emphasize a potential role of IRF5 in the regulation not only of lipid metabolism, but also its intracellular processing. Moreover, this function can be, at least in part, attributed to microglia in response to demyelinating lesions.

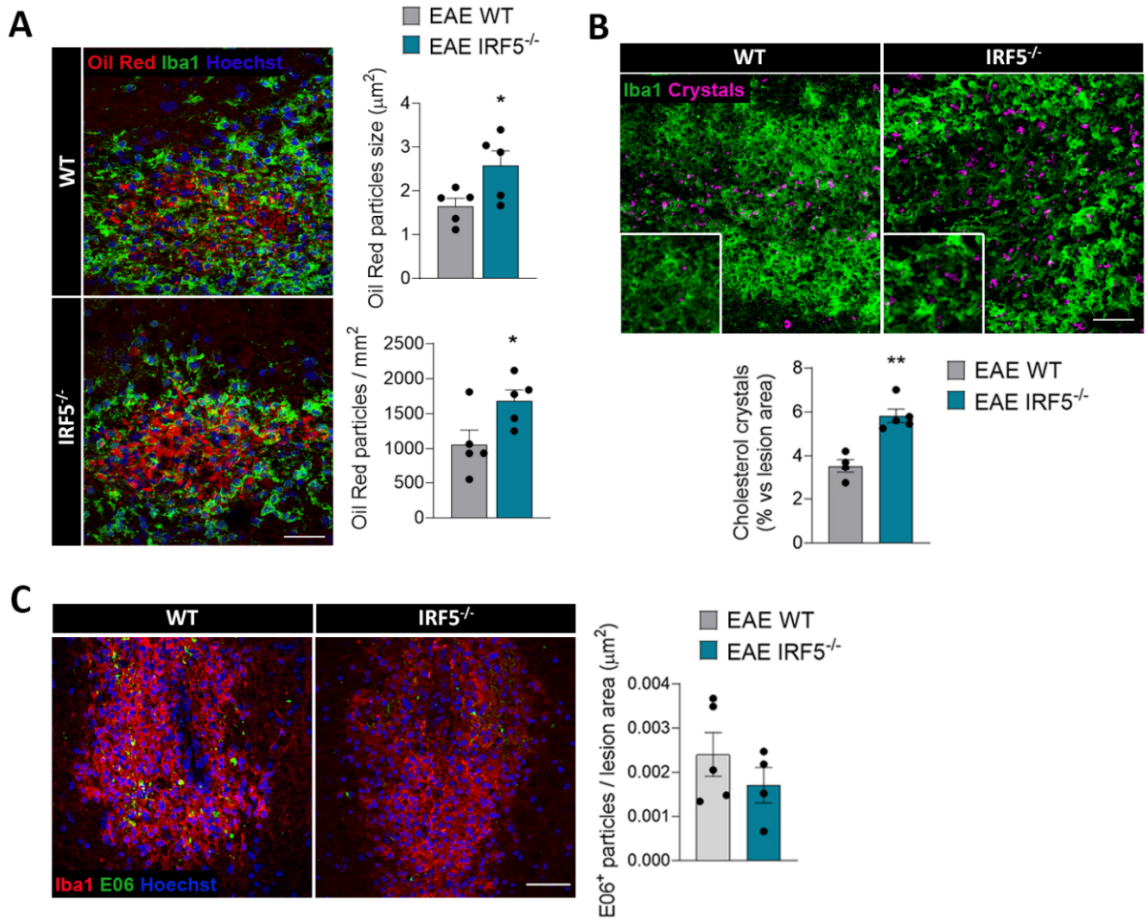

Figure 26. Altered lipid phagocytosis and processing after demyelination in *Irf5*$^{-/-}$ mice. *(B)* Staining of Oil Red O in LPC-induced lesions (14 dpi) in WT and *Irf5*$^{-/-}$ mice. Histograms show the number and size of ORO^{+} particles. Scale bar = 25 µm. ***(C)*** Representative images of cholesterol crystals Iba1^{+} microglia/macrophages in LPC-induced lesions (14 dpi), in both WT and *Irf5*$^{-/-}$ mice. Scale bar = = 25 µm. Histogram shows the number of crystals in relation to the lesioned area. (***D)*** Representative images of oxidized phosphatidylcholines (E06) and Iba1+ microglia/macrophages in LPC-induced lesions (14 dpi), in both WT and *Irf5*$^{-/-}$ mice. Histogram shows the number of E06^{+} particles normalized to the lesion area. Scale bar = 50 µm. Data are presented as mean ± SEM (n= 4-5). *p < 0.05, **p<0.01.

To sum up, the results described in this section define a role of IRF5 transcription factor modulating myelin debris clearance. Irf5-/- microglia/macrophage accumulated excessive myelin debris, which triggered cholesterol crystal formation and lipid droplets accumulation, thereby inducing a maladaptive immune response that blocks tissue remyelination.

Part III. Role of mitochondrial dynamics in microglial activation and metabolic switch

Microglia can adapt their metabolism in response to extracellular stimuli, by remodeling their sources for energy generation. The field of immunometabolism, which comprises this kind of processes, has been extensively investigated due the potential of targeting specific metabolic pathways as therapy for diverse pathologies. However, the specifics behind this metabolic switch are not entirely elucidated. Here, we have analyzed metabolic reprogramming of microglia, focusing on the functional state of mitochondria during this process and the role of mitochondrial dynamics in it. In addition, in order to potentially define metabolic reprogramming of microglia throughout the course of EAE, we have optimized magnetic-activated cell sorting (MACS)-sorted microglia serum-free cultures and characterized their metabolic reprogramming capacity.

Metabolic reprogramming in microglia is not associated with mitochondrial damage

First, to test whether microglia metabolic reprogramming from OXPHOS to glycolysis upon pro-inflammatory challenge is associated with mitochondrial damage or dysfunction, we set up an *in vitro* protocol to study the metabolic switch, and we measured real time OCR and ECAR as indicative of mitochondrial respiration and glycolysis, respectively. Cells treated with classical pro-inflammatory factors (LPS and IFN-γ) for 24 hours showed a flat profile regarding OXPHOS, and all the parameters (basal OCR, ATP-linked respiration, and spare respiratory capacity) related to this molecular process were practically abolished (Fig. 27A), as previously described (Orihuela et al., 2016). This outcome points out to a robust metabolic shift from OXPHOS to glycolysis to rapidly obtain energy, upon inflammatory stimulation.

Conversely, microglia treated with anti-inflammatory factors (IL-4 and IL-13) showed a significant increase in basal OCR, spare respiratory capacity, and ATP-linked respiration, suggesting that mitochondrial OXPHOS was boosted (Fig. 27A). In contrast, ECAR measurement showed an increase in basal glycolysis in both pro- and anti-inflammatory microglia (Fig. 27B), suggesting that activated microglia have higher energetic demands independently of their phenotype. Moreover, inhibition of mitochondrial F_0F_1-ATP synthase

with oligomycin, provoking a blockage of OXPHOS, increased the glycolytic rate in control and anti-inflammatory microglia but not in pro-inflammatory microglia (Fig. 27B). Finally, the basal ratio between mitochondrial OCR and the glycoPER, the latter being specific for the release of protons to the extracellular medium during glycolysis, was significantly diminished in pro-inflammatory microglia (Fig. 27C). These results further support the idea that pro-inflammatory microglia metabolism relies exclusively on glycolysis.

In other immune cells, such as dendritic cells, the metabolic switch to glycolysis occurs within minutes after TLR activation with LPS (Everts et al., 2014). However, acute treatment with LPS + IFN-γ did not induce any change in microglial OCR-associated parameters (Fig. 27D). Further time-course analysis demonstrated that the metabolic switch caused by these pro-inflammatory factors began after approximately 2 h, was clear after 6 h, and completed with a 24-hour-treatment (Fig. 27E).

Because OXPHOS takes place in the mitochondrial inner membrane and is determinant for proton flux and ΔΨm maintenance, we hypothesized that the arrest of mitochondrial respiration caused by pro-inflammatory stimuli could induce a collapse in ΔΨm. To check whether ΔΨm was altered in microglia under this condition, we performed live cell imaging of Rh123 fluorescent dye under quenching conditions (Corona and Duchen, 2014). The addition of the mitochondrial OXPHOS uncoupler FCCP to the primary microglia provoked the release of Rh123 from the mitochondria. This consequently increased Rh123 cytoplasmic fluorescence 2-fold over baseline (100%) both in control microglia and in microglia treated with LPS + IFN-γ (Fig. 28A), indicating that basal mitochondrial potential is maintained in pro-inflammatory microglia, despite the arrest of OXPHOS.

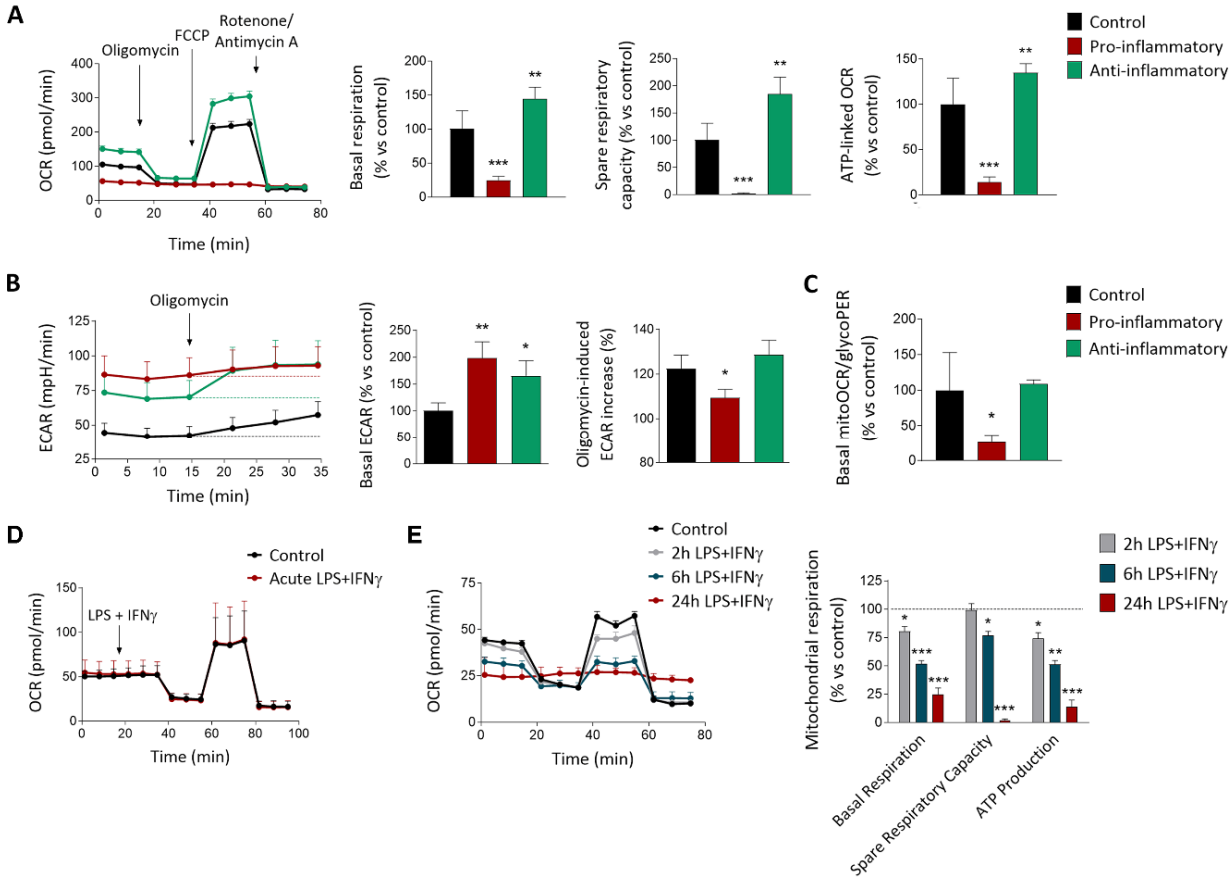

Figure 27. Robust metabolic reprogramming to glycolysis after 24 hours of pro-inflammatory stimulation in microglia. ***(A)*** Representative experiment of OCR analysis in control microglia and in microglia after 24 hours of pro-inflammatory (LPS + IFN-γ) and anti-inflammatory (IL-4 + IL-13) stimulations. Histograms show metabolic parameters obtained by the analysis of this metabolic profile compared to control cells (n = 7 experiments). ***(B)*** ECAR measurement of control microglia and microglia after 24-hour incubation with pro- and anti-inflammatory factors (n = 7). Histograms show basal ECAR and the increase provoked by the acute treatment with oligomycin, relative to control cells. One-way ANOVA followed by Bonferroni post-hoc test. ***(C)*** Ratio between basal OCR and basal glycoPER in control and both pro-inflammatory and anti-inflammatory microglia. These parameters were obtained using the XF Glycolytic Rate Assay test (n = 3). ***(D)*** Metabolic profile of microglia after acute treatment with LPS and IFNγ. This treatment was added after the basal measurement of OCR and prior to the addition of oligomycin (n = 3). ***(E)*** Metabolic profile of microglia treated during different time lapses with LPS and IFNγ. Histograms shows the metabolic parameters compared to control cells (n = 3). Data are presented as means ± SEM. *p < 0.05, ***p < 0.001.

To further assess mitochondrial integrity, we measured resting $[Ca^{2+}]_{mit}$ using Fluo-4. We recorded $[Ca^{2+}]_{cyt}$ upon addition of FCCP in the absence of extracellular Ca^{2+}, which is indicative for $[Ca^{2+}]_{mit}$ (Brocard et al., 2001). Again, we observed no significant differences in the release of mitochondrial calcium from the mitochondrial matrix to the cytosol after the addition of FCCP (Fig. 28B). Moreover, as OXPHOS is commonly accompanied by ROS production, we tested whether there were differences in this process. Pro-inflammatory stimulation of microglia induced a significant increase in ROS production, as revealed with

the dichlorofluorescein diacetate dye (DCFDA; Invitrogen) despite the blockage of OXPHOS (Fig. 28C). All these results show that pro-inflammatory activation and its subsequent lack of OXPHOS activity in microglia are neither cause nor consequence of any mitochondrial dysfunction or alteration in their ΔΨm, although it generates oxidative stress.

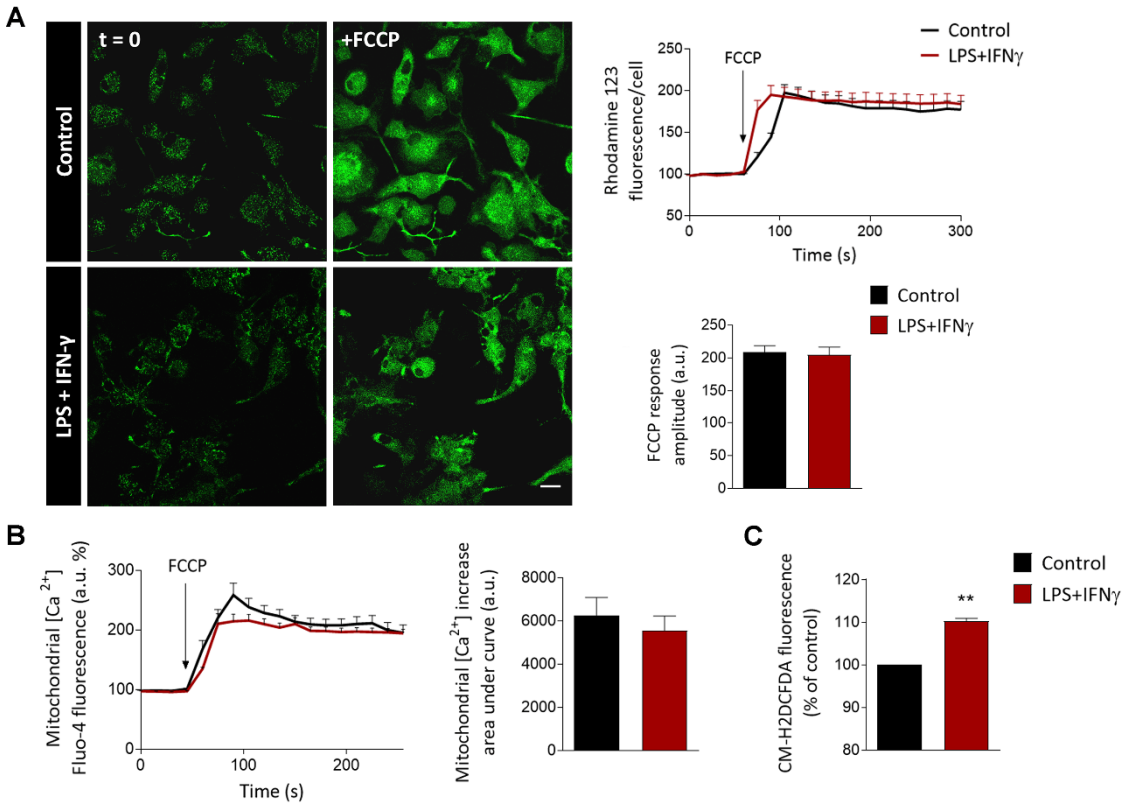

Figure 28. Mitochondria maintain its functionality despite the lack of OXHOS upon pro-inflammatory stimulation of microglia. ***(A)*** Measurement of mitochondrial potential, represented as the increase in cytoplasmic Rh123 fluorescence measured after acute exposure to FCCP in control and LPS+IFNγ treated microglia (n = 50-75 cells from three independent experiments). ***(B)*** Measurement of mitochondrial-specific calcium represented as the increase in cytoplasmic Fluo-4 fluorescence in a Ca2+-free medium, after exposure to FCCP, in control and LPS+IFNγ treated cells (n = 50-75 cells from three independent experiments). ***(C)*** Reactive oxygen species quantification in control and pro-inflammatory cells (n = 3 experiments performed in triplicate). Data are presented as means ± SEM. *p < 0.05, ***p < 0.001.

Maintaining ΔΨm is essential to prevent the release of pro-apoptotic factors into the cytosol and subsequent cell death. Indeed, despite the blockage of OXPHOS, LPS + IFN-γ stimulation did not induce significant microglia cell death in comparison to the control microglia (Fig. 29A). We hypothesized that ΔΨm could be maintained in cells with inhibited respiration through the reverse operation of F_0F_1-ATP synthase and the adenine nucleotide translocase (ANT), which pumps H^+ out of the matrix (Chinopoulos, 2011). To test this hypothesis, we

analyzed the impact of the F_0F_1-ATP synthase and ANT in cell viability and ΔΨm. Indeed, treatment of LPS + IFN-γ stimulated microglia with oligomycin, a F_0F_1-ATP synthase inhibitor, induced a significant increase in microglial cell death (Fig. 29A). In contrast, bongkrekic acid, an inhibitor of ANT (Henderson and Lardy, 1970), did not induce any changes in microglial cell death (Fig. 29A). Accordingly, a role of F_0F_1-ATP synthase in mitochondrial ΔΨm maintenance in pro-inflammatory microglia was further corroborated by live cell imaging of TMRE, a fluorescent dye that accumulates in active mitochondria. Addition of oligomycin induced a significant decrease in ΔΨm in proinflammatory microglia but not in control microglia (Fig. 29B), supporting the idea that mitochondrial integrity in active pro-inflammatory microglia depends, at least partially, on the activity of the ATP synthase.

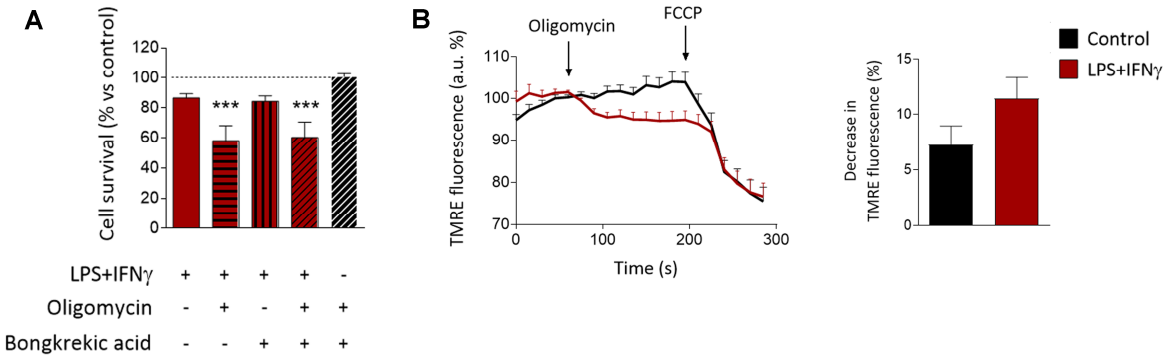

Figure 29. Involvement of F_0F_1-ATP synthase and ANT in ΔΨm maintenance upon pro-inflammatory stimulation of microglia. ***(A)*** Microglial viability after 24-hour treatment with LPS+IFNγ, oligomycin and/or bongkrekic acid, compared to control cells. One-way ANOVA followed by Bonferroni post-hoc analysis (n = 3 experiments performed in triplicate). ***(B)*** Effect of ATPase inhibitor oligomycin in mitochondrial potential of control and LPS+IFN-γ treated cells (n = 70-80 cells from three independent experiments). Data are presented as means ± SEM. ***p < 0.001.

Mitochondrial fission inhibition affects microglial activation but does not revert mitochondrial metabolic reprogramming

Previous data have showed that activation of microglia with LPS induced a transient shortening of mitochondria by fission after 2 hours. Similarly, we detected a shortening of mitochondrial length after 2 hours of LPS + IFN-γ treatment, an effect that was reverted in the presence of the mitochondrial fission inhibitor Mdivi-1 (data not shown; Montilla et al., 2021). Because microglial metabolic switch had been previously associated with mitochondrial fission, we further analyzed this hypothesis in our cultures using Mdivi-1.

First, we assessed whether the Mdivi-1 treatment would have an effect on microglia in control conditions. A 24-h treatment with Mdivi-1 (50 μM) provoked a morphological change in microglia, with a significant increase in cytoplasm circularity, indicating that Mdivi-1 treatment induces an amoeboid morphology (Fig. 30A). This characteristic can be associated with a harmful effect in the cell or, alternatively, with an activation process. However, we found no differences in cell viability (Fig. 30B) or the basal expression of pro- and anti-inflammatory markers (iNOS and MNR, respectively; Fig. 30C) in relation to control microglia.

However, Mdivi-1 reduced significantly the increased levels of iNOS in response to LPS and IFN-γ stimulation while having no effect on MNR levels (Fig. 30D). We further analyzed by qPCR the expression of different pro-inflammatory mediators. Treatment of microglia with LPS + IFN-γ induced an increase in all the proinflammatory gene expression assessed (*Ccl2*, *Il1b*, *iNOS*) with respect to control cells, but also the expression of *Arg1*, an anti-inflammatory mediator known to carry an opposite function to iNOS regarding cellular metabolism (Rath et al., 2014). The addition of Mdivi-1 significantly reduced the overexpression of all these mediators. (Fig. 30E). These results suggest that Drp1-dependent mitochondrial fission is potentially involved in microglial activation.

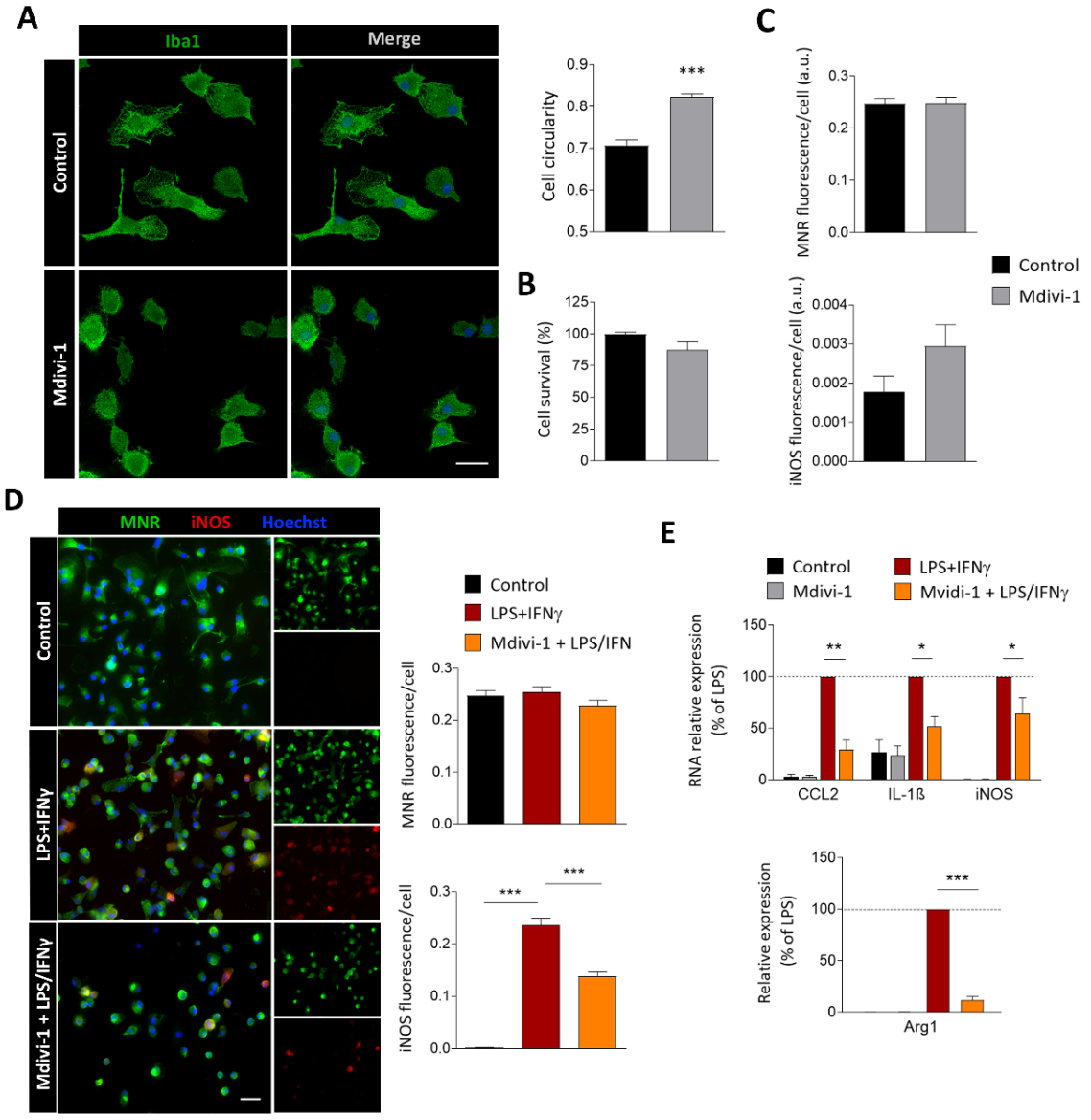

Figure 30. Mitochondrial fission inhibition reduces microglial inflammatory markers. ***(A)*** Representative images of Iba1⁺ control and Mdivi-1 treated microglia. Scale bar = 25 µm. Histogram represents the circularity of the cells (n = 200 cells from three independent experiments). ***(B)*** Microglial viability in control and Mdivi-1 cells, measured by calcein assay (n = 3 experiments performed in triplicate). ***(C)*** Expression of anti-inflammatory (MNR) and pro-inflammatory mediators (iNOS) in control and Mdivi-1 treated microglia (n = 4 independent experiments performed in duplicate). ***(D)*** Immunostaining of MNR and iNOS in control microglia and cells treated with LPS+IFNγ or Mdivi-1 and LPS+IFNγ. Scale bar = 40 µm. Histograms represent the mean fluorescence of the staining per cell (n = 4 independent experiments performed in duplicate). One-way ANOVA followed by Bonferroni post-hoc analysis. ***(E)*** qPCR analysis of pro-inflammatory (top) and an anti-inflammatory mediator (bottom) in control microglia, as well as in microglia treated with Mdivi-1, LPS+IFNγ, and Mdivi-1 + LPS+IFNγ (n = 4 experiments performed in duplicate). Data are expressed relative to the expression in LPS+IFNγ. One-way ANOVA followed by Bonferroni post-hoc analysis. Data are presented as means ± SEM. *p < 0.05, **p < 0.005, ***p < 0.001.

Next, we checked whether the impact of Mdivi-1 on microglial activation could affect microglial metabolic reprogramming capacity. Interestingly, in addition to the blockage of Drp1-dependent mitochondrial fission, Mdivi-1 provokes an acute and reversible inhibition of mitochondrial complex I in neurons (Bordt et al., 2017). To determine the direct impact of Mdivi-1 on microglial bioenergetics, we treated microglia with Mdivi-1 for 1 h and 24 h, and we measured microglial OCR. Despite a reduction in mitochondrial respiration after 1 h, the effect was transient and disappeared at 24 h (Fig. 31A, B). Next, we analyzed the impact of Mdivi-1 on the metabolic switch of pro-inflammatory microglia. The treatment with Mdivi-1 did not revert the absence of OXPHOS-related parameters in cells stimulated with LPS + IFN-γ to recover the normal bioenergetics profile (Fig. 31B). These results indicate that, although Drp1-mediated mitochondrial fission could modulate or contribute to microglia activation, it does not play an active role in the metabolic switch produced upon inflammatory paradigms.

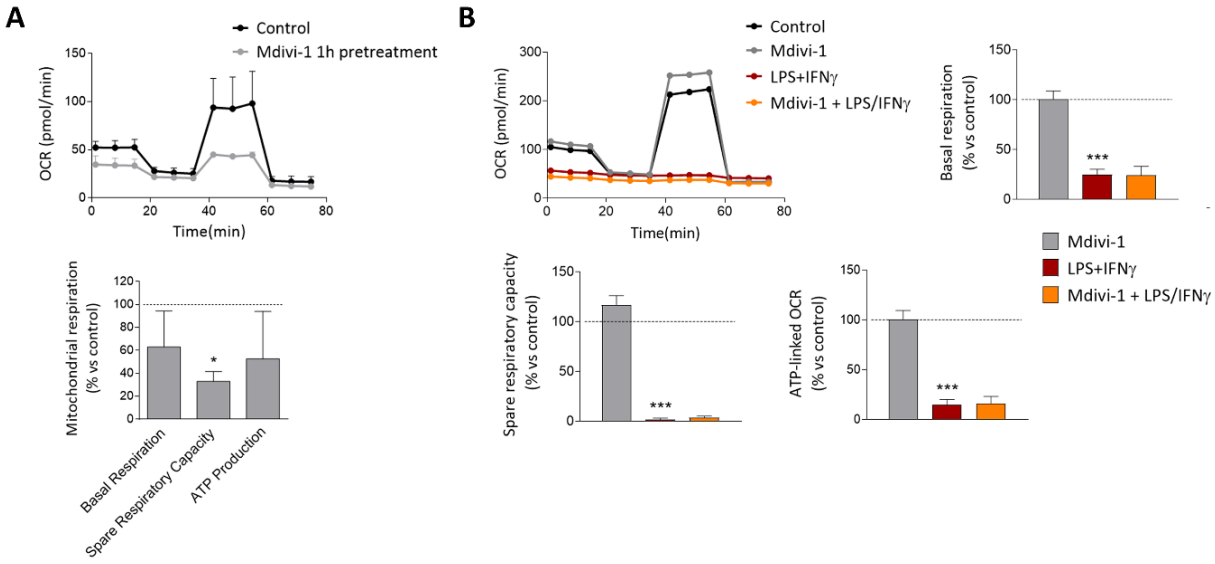

Figure 31. Mitochondrial fission inhibition does not revert mitochondrial metabolic reprogramming. ***(A)*** Metabolic profile of control and microglia treated for 1 hour with Mdivi-1 (above). Histogram shows the metabolic parameters related to OCR of Mdivi-1 treated cells, compared to the control ones (n = 3). ***(B)*** Metabolic profile of control microglia, as well as microglia treated for 24 hours with Mdivi-1, LPS+IFNγ and Mdivi-1 + LPS+IFNγ. Histograms show the metabolic parameters related to OCR compared to control microglia (n = 3). Data are presented as means ± SEM. *p < 0.05, ***p < 0.001. One-way ANOVA followed by Bonferroni post-hoc analysis.

Functional and metabolic characterization of microglia culture in a free-serum medium

Given the relevance of the metabolic state of microglia in its activation and their functions, we hypothesized that the metabolic phenotype of these cells can evolve during the development of pathological conditions, like MS. Indeed, mononuclear phagocytes modify their activation throughout the progression of EAE (Locatelli et al., 2018), and this is potentially associated with changes in intracellular metabolism.

In an attempt to test this hypothesis, we optimized a protocol for microglia isolation from adult rodents using MACS and subsequent culture in serum-free conditions. Serum can potentially perturb microglial phenotype, as these cells commonly present amoeboid morphology and high proliferative rate when cultured in the presence of serum. Bohlen and colleagues recently identified three essential factors for microglial survival in the absence of serum: TGF-β2, IL-34, and cholesterol (TIC factors; Bohlen et al., 2017). We have further characterized both functionally and metabolically microglia isolated by MACS from rat brains and cultured without serum and in presence of TIC factors. Cells in these conditions could potentially serve us to analyze the metabolic state in animals at different EAE stages.

First, we analyzed the morphology of the cells based on Iba1 immunostaining, and observed a significant increase in the number of processes and a decrease in the cell body area in microglia cultured without serum (defined medium; Fig. 32A). In contrast, cells cultured with serum presented an amoeboid-like phenotype. Thus, microglia acquired a highly ramified morphology in absence of serum, with multiple processes branching off the soma, resembling normal, surveillant microglia *in vivo*.

In physiological conditions, microglia constantly survey the brain parenchyma, being this function pivotal for their role. We performed live imaging of microglia in presence and absence of serum, and the latter showed higher motility parameters. Specifically, the mean speed of microglia in basal conditions was enhanced in the defined medium, and the distances travelled were longer (Fig. 32B). Again, these data support the idea that microglia isolated with MACS and cultured without serum resembles physiological microglia *in situ*. Other functional characterizations were performed and the outcomes pointed out to similar conclusions (data not shown; Montilla et al., 2020).

Lastly, as we aimed to analyze the metabolic state of microglia from EAE animals, we assessed whether primary microglia grown in defined medium respond to pro- and anti-inflammatory factors in a canonical way, being able to redirect their metabolism. Microglia cultured without serum showed a significant reduction in OXPHOS after pro-inflammatory stimulation (LPS and IFN-γ), similarly to serum-exposed microglia (Fig. 32C). In contrast, mitochondrial metabolism did not significantly change in microglia cultured in defined medium after exposure to anti-inflammatory factors (Fig. 32C). This can be associated with a basal shift to an anti-inflammatory phenotype in these cells (Cherry et al., 2014). Moreover, the OCR/ECAR ratio was significantly decreased after exposure to pro-inflammatory stimuli in both culture models (Figure 32D), thus indicating that microglia isolated by MACS and cultured without serum can properly undergo metabolic reprogramming and shift to a glycolytic phenotype.

This methodology can potentially be helpful for understanding the metabolic state of microglia during EAE development, as microglia can be MACS-isolated from CNS and their metabolism subsequently analyzed at different EAE stages. Nevertheless, more insights in whether microglia would maintain their phenotype during the isolating protocol are needed.

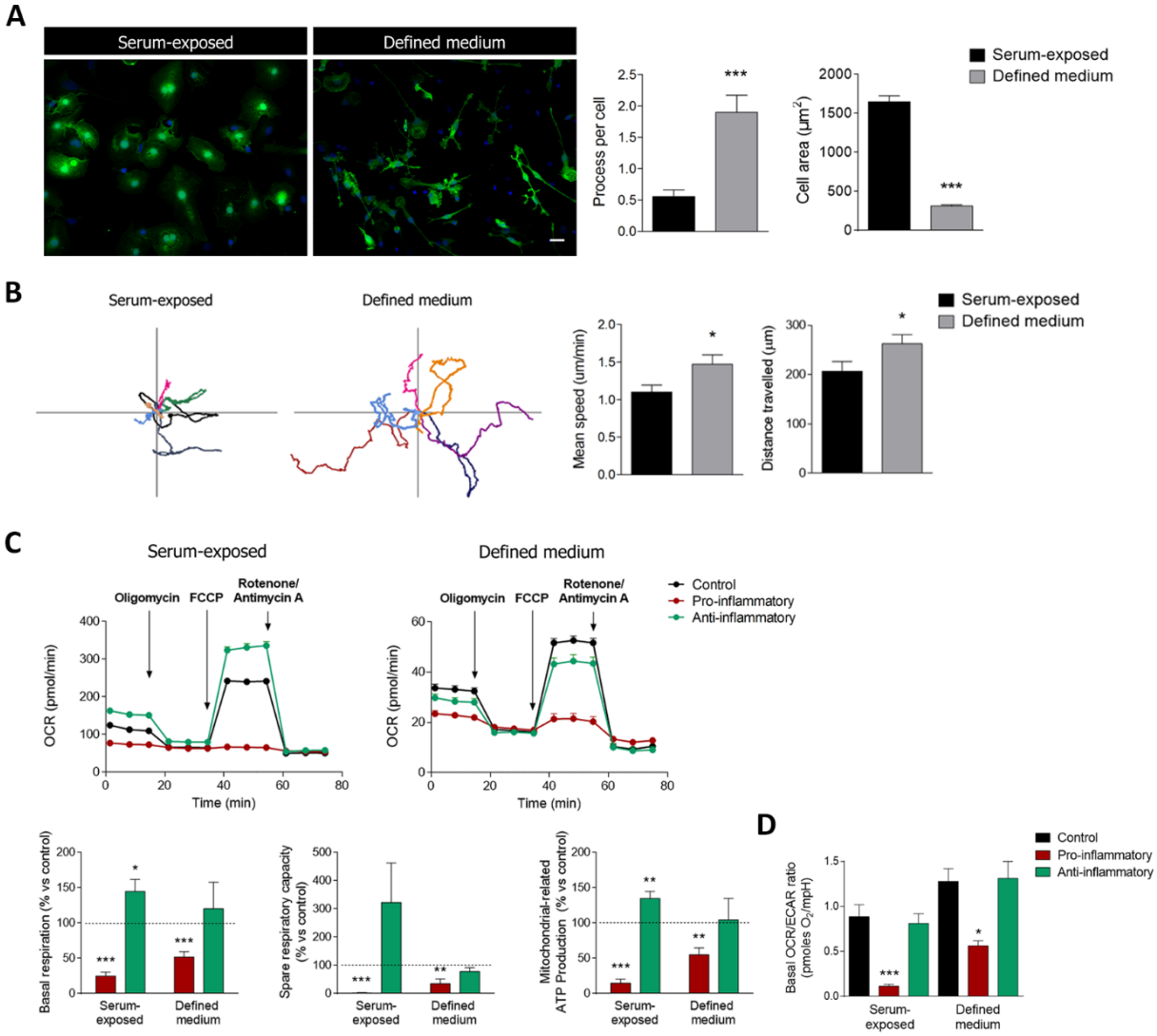

Figure 32. Microglia cultured in serum-free conditions display physiological features and maintain metabolic reprogramming. ***(A)*** Representative images of Iba1⁺ microglia cultured in the presence and absence (defined medium) of serum. Scale bar = 25 µm. Histograms represent the morphological characterization of microglia in both conditions (n = 20-30 cells, 3 independent experiments). ***(B)*** (Left) Representative trajectories of single microglia in presence and absence of serum, represented as differentially coloured lines. The point of intersection of the axes constitutes the initial position of the cells. (Right) Histograms represent the mean speed of their movement as well as the distance travelled by the cells (n = 20 cells, 3 independent experiments). ***(C)*** (Top) Metabolic profiles of microglia with and without serum, after 24h incubations with pro-inflammatory or anti-inflammatory factors. (Bottom) Metabolic parameters of microglia in these conditions. Data are normalized with respect to the control cells (n = 5–8 independent experiments). (D) OCR/ECAR ratio obtained from the basal levels of each parameter (n = 5–8 independent experiments). For each experiment, 6 to 8 replicates were used. * $p < 0.05$, ** $p < 0.005$, *** $p < 0.001$.

This initial characterization proved that we can properly assess the metabolic profile of microglia isolated from mice. The absence of serum in the medium would avoid artificial activation or modifications to the cell phenotype. As a first approach to analyze the metabolic state of microglial from *in vivo* conditions, we intraperitoneally injected saline

and LPS (3 mg/kg) to mice 24 hours prior to the isolation of brain microglia (Fig. 33A). LPS was injected to provoke systemic inflammatory effects, including microglial activation and neuroinflammation (Zhao et al., 2019). The metabolic profile of these freshly-isolated cells was subsequently measured using the Seahorse Analyzer, and we detected nearly significant decreases in the OXPHOS profile and OXPHOS-related parameters in microglia isolated from LPS-treated mice (Fig. 33B), suggesting a partial switch to glycolytic pathways in these cells. However, the number of cells that can be successfully isolated from adult mice following this protocol entails a limiting variable for future investigations, as well as the possible alteration in the microglial activation state due to manipulation.

While further optimization of the isolation protocol is needed, this method could potentially allow us to analyze the evolution of microglial metabolic phenotype throughout the development of EAE and other demyelinating models. This would, in turn, facilitate the therapeutical targeting of microglial metabolic reprogramming to modulate cell activation and the deleterious, associated events during the progression of these disorders.

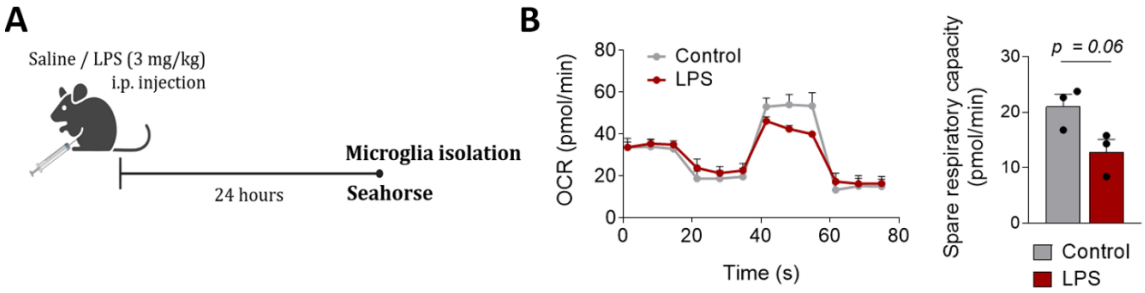

Figure 33. Freshly-isolated microglia display partial metabolic switch in mice after LPS treatment. ***(A)*** Experimental paradigm, indicating that microglia were isolated from control and LPS-treated mice, and their metabolic profile subsequently assessed using Seahorse Analyzer. ***(B)*** (Left) Metabolic profiles of microglia isolated from control and LPS-treated mice. (Right) Spare respiratory capacity measurement, obtained through the analysis of the metabolic profiles of both cell groups.

DISCUSSION

Part I. Specific role of microglia in experimental autoimmune encephalomyelitis development

Microglial cells actively participate in neurodegenerative pathology development. Thus, the analysis of their specific role in these disorders has lately emerged as an important focus of research, seeking for therapeutic approaches for diseases like MS (Guerrero and Sicotte, 2020). In this work, we depleted microglial population using the CSF-1R antagonist, PLX5622, in order to assess its effect in EAE development. The specificity of this treatment has been questioned lately, as some studies observed alterations in myeloid and lymphoid populations in peripheral tissues (Lei et al., 2020; Spiteri et al., 2022). However, we did not find any alterations in immune populations, including macrophages, neither in spleen nor blood in our experimental conditions. Nevertheless, CSF1R inhibition side effects on meningeal/perivascular macrophages were previously described (Kerkhofs et al., 2020), a feature that may contribute to the changes observed in the EAE course and cannot be ruled out as a possible root for the results obtained.

Microglia limit macrophage dispersion into CNS parenchyma after EAE

We here showed that microglial depletion provoked a massive infiltration of $CCR2^{+}$ peripheral macrophages during EAE progression in comparison to control mice, which could constitute a compensatory mechanism. Indeed, we identified that infiltrating monocytes started developing a microglial-like phenotype, even promoting the expression of CSF-1R. In accordance, it has been previously identified that CNS environment is able to induce microglial gene expression in myeloid populations (Bennett et al., 2018). Importantly, infiltrating macrophages colonized the whole CNS parenchyma, occupying both white and gray matter of the spinal cord in PLX5622-treated mice, and their location is not limited to demyelinating lesions as in control EAE mice. These data suggest that microglia limit and control the infiltration, proliferation or survival of macrophages in CNS, leading to a higher number of the latter in demyelinated lesions after microglial depletion. Indeed, previous data using parabiosis in the EAE model demonstrated that peripheral macrophage infiltration is preceded by microglia cell death (Ajami et al., 2011). Besides, microglia also control the dispersion of these infiltrating macrophages throughout the parenchyma. Consistently, microglia surround and confine infiltrating macrophages into

the CNS parenchyma, limiting their dispersion after LPC-induced demyelination (Plemel et al., 2020).

Altogether, our data suggest that microglia interfere with peripheral macrophage dynamics by controlling their entry and migration. This function of microglia could potentially serve as a mechanism to limit peripherally derived CNS inflammation and to maintain the "CNS immune-privileged" status.

Microglia depletion reduced T cell reactivation and delayed EAE onset

Microglia ablation induced a consistent delay in the appearance of the first symptoms in EAE. This suggests that microglia play a role in the effector stage of this disease model. Indeed, inhibition of CCR2-dependent recruitment of monocytes to the CNS blocked EAE progression, but not the onset, suggesting that microglia contribute to EAE onset whereas macrophages are essential to its development up to the paralytic stage (Ajami et al., 2011).

Specifically, we observed that microglial ablation caused an alteration in antigen presentation to the first T cells arriving to the CNS. Frequently, DCs have been identified as the main APCs during EAE (Greter et al., 2015; Giles et al., 2018; Mundt et al., 2019), but contribution of other cells was not discarded. Our data demonstrated that microglial ablation reduced the expression of co-stimulatory molecules (CD80 and CD86) in dendritic cells and infiltrated/CNS-resident macrophages, being these molecules essential for antigen presentation. This suggests microglial early activation and related neuroinflammation after EAE induction potentially promotes antigen presentation capacity in other cell types. This result is in accordance to those obtained in a virus model, in which PLX5622 also alters T cell local reactivation in CNS decreasing B7 co-stimulatory signals in $CD11c^+$ cells (Funk and Klein, 2019), highlighting the relevance of microglia in orchestrating the CNS immune response. Indeed, chronic activation of innate immune response at different levels by microglia is believed to be a major contributor to neurodegenerative conditions (Amor et al., 2014).

Numerous studies determined that microglia activation occurs during the onset and peak of EAE and that this activation and related events are necessary to EAE development. Thus, expression of the p40 subunit of IL-12 and IL-23 by microglia control T cell

encephalogenicity and the deletion of p40 in microglial cells decreases EAE severity by shifting T cell response towards a Th2 phenotype, rather than Th1 (Becher et al., 2003). Another important signal for microglia activation is the transforming growth factor β (TGF-β)-activated kinase 1 (TAK1). Accordingly, microglia selective ablation of TAK1 blocks its activation, the subsequent release of pro-inflammatory mediators such as IL-1β and CCL2, and the infiltration of immune cells, thus completely suppressing EAE development (Goldmann et al., 2013). Similarly, microglial paralysis provoked by the treatment of ganciclovir in CD11b-HSVTK transgenic mice led to a repression of clinical EAE (Heppner et al., 2005). Overall, our data, in accordance to previous studies, indicate that microglia and its persistent and overt activation has a detrimental role in CNS autoimmunity onset, and the targeting of this process in order to either prevent it or suppress it may be a therapeutic option.

Microglia are not necessary for recovery and remyelination after EAE immunization

Serial block-face scanning electron microscopy (SBF-SEM) studies showed that monocyte-derived macrophages associate with nodes of Ranvier and initiate demyelination, whereas microglia appear to mainly clear myelin debris during EAE (Yamasaki et al., 2014). Similarly, during EAE, microglia displayed a weakly immune-activated phenotype whereas infiltrated macrophages are highly immune reactive (Vainchtein et al., 2014). Surprisingly, we observed that the excess of infiltrating macrophages in the CNS parenchyma after microglia deletion did not trigger an exacerbated progression of EAE motor symptomatology, even though the accumulation of these cells has been described as determinant for EAE progression (Ajami et al., 2011). Moreover, both microglia and macrophages are involved in the recovery phase, promoting myelin phagocytosis and favouring oligodendrocyte differentiation and remyelination through the release of diverse factors (Miron and Franklin, 2014; Zabala et al., 2018). Thus, $CCR2^{+}$ infiltrated macrophages can compensate for microglia cell loss and are able to promote remyelinating processes, which are thus not specifically linked to microglial actions.

Targeting CSF-1R has also been tried in different EAE models and at different time windows leading to diverse outcomes. Thus, inhibiting CSF-1R with PLX5622 after EAE onset attenuated EAE pathology and promoted recovery (Nissen et al., 2018). However, blocking

CSF-1R with PLX3397 at later stages in EAE exacerbated neuroinflammation and neurological damage in a model of progressive MS (Tanabe et al., 2019). This study was performed in non-obese diabetic NOD mice, which have a genetic background of high innate immunity activation. In addition, these mice present aberrant activation of microglia that leads to exacerbated symptoms at the chronic phase, probably because immune resolution and recovery is affected. Indeed, microglia depletion in the chronic phase (not tested before) blocked EAE progression. Thus, the results of these studies are not comparable with ours because both the genetic background of the mice and the time window of the treatment are different.

Intriguingly, microglia depletion exacerbates demyelination and impairs remyelination in a neurotropic coronavirus infection model of demyelination (Sariol et al., 2020). The authors showed a higher accumulation of damaged myelin deposits and debris in microglia-depleted mice, that led to impaired myelin repair and prolonged clinical disease. They proposed that microglial functions could not be compensated by infiltrating macrophages. These results, although observed in a different MS model, are in apparent contradiction with our data. We did not detect a deficit in remyelination suggesting that in our model macrophages compensate and efficiently phagocytose myelin to promote repair mechanisms. Altogether, along with the results obtained in our study, show that microglia have distinct roles at different stages of the EAE. Nevertheless, they are not strictly necessary for the development of those phases.

To sum up, our microglia ablation strategy demonstrated that microglia limit the infiltration and dispersion of peripheral macrophages throughout the CNS, in response to EAE induction. Moreover, our results suggest that microglia are not essential for the development of this MS model, nor for proper remyelination processes. On the other hand, we described a microglia-related mechanism promoting early antigen presentation in the CNS, by modulating the expression of B7 co-stimulatory molecules in other APCs, such as DCs and other myeloid populations. This lack of antigen presentation to infiltrating T cells delays the reactivation of these lymphoid cells and therefore provokes a slowdown of EAE early events.

Part II. Role of IRF5 transcription factor in demyelination and remyelination

In this section of the Doctoral Thesis, we focused on the role of IRF5 transcription factor in demyelination and remyelination. We have recently identified purinergic receptor P2X4 as a new target to control microglia activation and to potentiate myelin phagocytosis and remyelination in MS animal models (Zabala et al., 2018); of note, the IRF8-IRF5 transcriptional axis is a critical regulator for the shifting of microglia towards a $P2X4R^+$ reactive phenotype. Moreover, polymorphisms in the human *Irf5* gene have been associated with the development of immune-mediated diseases, including MS (Kristjansdottir et al., 2008). However, its function in the development of this pathology is unknown. In this section, our data show that mice deficient for IRF5 transcription factor showed an accumulation of damaged myelin and an impairment in remyelination and recovery in MS animal models.

Dual role of IRF5 in EAE development

When assessing EAE progression, we observed a potential dual role of IRF5. While the deficiency of this transcription factor was beneficial at initial phases of the model, provoking a delay in the onset of the motor symptoms, it exacerbated neurological damage at the chronic stage of the EAE.

Given the role of IRF5 in immune cells response and activation, the delay in the onset of the disease is potentially linked to a failure in the initial priming. Similarly, other IRF transcription factors are involved in EAE development. Thus, mice lacking *Irf*1, *Irf*3 or *Irf*8 either have a significant amelioration of the EAE pathogenesis (in the case of IRF1 and IRF3), or are completely resistant to EAE (IRF8) (Tada et al., 1997; Fitzgerald et al., 2014; Yoshida et al., 2014). These transcription factors regulate the expression of interferon-induced genes as well as type I interferons, and are key players in the pro-inflammatory activation of myeloid cells as well as in immune priming in the periphery after MOG immunization (Buch et al., 2003; Tamura et al., 2008). In particular, IRF5 plays an important role in the induction of pro-inflammatory cytokines, contributing to the plasticity and polarization of macrophages to an inflammatory phenotype, and promoting the initiation of a potent Th1-Th17 response, associated to a boost of EAE disease progression (Krausgruber et al., 2011; Yoshida et al., 2014). In the light of these data, we hypothesize that EAE onset delay in *Irf5*$^-$

$^{/-}$ mice could be due to a direct impact of IRF5 on initial immune reaction. Indeed, *Irf5* is not only expressed in myeloid cells but it is also present in lymphoid cells and regulates T cell function and migration (Yan et al., 2020). In contrast, the role of IRF5 in other myeloid cells, like neutrophils, is residual at least in other inflammation models (Weiss et al., 2015).

Surprisingly, our results showed for the first time that IRF5 is necessary for EAE recovery in the chronic phase. This role of IRF5 in axonal recovery is also supported by the detrimental effect of *Irf5* deletion in the remyelinating processes in LPC-injected mice, a model lacking adaptive immune activation. Of note, the fact that pro-regenerative properties were aberrant in these animals diverges with the canonical inflammatory functions accredited to IRF5 (Krausgruber et al., 2011). As lymphoid, T cell-related responses were not altered in *Irf5*$^{-/-}$ mice (previous data in the lab), we hypothesized that the effect could be attributed to an alteration in microglia/macrophage functions. Previous data in the laboratory also demonstrated that *Irf5*$^{-/-}$ mice, despite having an ameliorated immune reaction, exhibited a higher inflammatory response of the meninges and higher infiltration of $CD3^{+}$ T cells after LPC injections.

The role of inflammation in promoting neural repair is gaining increasing recognition. Products of macrophages as well as of microglia, their CNS counterparts, facilitate the regeneration of axons (David et al., 1990; Yin et al., 2006) and promote remyelination in animal models of demyelination. Indeed, their deficiency retards axonal repair processes (Kotter et al., 2006; Kondo et al., 2011; Sun et al., 2017; Cantuti-Castelvetri et al., 2018). In addition, microglia/macrophages play well-described roles in myelin clearance after demyelination (Neumann et al., 2009; Lampron et al., 2015), and a failure in this process can lead to inefficient remyelination due to an inhibitory effect of myelin debris in OPCs differentiation (Plemel et al., 2013; Lampron et al., 2015). *Irf5*$^{-/-}$ mice showed a deficit in myelin phagocytosis and a higher accumulation of myelin debris in EAE lesions, a fact that could explain the deficits on recovery. Moreover, proper processing of internalized myelin in microglia/macrophages is essential to maintain a phagocytic, anti-inflammatory phenotype (Bogie et al., 2014; Berghoff et al., 2021), this way generating a pro-regenerative positive feedback. In turn, phagocytosis of myelin in aged microglia/macrophages after demyelination results in cholesterol accumulation in these cells, leading to a maladaptive

inflammatory response that impairs remyelination (Cantuti-Castelvetri et al., 2018). Our data, showing an overload of lipids, could explain the exacerbated inflammatory and immune reaction after LPC injection in *Irf5*$^{-/-}$ mice.

Conventional views hold that dysregulated immune attacks against myelin cause the characteristic focal lesions of inflammatory demyelination. However, neither the immune triggers nor their targets have been completely identified, and despite potent immune-modulating therapies, the progression to disability remains inevitable for most patients. Given these limitations, the notion of these aberrant autoimmune responses on myelin from the "outside-in" has been countered by the argument that pathology of CNS myelin precedes and triggers inflammatory demyelination from the "inside-out" (Matute and Pérez-Cerdá, 2005). Accordingly, a recent study demonstrated that subtle biochemical alterations in myelin, in the absence of overt demyelination, is sufficient to elicit severe secondary demyelinating inflammatory reactions (Caprariello et al., 2018). Similarly, the fact that an alteration in myelin processing in *Irf5*$^{-/-}$ mice is able to promote a secondary immune and inflammatory reaction that exacerbates demyelination may support the "inside-out" model.

Failure in OPCs recruitment in* Irf5$^{-/-}$ *mice after LPC-induced demyelination lesions

Our study suggests both an alteration in OPCs recruitment towards the lesions after LPC-induced demyelination in the spinal cord, and a failure in myelin processing. One possible cause behind the alteration in OPC recruitment could be an abnormality in the extracellular matrix and the glial scar formation surrounding LPC lesions. The extracellular environment and ECM are significantly altered within MS plaques (Van Horssen et al., 2007), and these changes limit remyelination specially in chronic lesions. The ECM is composed of proteoglycans, hyaluronan and multiple protein components such as collagen, fibronectin and laminin, that could influence OPC migration and differentiation (You and Gupta, 2018). In particular, we observed that hyaluronan, an ECM component that blocks OPCs maturation and subsequent remyelination (Sloane et al., 2010), as well as astrocytes are located exclusively in the periphery of LPC lesions in *Irf5*$^{-/-}$ mice. As astrocytes are the main producers of extracellular matrix, our data support the hypothesis that the ECM could be altered or even absent in the core of the lesions of *Irf5*$^{-/-}$ mice. The strong glial scar formed around *Irf5*$^{-/-}$ lesions could also constitute a direct, physical barrier for OPC entrance,

although glial scar rather aids than prevents axon regeneration after spinal cord injury (Anderson et al., 2016). Moreover, astrocytic scar was described not to limit remyelination in EAE (Haindl et al., 2019). In our experimental setting, the sequence of events after LPC-induced lesions might be crucial for understanding if the scar impedes proper repairing mechanisms. In addition, alternative mechanisms may account for the OPC recruitment failure. This includes the lack in *Irf5*$^{-/-}$ mice of OPC chemoattraction by BDNF released from microglia, following activation of the IRF5-P2X4 axis (Zabala et al., 2018; Haindl et al., 2019). Finally, the aberrant inflammatory reaction observed inside the lesions may also alter the expression of chemotactic or chemorepellent molecules, governing OPC migration.

Irf5 regulate myelin-derived cholesterol metabolism in microglia in demyelinating lesions

Our data point out to an alteration of myelin phagocytosis and degradation in *Irf5*$^{-/-}$ microglia, leading to an aberrant accumulation of myelin debris that blocks remyelination. Microglial P2X4^{+} reactive state, modulated by IRF5 (Masuda et al., 2014), is characterized by more phagocytic capacity (Zabala et al., 2018). Therefore, it is possible that P2X4 downregulation secondary to *Irf5* deletion could explain the phagocytic deficits and the subsequent outcome in EAE. However, our transcriptomic data revealed a direct involvement of IRF5 in the transcriptional control of additional genes. Indeed, in addition to the expected decrease of immune response-related genes, *Irf5*$^{-/-}$ microglia showed a downregulation of two previously unidentified signaling pathways, GTPases signaling and intracellular metabolism, postulating new roles of IRF5 in microglial functions.

Cdc42 GTPase signaling is known to mediate actin remodeling and membrane extension in microglia, favouring processes such as cell motility (Rong et al., 2020) and the formation of phagocytic cups, that precedes phagocytosis of neurons (Barcia et al., 2012). Previous data from the literature have suggested the connection of another IRF transcription factor, IRF8, with microglial and macrophage motility. Indeed, macrophages lacking IRF8 are not able to migrate toward the epicenter of the lesion after SCI, and remain widely scattered in the injured spinal cord, leading to higher axonal loss and poor functional outcomes (Kobayakawa et al., 2019). However, although *Irf5*$^{-/-}$ microglial motility was affected *in vitro*, *Irf5*$^{-/-}$ mice did not present a deficient migration of microglia and macrophages into the

lesions, neither at early stages (4 dpi) nor at later phases after LPC-induced demyelination or in EAE chronic lesions. Despite that, we cannot exclude that the deficit in myelin debris phagocytosis in EAE and LPC lesions in *Irf5*$^{-/-}$ mice is due to the alteration in the Cdc42 GTPase signaling pathway.

On the other hand, *Irf5*$^{-/-}$ microglia showed downregulation in genes associated with lipid phagocytosis and metabolism. This transcriptional program encompasses a gene signaling pathway that may enable microglia to enhance their phagocytic properties, their lysosome degradative capacity and the ability to facilitate lipid trafficking in microglia. Thus, a failure to induce this transcriptional program in *Irf5*$^{-/-}$ microglia results in aberrant lipid and lipid-related structures accumulation, such as lipid droplets (LDs) and pathogenic cholesterol crystals. A similar phenotype was described in microglia lacking TREM2, an immune receptor involved in phagocytosis in microglia, as well as in aged microglia/macrophages (Cantuti-Castelvetri et al., 2018; Nugent et al., 2020). Cholesterol crystals formed by aged microglia propagate a maladaptive pro-inflammatory response after LPC injections, although it remains unclear how inflammasome activation diminishes remyelination (Cantuti-Castelvetri et al., 2018). In turn, LD-accumulating microglia represent a dysfunctional and pro-inflammatory state in the aging brain (Marschallinger et al., 2020), further highlighting the importance of a correct lipid processing by microglia after demyelination. A recent work showed that TREM2$^{-/-}$ microglia abnormally enhances LD production upon excessive myelin challenge, promoting pathogenic events (Nugent et al., 2020). Alternatively, LDs biogenesis in phagocytes was described to be required for remyelination (Gouna et al., 2021), and these structures also participate in other immune-related mechanisms, such as antiviral responses (Monson et al., 2021). Besides, the altered lipid phenotype we identified in *Irf5*$^{-/-}$ microglia is reminiscent of macrophage foam cells in atherosclerotic lesions (Moore and Tabas, 2011). Indeed, familial cases of atherosclerosis linked to mutations in the *LIPA* gene (encoding the lysosome enzyme lipase) lead to a cholesterol ester (CE) storage disorder, suggesting that aberrant accumulation of this lipid is pathogenic (Du et al., 2004). CE accumulation may mediate toxicity generation of oxidized metabolites and lipid peroxidation products of mono- or polyunsaturated fatty acyl chains (Choi et al., 2017). In light of the above, it is possible that unresolved inflammation, caused

by defective cholesterol efflux in *Irf5*$^{-/-}$ mice, impedes the anti-inflammatory, pro-regenerative effects of microglia/macrophages that drive OPCs differentiation.

In addition to cholesterols, IRF5-deficient microglia showed altered metabolism of phospholipid, such as phosphatidylinositols (PIs) and plasmalogens. *In vitro* analysis by LC/MS showed a decrease in the concentration of these lipids after myelin degradation; similarly, we identified a failure in PI metabolism by RNA sequencing. Of note, phospholipid localization modulates microglial functions via Cdc42 *in vitro* (Tokizane et al., 2017). Furthermore, phosphatidylinositols are known to participate in a myriad of signaling pathways, including those involved in lipid metabolism. Thus, a reduction in PI levels after phagocytosis of myelin in IRF5-deficient microglia may alter their regenerative capacity. Finally, we also observed a decrease in plasmalogens levels both *in vitro* by LC/MS and by MALDI-IMS in microglia responding to LPC lesions. This decrease may impair the endogenous antioxidant capacity to protect ROS-vulnerable myelin (Luoma et al., 2015) and the requirement of plasmalogens for the correct and timely differentiation of myelinating cells (Da Silva et al., 2014).

All the findings described in this section point to a complex role of IRF5 that evolves from detrimental to beneficial, a finding in correlation with the complex role of microglia/macrophages along the MS pathology. Importantly, we describe a role of IRF5 not only in the modulation of the immune response but also directly regulating lipid uptake and subsequent intracellular degradation. This aberrant lipid processing, in the context of demyelination, could potentially induce altered inflammatory states in microglia and reduce regenerative processes.

Part III. Role of mitochondrial dynamics in microglial activation and metabolic switch

The relationship between immune cell energy metabolism and function was uncovered in the 60s by demonstrating functional changes in immune cells after blocking of specific energetic routes (Oren et al., 1963). Accordingly, immunometabolism has recently emerged as an important focus of research, as it opens a novel therapeutic approach for inflammatory and autoimmune diseases. Thus, effector immune cells such as microglia/macrophages undergo a metabolic reprogramming process that are distinctly associated with immunological function (Kelly and O'Neill, 2015; Andrejeva and Rathmell, 2017). We have here monitored this effect in primary microglia and its consequences in mitochondrial integrity; moreover, we have checked whether this metabolic switch is associated with mitochondrial dynamics. Notably, we found that ablation of OXPHOS in activated microglia is not due to a disruption of mitochondrial integrity. Moreover, we have also observed that Drp1-dependent mitochondrial fission, although potentially involved in microglial activation, does not play an essential role in metabolic reprogramming of microglia.

Microglia maintain mitochondrial function upon metabolic reprogramming

Upon pro-inflammatory stimulation, cells are able to redirect their entire metabolic processes to the glycolytic pathway to rapidly obtain energy. This process is an outcome of different molecular pathways; nevertheless, the precise mechanisms involved are yet to be defined. In this study, we have observed that halting OXPHOS machinery is not associated with mitochondrial damage or dysfunction nor with microglia cell death. This is opposed to the idea that dysfunctional mitochondria would be the reason underlying the switch in metabolism and, eventually, the development of cancer cells (Warburg, 1956). In turn, functional mitochondria produce ROS to support not only the development of cancer cells but also the pro-inflammatory state of macrophages (West et al., 2011; Porporato et al., 2018). Thus, TLR activation in macrophages induced mitochondrial ROS generation, an essential step for efficient intracellular bacteria killing (West et al., 2011). We observed that $\Delta\Psi m$ was maintained in pro-inflammatory microglia through the reverse operation of F_0F_1-ATP synthase and that this protects microglia from cell death. Indeed, the blockage of complexes I, III, and IV abolishes H1 translocation and it would lead to a transient drop in $\Delta\Psi m$. However, the F1 subunit of F_0F_1-ATP synthase can hydrolyse mitochondrial ATP

under these circumstances and drive the F_0 rotor to pump H1 out of the matrix to be able to maintain the ΔΨm (Kinosita et al., 2004). Thus, mitochondria of pro-inflammatory microglia would become consumer rather than ATP generator, further increasing the energetic demand of the cells (Solaini et al., 2010). However, we have not found any essential role in the ANT reversal activity, which has also been described as key in ΔΨm maintenance process in similar paradigms (Chinopoulos, 2011).

Mitochondrial dynamics modulate microglial activation but not metabolic reprogramming

Signaling events mediated by extracellular signals can regulate the metabolic pathways in immune cells such as macrophages or microglia (Wang et al., 2019). Accordingly, diverse cellular functions have been associated with metabolic reprogramming, including those related to mitochondrial function in general. Previous data suggested that mitochondrial dynamics contribute to this mechanism (Nair et al., 2019). Our results demonstrated that Mdivi-1, a putative mitochondrial fission inhibitor, reduced the enhancement of markers associated with microglial activation after LPS and IFN-γ exposure. This effect on microglial activation is consistent with other studies (Katoh et al., 2017; Nair et al., 2019). Drp1-mediated mitochondrial fission has been associated with enhanced activation of both p38 and NF-KB, both mediators of signaling cascades leading to the expression of pro-inflammatory genes, in a paradigm of diabetic nephropathy (Zhang et al., 2015). Moreover, blocking Drp1-dephosphorylation with oleuropein reduced the production of proinflammatory factors in microglia as well (Park et al., 2017). In contrast, blockage of mitochondrial fission with Mdivi-1 did not avoid the microglial metabolism switch to glycolysis upon LPS plus IFN-γ exposure, nor did it provoke any effect in the control cells. We concluded that mitochondria fission does not contribute to the metabolic switch in microglia. This result is apparently at odds with previous results (Nair et al., 2019b). The contradiction may be explained on the basis of the different paradigm used; in the study from Nair and colleagues, microglia was pre-treated with Mdivi-1 (25 μM) for 1 h before LPS stimulation (100 ng/ml. 24 h). We, in contrast, blocked mitochondrial fission with Mdivi-1 (50 μM) during the whole LPS (10 ng/ml) plus IFN-γ (20 ng/ml) treatment (24 h).

On the other hand, metabolism plays a key role in the plasticity of immune cells. Pro-inflammatory microglia convert arginine into NO trough iNOS activity (Rath et al., 2014;

Yang and Ming, 2014). Upregulation of iNOS under pro-inflammatory conditions, and the resulting generation of NO, contributes to the detention of mitochondrial respiration, both in immune cells and astrocytes (Bolaños et al., 1994; Everts et al., 2012). In accordance, editing macrophage and microglia (re)polarization is emerging as a new therapeutic approach, and iNOS has been described as a target. Indeed, iNOS inhibition improves metabolic and phenotypic reprograming to anti-inflammatory macrophages (Van den Bossche et al., 2016). Despite the fact that Mdivi-1 treatment consistently reduced iNOS expression in pro-inflammatory microglia, we did not detect any significant improvement on mitochondrial respiration. There are two possible interpretations. The complete blockage of iNOS activity and total abolishment of NO production, as observed with other iNOS inhibitor like 1400W (Garvey et al., 1997), could be required to prevent the metabolic switch. In this sense, Mdivi-1 only partially reduced iNOS expression in our pro-inflammatory microglia. Alternatively, signaling pathways controlling metabolic switch could differ from those regulating phenotypic expression. Indeed, iNOS inhibition does not affect phenotypic polarization of cells nor the inflammatory cytokines secretion in macrophages (Van den Bossche et al., 2016). Accordingly, the effect of Mdivi-1 on pro-inflammatory gene expression does not produce any change on metabolism.

In summary, the current study sheds some light into the role of mitochondria in the metabolic reprogramming process in microglia. Pro-inflammatory stimuli dampen mitochondrial function without compromising their integrity, and our results point F_0F_1-ATP synthase as a key regulator of mitochondrial potential and cell viability maintenance in these conditions. In addition, we concluded that mitochondrial dynamics, fusion-fission, although potentially involved in pro-inflammatory gene expression, do not contribute to microglial glycolytic switch after pro-inflammatory stimulation.

Ex vivo model to study microglial metabolism switch

We also optimized and characterized primary microglia isolated by MACS and cultured in a chemically defined medium with previously identified factors that promote microglial survival (Bohlen et al., 2017). The absence of serum is known to provoke a ramified morphology that mirrors that acquired by these cells *in vivo* in the normal adult brain. Besides, we identified the obtained phenotype as a more representative example of resting microglia observed in physiological conditions, ranging from a downregulation of activation

markers to a reduction of different functionalities typically associated to the activated state of microglia, including phagocytosis. Importantly, the capacity of the cells to polarize to pro- or anti-inflammatory profiles when exposed to common agents, as well as the metabolic reprogramming that cells suffer during this process remained mainly unaltered.

Serum-free culture conditions are essential to reproduce the physiological condition of the extracellular fluid of the CNS, which is similar to the cerebrospinal fluid (CSF). Normal CSF contains extremely low levels of proteins and factors. In this study, we corroborated that the chemically defined medium more closely reproduce the *in vivo* extracellular medium than the typical serum-containing medium, and lead to a morphological and functional microglia state resembling homeostatic microglia *in vivo*. Moreover, the increased dynamics of microglia cultured in defined medium also mimic the ones observed in physiological conditions. Microglia cultured in these conditions decrease the OCR/ECAR ratio after exposure to pro-inflammatory stimuli, demonstrating that microglia undergo a metabolic reprogramming under these conditions. In contrast, microglia cultured in defined medium did not show a clear increase in basal OXPHOS nor OXPHOS-related parameters after exposure to anti-inflammatory cytokines. Altogether, data suggest that metabolic stimulation with anti-inflammatory factors did not induce any metabolic change in microglia cultured in defined medium. These difference with regards to serum-exposed microglia may suggest that microglia in defined medium are slightly shifted toward an anti-inflammatory phenotype (Cherry et al., 2014).

Moreover, when we studied metabolism switch in freshly isolated after *in vivo* treatment of mice with LPS, we did not clearly observe the metabolic switch towards glycolysis. Previous observations in the laboratory indicate that microglia activation quickly reverses after removing pro- and anti-inflammatory factors. Thus, it is possible that the metabolic switch happening *in vivo* reverses during the process of microglia isolation. In addition, the whole process of microglia isolation and purification could also alter the activation state of microglia. Indeed, transcriptomic studies emphasize the necessity of performing microglia isolation in the absence of enzymatic digestion and at 4ºC to avoid excessive microglia cell activation during the manipulation processes.

CONCLUSIONS

The conclusions of this work are as follows:

1. **Microglia limit macrophage infiltration** and dispersion throughout CNS parenchyma during EAE development.
2. **Microglia modulate antigen presentation and T cell reactivation** at early stages of the EAE.
3. **Microglia are not essential** triggering EAE nor in the subsequent regeneration in its chronic phase.

These findings indicate that microglia interact with immune cells during the development of EAE, by impeding macrophage access and spreading into the CNS as well as by promoting T cell reactivation and clonal expansion.

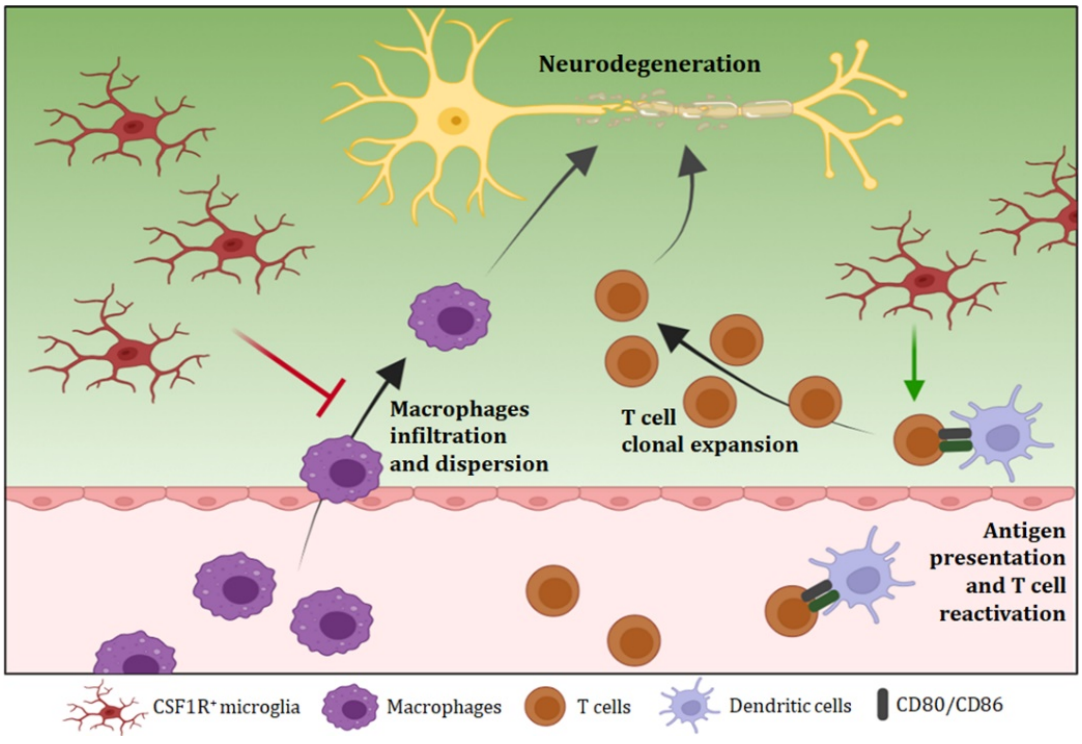

4. **IRF5 plays a dual role in EAE** development as its deletion delays EAE onset and aggravates motor symptoms and tissue damage in the EAE chronic phase.
5. IRF5 **deficiency exacerbates LPC-induced demyelinating lesions** in the spinal cord and limits OPC recruitment towards the injury site.
6. IRF5 modulates microglial essential functions like **phagocytosis and motility**.
7. **IRF5 regulates lipid homeostasis in microglia** as its deficiency induces an accumulation of cholesterol esters, lipid droplets and cholesterols crystals, that exacerbates demyelinating lesions.

We identified a novel role of IRF5 modulating lipid homeostasis in microglia, that favours myelin uptake and subsequent degradation in EAE and lysolecithin-induced lesions and promotes regenerative processes after demyelination.

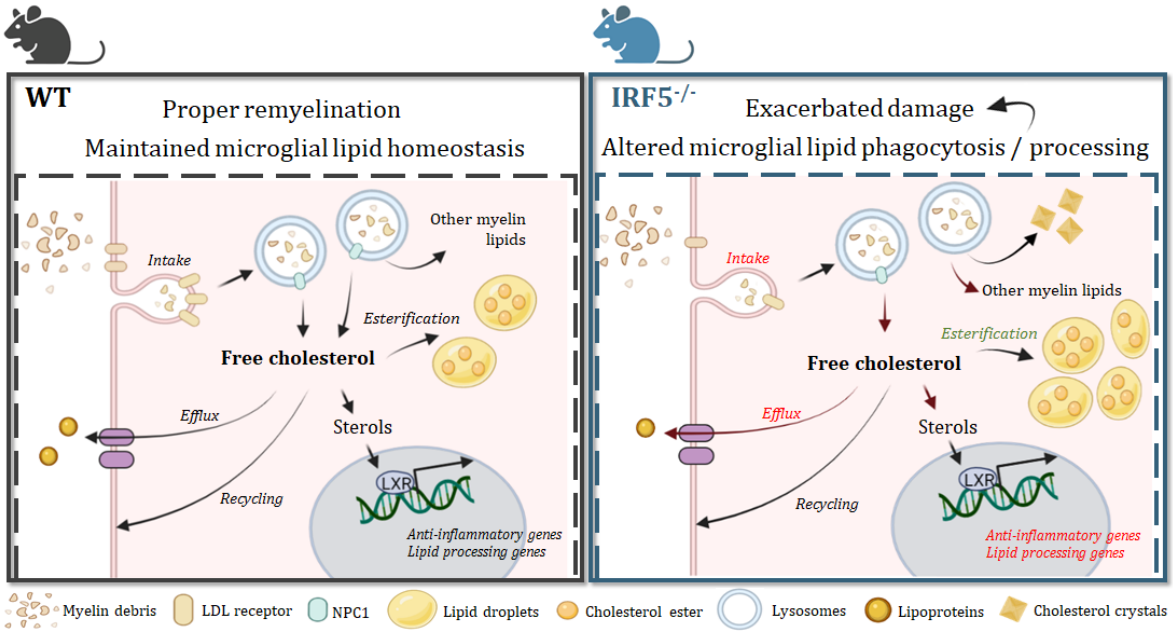

8. **Microglial metabolic reprogramming** is not due to mitochondrial dysfunction.
9. **Mitochondrial dynamics are involved in microglial activation**, but not in metabolic reprogramming processes.
10. **Microglia display physiological features in serum-free conditions**, and maintain metabolic switch capacity.

These results show that microglial activation and metabolic reprogramming does not compromise mitochondrial integrity. Moreover, mitochondrial dynamics processes, including fission and fusion, are potentially involved in pro-inflammatory activation of microglia, but do not in the associated metabolic switch.

Altogether, the results of this Thesis broaden current understanding on the role of microglia in demyelinating disorders, as well as on the mechanisms underlying their activation in response to inflammation and demyelination.

REFERENCES

Aggarwal, S., Yurlova, L., and Simons, M. (2011). Central nervous system myelin: Structure, synthesis and assembly. *Trends Cell Biol.* 21, 585–593. doi:10.1016/j.tcb.2011.06.004.

Ajami, B., Bennett, J. L., Krieger, C., McNagny, K. M., and Rossi, F. M. V (2011). Infiltrating monocytes trigger EAE progression, but do not contribute to the resident microglia pool. *Nat. Neurosci.* 14, 1142–1149. doi:10.1038/nn.2887.

Ajami, B., Bennett, J. L., Krieger, C., Tetzlaff, W., and Rossi, F. M. V. (2007). Local self-renewal can sustain CNS microglia maintenance and function throughout adult life. *Nat. Neurosci.* 10, 1538–1543. doi:10.1038/nn2014.

Al Mamun, A., Chauhan, A., Qi, S., Ngwa, C., Xu, Y., Sharmeen, R., et al. (2020). Microglial IRF5-IRF4 regulatory axis regulates neuroinflammation after cerebral ischemia and impacts stroke outcomes. *Proc. Natl. Acad. Sci. U. S. A.* 117, 1742–1752. doi:10.1073/pnas.1914742117.

Almuttaqi, H., and Udalova, I. A. (2019). Advances and challenges in targeting IRF5, a key regulator of inflammation. *FEBS J.* 286, 1624–1637. doi:10.1111/febs.14654.

Amor, S., Peferoen, L. A. N., Vogel, D. Y. S., Breur, M., van der Valk, P., Baker, D., et al. (2014). Inflammation in neurodegenerative diseases - an update. *Immunology* 142, 151–166. doi:10.1111/imm.12233.

Anderson, M. A., Burda, J. E., Ren, Y., Ao, Y., O'Shea, T. M., Kawaguchi, R., et al. (2016). Astrocyte scar formation AIDS central nervous system axon regeneration. *Nature* 532, 195–200. doi:10.1038/nature17623.

Andrejeva, G., and Rathmell, J. C. (2017). Similarities and Distinctions of Cancer and Immune Metabolism in Inflammation and Tumors. *Cell Metab.* 26, 49–70. doi:10.1007/s11065-015-9294-9.Functional.

Antony, J. M., Van Marle, G., Opii, W., Butterfield, D. A., Mallet, F., Yong, V. W., et al. (2004). Human endogenous retrovirus glycoprotein-mediated induction of redox reactants causes oligodendrocyte death and demyelination. *Nat. Neurosci.* 7, 1088–1095. doi:10.1038/nn1319.

Arnoux, I., and Audinat, E. (2015). Fractalkine signaling and microglia functions in the developing brain. *Neural Plast.* 2015. doi:10.1155/2015/689404.

Bachiller, S., Jiménez-Ferrer, I., Paulus, A., Yang, Y., Swanberg, M., Deierborg, T., et al. (2018). Microglia in neurological diseases: A road map to brain-disease dependent-inflammatory response. *Front. Cell. Neurosci.* 12, 1–17. doi:10.3389/fncel.2018.00488.

Bakhuraysah, M. M., Theotokis, P., Lee, J. Y., Alrehaili, A. A., Aui, P. M., Figgett, W. A., et al. (2021). B-cells expressing NgR1 and NgR3 are localized to EAE-induced inflammatory infiltrates and are stimulated by BAFF. *Sci. Rep.* 11, 1–16. doi:10.1038/s41598-021-82346-6.

Barcia, C., Ros, C. M., Annese, V., Sauvage, M. A. C. De, Ros-Bernal, F., Gómez, A., et al. (2012). ROCK/Cdc42-mediated microglial motility and gliapse formation lead to phagocytosis of degenerating dopaminergic neurons in vivo. *Sci. Rep.* 2, 1–13. doi:10.1038/srep00809.

Barnett, M. H., and Prineas, J. W. (2004). Relapsing and Remitting Multiple Sclerosis: Pathology of the Newly Forming Lesion. *Ann. Neurol.* 55, 458–468. doi:10.1002/ana.20016.

Becher, B., Durell, B. G., and Noelle, R. J. (2003). IL-23 produced by CNS-resident cells controls T cell encephalitogenicity during the effector phase of experimental autoimmune encephalomyelitis. *J. Clin. Invest.* 112, 1186–1191. doi:10.1172/jci19079.

Bennett, F. C., Bennett, M. L., Yaqoob, F., Mulinyawe, S. B., Grant, G. A., Hayden Gephart, M., et al. (2018). A Combination of Ontogeny and CNS Environment Establishes Microglial Identity. *Neuron* 98, 1170-1183.e8. doi:10.1016/j.neuron.2018.05.014.

Bennett, J., Basivireddy, J., Kollar, A., Biron, K. E., Reickmann, P., Jefferies, W. A., et al. (2010). Blood–brain barrier disruption and enhanced vascular permeability in the multiple sclerosis model EAE. *J. Neuroimmunol.* 229, 180–191. doi:10.1016/J.JNEUROIM.2010.08.011.

Bennett, M. L., and Bennett, F. C. (2020). The influence of environment and origin on brain resident macrophages and implications for therapy. *Nat. Neurosci.* 23, 157–166. doi:10.1038/s41593-019-0545-6.

Berghoff, S. A., Spieth, L., Sun, T., Hosang, L., Schlaphoff, L., Depp, C., et al. (2021). Microglia facilitate repair of demyelinated lesions via post-squalene sterol synthesis. *Nat. Neurosci.* 24, 47–60. doi:10.1038/s41593-020-00757-6.

Bernier, L. P., York, E. M., Kamyabi, A., Choi, H. B., Weilinger, N. L., and MacVicar, B. A. (2020). Microglial metabolic flexibility supports immune surveillance of the brain parenchyma. *Nat. Commun.* 11. doi:10.1038/s41467-020-15267-z.

Bieber, A. J., Kerr, S., and Rodriguez, M. (2003). Efficient central nervous system remyelination requires T cells. *Ann. Neurol.* 53, 680–684. doi:10.1002/ana.10578.

Bjornevik, K., Cortese, M., Healy, B. C., Kuhle, J., Mina, M. J., Leng, Y., et al. (2022). Longitudinal analysis reveals high prevalence of Epstein-Barr virus associated with multiple sclerosis. *Science* 375, 296–301. doi:10.1126/science.abj8222.

Bligh, E., and Dyer, W. (1959). A rapid method of total lipid extraction and purification. *Can. J. Biochem. Physiol.* 37, 911–917. Available at: www.nrcresearchpress.com.

Bogie, J. F. J., Jorissen, W., Mailleux, J., Nijland, P. G., Zelcer, N., Vanmierlo, T., et al. (2014). Myelin alters the inflammatory phenotype of macrophages by activating PPARs. *Acta Neuropathol. Commun.* 1. doi:10.1186/2051-5960-1-43.

Bogie, J. F. J., Timmermans, S., Huynh-Thu, V. A., Irrthum, A., Smeets, H. J. M., Gustafsson, J. Å., et al. (2012). Myelin-Derived Lipids Modulate Macrophage Activity by Liver X Receptor Activation. *PLoS One* 7, 1–10. doi:10.1371/journal.pone.0044998.

Bohlen, C., Bennett, F., Tucker, A., Collins, H., Mulinyawe, S., and Barres, B. (2017). Diverse requirements for microglial survival, specification, and function revealed by defined-medium cultures. *Neuron* 94, 759–773. doi:10.1016/j.neuron.2017.04.043.Diverse.

Bolaños, J. P., Peuchen, S., Heales, S. J. R., Land, J. M., and Clark, J. B. (1994). Nitric Oxide-Mediated Inhibition of the Mitochondrial Respiratory Chain in Cultured Astrocytes. *J. Neurochem.* 63, 910–916. doi:10.1046/j.1471-4159.1994.63030910.x.

Bordt, E. A., Clerc, P., Roelofs, B. A., Saladino, A. J., Tretter, L., Adam-Vizi, V., et al. (2017). The Putative Drp1 Inhibitor mdivi-1 Is a Reversible Mitochondrial Complex I Inhibitor that Modulates Reactive Oxygen Species. *Dev. Cell* 40, 583-594.e6. doi:10.1016/j.devcel.2017.02.020.

Brocard, J. B., Tassetto, M., and Reynolds, I. J. (2001). Quantitative evaluation of mitochondrial calcium content in rat cortical neurones following a glutamate stimulus. *J. Physiol.* 531, 793–805. doi:10.1111/j.1469-7793.2001.0793h.x.

Browne, P., Chandraratna, D., Angood, C., Tremlett, H., Baker, C., Taylor, B. V., et al. (2014). Atlas of multiple sclerosis 2013: A growing global problem with widespread inequity. *Neurology* 83, 1022–1024. doi:10.1212/WNL.0000000000000768.

Bruttger, J., Karram, K., Wörtge, S., Regen, T., Marini, F., Hoppmann, N., et al. (2015). Genetic Cell Ablation Reveals Clusters of Local Self-Renewing Microglia in the Mammalian Central Nervous System. *Immunity* 43, 92–106. doi:10.1016/j.immuni.2015.06.012.

Buch, T., Uthoff-Hachenberg, C., and Waisman, A. (2003). Protection from autoimmune brain inflammation in mice lacking IFN-regulatory factor-1 is associated with Th2-type cytokines. *Int. Immunol.* 15, 855–859. doi:10.1093/intimm/dxg086.

Butovsky, O., and Weiner, H. L. (2018). Microglial signatures and their role in health and disease. *Nat. Rev. Neurosci.* 19, 622–635. doi:10.1038/s41583-018-0057-5.

Cantuti-Castelvetri, L., Fitzner, D., Bosch-Queralt, M., Weil, M.-T., Su, M., Sen, P., et al. (2018). Defective cholesterol clearance limits remyelination in the aged central nervous system. *Science* 359, 684–688.

Caprariello, A. V., Rogers, J. A., Morgan, M. L., Hoghooghi, V., Plemel, J. R., Koebel, A., et al. (2018). Biochemically altered myelin triggers autoimmune demyelination. *Proc. Natl. Acad. Sci. U. S. A.* 115, 5528–5533. doi:10.1073/pnas.1721115115.

Cayre, M., Falque, M., Mercier, O., Magalon, K., and Durbec, P. (2021). Myelin Repair: From Animal Models to Humans. *Front. Cell. Neurosci.* 15, 1–20. doi:10.3389/fncel.2021.604865.

Chastain, E. M. L., Duncan, D. S., Rodgers, J. M., and Miller, S. D. (2011). The role of antigen presenting cells in multiple sclerosis. *Biochim. Biophys. Acta - Mol. Basis Dis.* 1812, 265–274. doi:10.1016/j.bbadis.2010.07.008.

Chausse, B., Kakimoto, P. A., and Kann, O. (2021). Microglia and lipids: how metabolism controls brain innate immunity. *Semin. Cell Dev. Biol.* 112, 137–144. doi:10.1016/j.semcdb.2020.08.001.

Cherry, J. D., Olschowka, J. A., and Banion, M. K. (2014). Are Resting Microglia More M2? *Front. Immunol.* 5, 2–5. doi:10.3389/fimmu.2014.00594.

Chinopoulos, C. (2011). Mitochondrial consumption of cytosolic ATP: Not so fast. *FEBS Lett.* 585, 1255–1259. doi:10.1016/j.febslet.2011.04.004.

Chistiakov, D. A., Bobryshev, Y. V., and Orekhov, A. N. (2016). Macrophage-mediated cholesterol handling in atherosclerosis. *J. Cell. Mol. Med.* 20, 17–28. doi:10.1111/jcmm.12689.

Choi, S. H., Sviridov, D., and Miller, Y. I. (2017). Oxidized cholesteryl esters and inflammation. *Biochim. Biophys. Acta - Mol. Cell Biol. Lipids* 1862, 393–397. doi:10.1016/j.bbalip.2016.06.020.

Cignarella, F., Filipello, F., Bollman, B., Cantoni, C., Locca, A., Mikesell, R., et al. (2020). TREM2 activation on microglia promotes myelin debris clearance and remyelination in a model of multiple sclerosis. *Acta Neuropathol.* 140, 513–534. doi:10.1007/s00401-020-02193-z.

Colonna, M., and Butovsky, O. (2017). Microglia function in the central nervous system during health and neurodegeneration. *Annu. Rev. Immunol.* 35, 441–468. doi:10.1146/annurev-immunol-051116-052358.

Compston, A., and Coles, A. (2008). Multiple sclerosis. *Lancet* 372, 1502–1517. doi:10.1016/S0140-6736(08)61620-7.

Constantinescu, C. S., Farooqi, N., O'Brien, K., and Gran, B. (2011). Experimental autoimmune encephalomyelitis (EAE) as a model for multiple sclerosis (MS). *Br. J. Pharmacol.* 164, 1079–1106. doi:10.1111/j.1476-5381.2011.01302.x.

Corona, J. C., and Duchen, M. R. (2014). Mitochondrial bioenergetics assessed by functional fluorescence dyes. *Neuromethods*. doi:10.1007/978-1-4939-1059-5_7.

Da Silva, T. F., Eira, J., Lopes, A. T., Malheiro, A. R., Sousa, V., Luoma, A., et al. (2014). Peripheral nervous system plasmalogens regulate Schwann cell differentiation and myelination. *J. Clin. Invest.* 124, 2560–2570. doi:10.1172/JCI72063.

Davalos, D., Grutzendler, J., Yang, G., Kim, J. V., Zuo, Y., Jung, S., et al. (2005). ATP mediates rapid microglial response to local brain injury in vivo. *Nat. Neurosci.* 8, 752–758. doi:10.1038/nn1472.

David, S., Bouchard, C., Tsatas, O., and Giftochristos, N. (1990). Macrophages can modify the nonpermissive nature of the adult mammalian central nervous system. *Neuron* 5, 463–469. doi:10.1016/0896-6273(90)90085-T.

De, S., Van Deren, D., Peden, E., Hockin, M., Boulet, A., Titen, S., et al. (2018). Two distinct ontogenies confer heterogeneity to mouse brain microglia. *Dev.* 145. doi:10.1242/dev.152306.

Deczkowska, A., Keren-Shaul, H., Weiner, A., Colonna, M., Schwartz, M., and Amit, I. (2018). Disease-Associated Microglia: A Universal Immune Sensor of Neurodegeneration. *Cell* 173, 1073–1081. doi:10.1016/j.cell.2018.05.003.

Dekkers, M. P. J., Nikoletopoulou, V., and Barde, Y. A. (2013). Death of developing neurons: New insights and implications for connectivity. *J. Cell Biol.* 203, 385–393. doi:10.1083/jcb.201306136.

Dendrou, C. A., Fugger, L., and Friese, M. A. (2015). Immunopathology of multiple sclerosis. *Nat. Rev. Immunol.* 15, 545–558. doi:10.1038/nri3871.

Dideberg, V., Kristjansdottir, G., Milani, L., Libioulle, C., Sigurdsson, S., Louis, E., et al. (2007). An insertion-deletion polymorphism in the Interferon Regulatory Factor 5 (IRF5) gene confers risk of inflammatory bowel diseases. *Hum. Mol. Genet.* 16, 3008–3016. doi:10.1093/hmg/ddm259.

Dobson, R., and Giovannoni, G. (2019). Multiple sclerosis – a review. *Eur. J. Neurol.* 26, 27–40. doi:10.1111/ene.13819.

Domercq, M., Sanchez-Gomez, M. V., Sherwin, C., Etxebarria, E., Fern, R., and Matute, C. (2007). System xc- and Glutamate Transporter Inhibition Mediates Microglial Toxicity to Oligodendrocytes. *J. Immunol.* 178, 6549–6556. doi:10.4049/jimmunol.178.10.6549.

Domercq, M., Szczupak, B., Gejo, J., Gómez-Vallejo, V., Padro, D., Gona, K. B., et al. (2016). PET imaging with [18F]FSPG evidences the role of system xc- on brain inflammation following cerebral ischemia in rats. *Theranostics* 6, 1753–1767. doi:10.7150/thno.15616.

Domercq, M., Vazquez-Villoldo, N., and Matute, C. (2013). Neurotransmitter signaling in the pathophysiology of microglia. *Front. Cell. Neurosci.* 7, 1–17. doi:10.3389/fncel.2013.00049.

Dong, Y., D'Mello, C., Pinsky, W., Lozinski, B. M., Kaushik, D. K., Ghorbani, S., et al. (2021a). Oxidized phosphatidylcholines found in multiple sclerosis lesions mediate neurodegeneration and are neutralized by microglia. *Nat. Neurosci.* 24, 489–503. doi:10.1038/s41593-021-00801-z.

Dong, Y., and Yong, V. W. (2019). When encephalitogenic T cells collaborate with microglia in multiple sclerosis. *Nat. Rev. Neurol.* 15, 704–717. doi:10.1038/s41582-019-0253-6.

Du, H., Schiavi, S., Wan, N., Levine, M., Witte, D. P., and Grabowski, G. A. (2004). Reduction of Atherosclerotic Plaques by Lysosomal Acid Lipase Supplementation. *Arterioscler. Thromb. Vasc. Biol.* 24, 147–154. doi:10.1161/01.ATV.0000107030.22053.1e.

Elmore, M. R. P., Hohsfield, L. A., Kramár, E. A., Soreq, L., Lee, R. J., Pham, S. T., et al. (2018). Replacement of microglia in the aged brain reverses cognitive, synaptic, and neuronal deficits in mice. *Aging Cell* 17. doi:10.1111/acel.12832.

Elmore, M. R. P., Najafi, A. R., Koike, M. A., Dagher, N. N., Spangenberg, E. E., Rice, R. A., et al. (2014). Colony-stimulating factor 1 receptor signaling is necessary for microglia viability, unmasking a microglia progenitor cell in the adult brain. *Neuron* 82, 380–397. doi:10.1016/j.neuron.2014.02.040.

Everts, B., Amiel, E., Van Der Windt, G. J. W., Freitas, T. C., Chott, R., Yarasheski, K. E., et al. (2012). Commitment to glycolysis sustains survival of NO-producing inflammatory dendritic cells. *Blood* 120, 1422–1431. doi:10.1182/blood-2012-03-419747.

Everts, B., Amiel, E., Huang, S. C. C., Smith, A. M., Chang, C. H., Lam, W. Y., et al. (2014). TLR-driven early glycolytic reprogramming via the kinases TBK1-IKKε supports the anabolic demands of dendritic cell activation. *Nat. Immunol.* 15, 323–332. doi:10.1038/ni.2833.

Falcão, A. M., van Bruggen, D., Marques, S., Meijer, M., Jäkel, S., Agirre, E., et al. (2018). Disease-specific oligodendrocyte lineage cells arise in multiple sclerosis. *Nat. Med.* 24, 1837–1844. doi:10.1038/s41591-018-0236-y.

Fan, Z., Zhao, S., Zhu, Y., Li, Z., Liu, Z., Yan, Y., et al. (2020). Interferon Regulatory Factor 5 Mediates Lipopolysaccharide-Induced Neuroinflammation. *Front. Immunol.* 11, 1–9. doi:10.3389/fimmu.2020.600479.

Fancy, S. P. J., Zhao, C., and Franklin, R. J. M. (2004). Increased expression of Nkx2.2 and Olig2 identifies reactive oligodendrocyte progenitor cells responding to demyelination in the adult CNS. *Mol. Cell. Neurosci.* 27, 247–254. doi:10.1016/j.mcn.2004.06.015.

Fiebich, B. L., Batista, C. R. A., Saliba, S. W., Yousif, N. M., and de Oliveira, A. C. P. (2018). Role of microglia TLRs in neurodegeneration. *Front. Cell. Neurosci.* 12, 1–10. doi:10.3389/fncel.2018.00329.

Filippi, M., Bar-Or, A., Piehl, F., Preziosa, P., Solari, A., Vukusic, S., et al. (2018). Multiple sclerosis. *Nat. Rev. Dis. Prim.*, 1–27.

Fitzgerald, D. C., O'Brien, K., Young, A., Fonseca-Kelly, Z., Rostami, A., and Gran, B. (2014). Interferon regulatory factor (IRF) 3 is critical for the development of experimental autoimmune encephalomyelitis. *J. Neuroinflammation* 11, 1–7. doi:10.1186/1742-2094-11-130.

Fourgeaud, L., Traves, P. G., Tufail, Y., Leal-Bailey, H., Lew, E. D., Burrola, P. G., et al. (2016). TAM receptors regulate multiple features of microglial physiology. *Nature* 532, 240–244. doi:10.1038/nature17630.

Frade, J. M., and Barde, Y. A. (1998). Microglia-derived nerve growth factor causes cell death in the developing retina. *Neuron* 20, 35–41. doi:10.1016/S0896-6273(00)80432-8.

Franklin, R. J. M., and Ffrench-Constant, C. (2017). Regenerating CNS myelin - From mechanisms to experimental medicines. *Nat. Rev. Neurosci.* 18, 753–769. doi:10.1038/nrn.2017.136.

Freya, T. G., and Mannellab, C. A. (2000). The internal structure of mitochondria. *Trends Biochem. Sci.* 25, 319–324. doi:10.1016/S0968-0004(00)01609-1.

Fumagalli, M., Lombardi, M., Gressens, P., and Verderio, C. (2018). How to reprogram microglia toward beneficial functions. *Glia* 66, 2531–2549. doi:10.1002/glia.23484.

Funk, K. E., and Klein, R. S. (2019). CSF1R antagonism limits local restimulation of antiviral CD8+ T cells during viral encephalitis. *J. Neuroinflammation* 16, 1–19. doi:10.1186/s12974-019-1397-4.

Gabandé-Rodríguez, E., Pérez-Cañamás, A., Soto-Huelin, B., Mitroi, D. N., Sánchez-Redondo, S., Martínez-Sáez, E., et al. (2019). Lipid-induced lysosomal damage after demyelination corrupts microglia protective function in lysosomal storage disorders. *EMBO J.* 38, 1–22. doi:10.15252/embj.201899553.

Garvey, E. P., Oplinger, J. A., Furfine, E. S., Kiff, R. J., Laszlo, F., Whittle, B. J. R., et al. (1997). 1400W is a slow, tight binding, and highly selective inhibitor of inducible nitric-oxide synthase in vitro and in vivo. *J. Biol. Chem.* 272. doi:10.1074/jbc.272.8.4959.

Gebara, E., Sultan, S., Kocher-Braissant, J., and Toni, N. (2013). Adult hippocampal neurogenesis inversely correlates with microglia in conditions of voluntary running and aging. *Front. Neurosci.* 7, 1–9. doi:10.3389/fnins.2013.00145.

Ghosh, S., Castillo, E., Frias, E. S., and Swanson, R. A. (2018). Bioenergetic regulation of microglia. *Glia* 66, 1200–1212. doi:10.1002/glia.23271.

Giles, D. A., Duncker, P. C., Wilkinson, N. M., Washnock-Schmid, J. M., and Segal, B. M. (2018). CNS-resident classical DCs play a critical role in CNS autoimmune disease. *J. Clin. Invest.* 128, 5322–5334. doi:10.1172/JCI123708.

Gimeno-Bayón, J., López-López, A., Rodríguez, M. J., and Mahy, N. (2014). Glucose pathways adaptation supports acquisition of activated microglia phenotype. *J. Neurosci. Res.* 92, 723–731. doi:10.1002/jnr.23356.

Ginhoux, F., Greter, M., Leboeuf, M., Nandi, S., See, P., Mehler, M. F., et al. (2010). Fate mapping analysis reveals that adult microglia derive from primitive macrophages. *Science* 330, 841–845. doi:10.1126/science.1194637.Fate.

Ginhoux, F., Lim, S., Hoeffel, G., Low, D., and Huber, T. (2013). Origin and differentiation of microglia. *Front. Cell. Neurosci.* 7, 1–14. doi:10.3389/fncel.2013.00045.

Ginhoux, F., and Prinz, M. (2015). Origin of microglia: Current concepts and past controversies. *Cold Spring Harb. Perspect. Biol.* 7, 1–15. doi:10.1101/cshperspect.a020537.

Glenn, J. A., Ward, S. A., Stone, C. R., Booth, P. L., and Thomas, W. E. (1992). Characterisation of ramified microglial cells: detailed morphology, morphological plasticity and proliferative capability. *J. Anat.* 180 (1), 109–18.

Goldmann, T., Wieghofer, P., Müller, P. F., Wolf, Y., Varol, D., Yona, S., et al. (2013). A new type of microglia gene targeting shows TAK1 to be pivotal in CNS autoimmune inflammation. *Nat. Neurosci. 2013 1611* 16, 1618–1626. doi:10.1038/nn.3531.

Goldmann, T., Wieghofer, P., Prutek, F., Hagemeyer, N., Frenzel, K., Staszewski, O., et al. (2016). Origin, fate and dynamics of macrophages at CNS interfaces. *Nat Immunol* 17, 797–805. doi:10.1038/ni.3423.Origin.

Gouna, G., Klose, C., Bosch-Queralt, M., Liu, L., Gokce, O., Schifferer, M., et al. (2021). TREM2-dependent lipid droplet biogenesis in phagocytes is required for remyelination. *J. Exp. Med.* 218. doi:10.1084/jem.20210227.

Grajchen, E., Hendriks, J. J. A., and Bogie, J. F. J. (2018). The physiology of foamy phagocytes in multiple sclerosis. *Acta Neuropathol. Commun.* 6, 124. doi:10.1186/s40478-018-0628-8.

Greter, M., Lelios, I., and Croxford, A. L. (2015). Microglia Versus Myeloid Cell Nomenclature during Brain Inflammation. *Front. Immunol.* 6, 249. doi:10.3389/FIMMU.2015.00249.

Guerrero, B. L., and Sicotte, N. L. (2020). Microglia in Multiple Sclerosis: Friend or Foe? *Front. Immunol.* 11, 1–8. doi:10.3389/fimmu.2020.00374.

Haindl, M. T., Köck, U., Zeitelhofer-Adzemovic, M., Fazekas, F., and Hochmeister, S. (2019). The formation of a glial scar does not prohibit remyelination in an animal model of multiple sclerosis. *Glia* 67, 467–481. doi:10.1002/glia.23556.

Hampton, D. W., Innes, N., Merkler, D., Zhao, C., Franklin, R. J. M., and Chandran, S. (2012). Focal immune-mediated white matter demyelination reveals an age-associated increase in axonal vulnerability and decreased remyelination efficiency. *Am. J. Pathol.* 180, 1897–1905. doi:10.1016/j.ajpath.2012.01.018.

Hardingham, G. E., Fukunaga, Y., and Bading, H. (2002). Extrasynaptic NMDARs oppose synaptic NMDARs by triggering CREB shut-off and cell death pathways. *Nat. Neurosci.* 5, 405–414. doi:10.1038/nn835.

Haschemi, A., Kosma, P., Gille, L., Evans, C. R., Burant, C. F., Starkl, P., et al. (2012). The sedoheptulose kinase CARKL directs macrophage polarization through control of glucose metabolism. *Cell Metab.* 15, 813–826. doi:10.1016/j.cmet.2012.04.023.

Hemmer, B., Kerschensteiner, M., and Korn, T. (2015). Role of the innate and adaptive immune responses in the course of multiple sclerosis. *Lancet Neurol.* 14, 406–419. doi:10.1016/S1474-4422(14)70305-9.

Henderson, P. J., and Lardy, H. A. (1970). Bongkrekic acid. An inhibitor of the adenine nucleotide translocase of mitochondria. *J. Biol. Chem.* 245, 1319–1326.

Heppner, F. L., Greter, M., Marino, D., Falsig, J., Raivich, G., Hövelmeyer, N., et al. (2005). Experimental autoimmune encephalomyelitis repressed by microglial paralysis. *Nat. Med.* 11, 146–152. doi:10.1038/nm1177.

Herst, P. M., Grasso, C., and Berridge, M. V. (2018). Metabolic reprogramming of mitochondrial respiration in metastatic cancer. *Cancer Metastasis Rev.* 37, 643–653. doi:10.1007/s10555-018-9769-2.

Hickman, S., Kingery, N., Ohsumi, T., Borowsky, M., Wang, L., Means, T., et al. (2013). The Microglial Sensome Revealed by Direct RNA Sequencing. *Evidence-Based Pract.* 2, 6, insert 2p. doi:10.1038/nn.3554.The.

Hoeffel, G., Chen, J., Lavin, Y., Low, D., Almeida, F. F., See, P., et al. (2015). C-Myb+ Erythro-Myeloid Progenitor-Derived Fetal Monocytes Give Rise to Adult Tissue-Resident Macrophages. *Immunity* 42, 665–678. doi:10.1016/j.immuni.2015.03.011.

Holland, R., McIntosh, A. L., Finucane, O. M., Mela, V., Rubio-Araiz, A., Timmons, G., et al. (2018). Inflammatory microglia are glycolytic and iron retentive and typify the microglia in APP/PS1 mice. *Brain. Behav. Immun.* 68, 183–196. doi:10.1016/j.bbi.2017.10.017.

Honda, K., and Taniguchi, T. (2006). IRFs: Master regulators of signalling by Toll-like receptors and cytosolic pattern-recognition receptors. *Nat. Rev. Immunol.* 6, 644–658. doi:10.1038/nri1900.

Huang, D. W., Sherman, B. T., and Lempicki, R. A. (2009). Systematic and integrative analysis of large gene lists using DAVID bioinformatics resources. *Nat. Protoc.* 4, 44–57. doi:10.1038/nprot.2008.211.

Huang, Y., Xu, Z., Xiong, S., Sun, F., Qin, G., Hu, G., et al. (2018). Repopulated microglia are solely derived from the proliferation of residual microglia after acute depletion. *Nat. Neurosci.* 21, 530–540. doi:10.1038/s41593-018-0090-8.

Hughes, A. N., and Appel, B. (2020). Microglia phagocytose myelin sheaths to modify developmental myelination. *Nat. Neurosci.* 23, 1055–1066. doi:10.1038/s41593-020-0654-2.

Jahan-Abad, A. J., Karima, S., Shateri, S., Baram, S. M., Rajaei, S., Morteza-Zadeh, P., et al. (2020). Serum pro-inflammatory and anti-inflammatory cytokines and the pathogenesis of experimental autoimmune encephalomyelitis. *Neuropathology* 40, 84–92. doi:10.1111/neup.12612.

Jain, A., and Holthuis, J. C. M. (2017). Membrane contact sites, ancient and central hubs of cellular lipid logistics. *Biochim. Biophys. Acta - Mol. Cell Res.* 1864, 1450–1458. doi:10.1016/j.bbamcr.2017.05.017.

Jay, T. R., Von Saucken, V. E., and Landreth, G. E. (2017). *TREM2 in Neurodegenerative Diseases*. Molecular Neurodegeneration doi:10.1186/s13024-017-0197-5.

Jeffery, N. D., and Blakemore, W. F. (1995). Remyelination of mouse spinal cord axons demyelinated by local injection of lysolecithin. *J. Neurocytol.* 24, 775–781. doi:10.1007/BF01191213.

Jiang, H. R., Milovanović, M., Allan, D., Niedbala, W., Besnard, A. G., Fukada, S. Y., et al. (2012). IL-33 attenuates EAE by suppressing IL-17 and IFN-γ production and inducing alternatively activated macrophages. *Eur. J. Immunol.* 42, 1804–1814. doi:10.1002/eji.201141947.

Jordão, M. J. C., Sankowski, R., Brendecke, S. M., Sagar, Locatelli, G., Tai, Y. H., et al. (2019). Single-cell profiling identifies myeloid cell subsets with distinct fates during neuroinflammation. *Science* 363. doi:10.1126/science.aat7554.

Katoh, M., Wu, B., Nguyen, H. B., Thai, T. Q., Yamasaki, R., Lu, H., et al. (2017). Polymorphic regulation of mitochondrial fission and fusion modifies phenotypes of microglia in neuroinflammation. *Sci. Rep.* 7, 1–14. doi:10.1038/s41598-017-05232-0.

Kawai, T., and Akira, S. (2009). The roles of TLRs, RLRs and NLRs in pathogen recognition. *Int. Immunol.* 21, 317–337. doi:10.1093/intimm/dxp017.

Kelly, B., and O'Neill, L. A. J. (2015). Metabolic reprogramming in macrophages and dendritic cells in innate immunity. *Cell Res.* 25, 771–784. doi:10.1038/cr.2015.68.

Keren-Shaul, H., Spinrad, A., Weiner, A., Matcovitch-Natan, O., Dvir-Szternfeld, R., Ulland, T. K., et al. (2017). A Unique Microglia Type Associated with Restricting Development of Alzheimer's Disease. *Cell* 169, 1276-1290.e17. doi:10.1016/j.cell.2017.05.018.

Kerkhofs, D., Van Hagen, B. T., Milanova, I. V., Schell, K. J., Van Essen, H., Wijnands, E., et al. (2020). Pharmacological depletion of microglia and perivascular macrophages prevents Vascular Cognitive Impairment in Ang II-induced hypertension. *Theranostics* 10, 9512–9527. doi:10.7150/thno.44394.

Kettenmann, H., Hanisch, U. K., Noda, M., and Verkhratsky, A. (2011). Physiology of microglia. *Physiol. Rev.* 91, 461–553. doi:10.1152/physrev.00011.2010.

Kierdorf, K., Erny, D., Goldmann, T., Sander, V., Schulz, C., Perdiguero, E. G., et al. (2013). Microglia emerge from erythromyeloid precursors via Pu.1-and Irf8-dependent pathways. *Nat. Neurosci.* 16, 273–280. doi:10.1038/nn.3318.

Kierdorf, K., and Prinz, M. (2017). Microglia in steady state. *J. Clin. Invest.* 127, 3201–3209. doi:10.1172/JCI90602.

Kinosita, K., Adachi, K., and Itoh, H. (2004). Rotation of F1-ATPase: How an ATP-driven molecular machine may work. *Annu. Rev. Biophys. Biomol. Struct.* 33, 245–268. doi:10.1146/annurev.biophys.33.110502.132716.

Kobayakawa, K., Ohkawa, Y., Yoshizaki, S., Tamaru, T., Saito, T., Kijima, K., et al. (2019). Macrophage centripetal migration drives spontaneous healing process after spinal cord injury. *Sci. Adv.* 5. doi:10.1126/sciadv.aav5086.

Kondo, Y., Adams, J. M., Vanier, M. T., and Duncan, I. D. (2011). Macrophages counteract demyelination in a mouse model of globoid cell leukodystrophy. *J. Neurosci.* 31, 3610–3624. doi:10.1523/JNEUROSCI.6344-10.2011.

Kotter, M. R., Li, W. W., Zhao, C., and Franklin, R. J. M. (2006). Myelin impairs CNS remyelination by inhibiting oligodendrocyte precursor cell differentiation. *J. Neurosci.* 26, 328–332. doi:10.1523/JNEUROSCI.2615-05.2006.

Kotter, M. R., Setzu, A., Sim, F. J., Van Rooijen, N., and Franklin, R. J. M. (2001). Macrophage depletion impairs oligodendrocyte remyelination following lysolecithin-induced demyelination. *Glia* 35, 204–212. doi:10.1002/glia.1085.

Krasemann, S., Madore, C., Cialic, R., Baufeld, C., Calcagno, N., El Fatimy, R., et al. (2017). The TREM2-APOE Pathway Drives the Transcriptional Phenotype of Dysfunctional Microglia in Neurodegenerative Diseases. *Immunity* 47, 566-581.e9. doi:10.1016/j.immuni.2017.08.008.

Krausgruber, T., Blazek, K., Smallie, T., Alzabin, S., Lockstone, H., Sahgal, N., et al. (2011). IRF5 promotes inflammatory macrophage polarization and T H1-TH17 responses. *Nat. Immunol.* 12, 231–238. doi:10.1038/ni.1990.

Kristjansdottir, G., Sandling, J. K., Bonetti, A., Roos, I. M., Milani, L., Wang, C., et al. (2008). Interferon regulatory factor 5 (IRF5) gene variants are associated with multiple sclerosis in three distinct populations. *J. Med. Genet.* 45, 362–369. doi:10.1136/jmg.2007.055012.

Kubota, Y., Takubo, K., Shimizu, T., Ohno, H., Kishi, K., Shibuya, M., et al. (2009). M-CSF inhibition selectively targets pathological angiogenesis and lymphangiogenesis. *J. Exp. Med.* 206, 1089–1102. doi:10.1084/jem.20081605.

Lampron, A., Larochelle, A., Laflamme, N., Préfontaine, P., Plante, M. M., Sánchez, M. G., et al. (2015). Inefficient clearance of myelin debris by microglia impairs remyelinating processes. *J. Exp. Med.* 212, 481–495. doi:10.1084/jem.20141656.

Lassmann, H., and van Horssen, J. (2016). Oxidative stress and its impact on neurons and glia in multiple sclerosis lesions. *Biochim. Biophys. Acta - Mol. Basis Dis.* 1862, 506–510. doi:10.1016/j.bbadis.2015.09.018.

Lassmann, H., and Bradl, M. (2017). Multiple sclerosis: experimental models and reality. *Acta Neuropathol.* 133, 223–244. doi:10.1007/s00401-016-1631-4.

Lee, Y. B., Nagai, A., and Kim, S. U. (2002). Cytokines, chemokines, and cytokine receptors in human microglia. *J. Neurosci. Res.* 69, 94–103. doi:10.1002/jnr.10253.

Lei, F., Cui, N., Zhou, C., Chodosh, J., Vavvas, D. G., and Paschalis, E. I. (2020). CSF1R inhibition by a small-molecule inhibitor is not microglia specific; Affecting hematopoiesis and the function of macrophages. *Proc. Natl. Acad. Sci. U. S. A.* 117, 23336–23338. doi:10.1073/pnas.1922788117.

Liddelow, S. A., Guttenplan, K. A., Clarke, L. E., Bennett, F. C., Bohlen, C. J., Schirmer, L., et al. (2017). Neurotoxic reactive astrocytes are induced by activated microglia. *Nature* 541, 481–487. doi:10.1038/nature21029.

Lloyd, A. F., Davies, C. L., Holloway, R. K., Labrak, Y., Ireland, G., Carradori, D., et al. (2019). Central nervous system regeneration is driven by microglia necroptosis and repopulation. *Nat. Neurosci.* 22, 1046–1052. doi:10.1038/s41593-019-0418-z.

Locatelli, G., Theodorou, D., Kendirli, A., Jordão, M. J. C., Staszewski, O., Phulphagar, K., et al. (2018). Mononuclear phagocytes locally specify and adapt their phenotype in a multiple sclerosis model. *Nat. Neurosci.* 21, 1196–1208. doi:10.1038/s41593-018-0212-3.

Lovett-Racke, A. E., Yang, Y., and Racke, M. K. (2011). Th1 versus Th17: Are T cell cytokines relevant in multiple sclerosis? *Biochim. Biophys. Acta - Mol. Basis Dis.* 1812, 246–251. doi:10.1016/j.bbadis.2010.05.012.

Lublin, F. D., and Reingold, S. C. (1996). Defining the clinical course of multiple sclerosis: Results of an international survey. *Neurology* 46, 907–911. doi:10.1212/WNL.46.4.907.

Lublin, F. D., Reingold, S. C., Cohen, J. A., Cutter, G. R., Thompson, A. J., Wolinsky, J. S., et al. (2014). Defining the clinical course of multiple sclerosis - The 2013 revisions. *Neurology* 83, 278–286.

Lucchinetti, C., Brück, W., Parisi, J., Scheithauer, B., Rodriguez, M., and Lassmann, H. (2000). Heterogeneity of multiple sclerosis lesions: Implications for the pathogenesis of demyelination. *Ann. Neurol.* 47, 707–717. doi:10.1002/1531-8249(200006)47:6<707::AID-ANA3>3.0.CO;2-Q.

Luoma, A. M., Kuo, F., Cakici, O., Crowther, M. N., Denninger, A. R., Avila, R. L., et al. (2015). Plasmalogen phospholipids protect internodal myelin from oxidative damage. *Free Radic. Biol. Med.* 84, 296–310. doi:10.1016/j.freeradbiomed.2015.03.012.

Madsen, P. M., Motti, D., Karmally, S., Szymkowski, D. E., Lambertsen, K. L., Bethea, J. R., et al. (2016). Oligodendroglial TNFR2 mediates membrane TNF-dependent repair in experimental autoimmune encephalomyelitis by promoting oligodendrocyte differentiation and remyelination. *J. Neurosci.* 36, 5128–5143. doi:10.1523/JNEUROSCI.0211-16.2016.

Mailleux, J., Vanmierlo, T., Bogie, J. F. J., Wouters, E., Lütjohann, D., Hendriks, J. J. A., et al. (2018). Active liver X receptor signaling in phagocytes in multiple sclerosis lesions. *Mult. Scler. J.* 24, 279–289. doi:10.1177/1352458517696595.

Marschallinger, J., Iram, T., Zardeneta, M., Lee, S. E., Lehallier, B., Haney, M. S., et al. (2020). Lipid-droplet-accumulating microglia represent a dysfunctional and proinflammatory state in the

aging brain. *Nat. Neurosci.* 23, 194–208. doi:10.1038/s41593-019-0566-1.

Masuda, T., Iwamoto, S., Yoshinaga, R., Nishiyama, A., Tsuda, M., Tamura, T., et al. (2014). Transcription factor IRF5 drives P2X4R+-reactive microglia gating neuropathic pain. *Nat. Commun.* 5, 1–11. doi:10.1038/ncomms4771.

Masuda, T., Sankowski, R., Staszewski, O., Böttcher, C., Amann, L., Sagar, et al. (2019). Spatial and temporal heterogeneity of mouse and human microglia at single-cell resolution. *Nature* 566, 388–392. doi:10.1038/s41586-019-0924-x.

Masuda, T., Sankowski, R., Staszewski, O., and Prinz, M. (2020). Microglia Heterogeneity in the Single-Cell Era. *Cell Rep.* 30, 1271–1281. doi:10.1016/j.celrep.2020.01.010.

Matute, C., Alberdi, E., Domercq, M., Pérez-Cerdá, F., Pérez-Samartín, A., and Sánchez-Gómez, M. V. (2001). The link between excitotoxic oligodendroglial death and demyelinating diseases. *Trends Neurosci.* 24, 224–230. doi:10.1016/S0166-2236(00)01746-X.

Matute, C., and Pérez-Cerdá, F. (2005). Multiple sclerosis: Novel perspectives on newly forming lesions. *Trends Neurosci.* 28, 173–175. doi:10.1016/j.tins.2005.01.006.

Matute, C., Torre, I., Pérez-Cerdá, F., Pérez-Samartín, A., Alberdi, E., Etxebarria, E., et al. (2007). P2X7 receptor blockade prevents ATP excitotoxicity in oligodendrocytes and ameliorates experimental autoimmune encephalomyelitis. *J. Neurosci.* 27, 9525–9533. doi:10.1523/JNEUROSCI.0579-07.2007.

Maxfield, F. R., and Tabas, I. (2005). Role of cholesterol and lipid organization in disease. *Nature* 438, 612–621.

McIntosh, A., Mela, V., Harty, C., Minogue, A. M., Costello, D. A., Kerskens, C., et al. (2019). Iron accumulation in microglia triggers a cascade of events that leads to altered metabolism and compromised function in APP/PS1 mice. *Brain Pathol.* 29, 606–621. doi:10.1111/bpa.12704.

Mildner, A., MacK, M., Schmidt, H., Brück, W., Djukic, M., Zabel, M. D., et al. (2009). CCR2+Ly-6Chi monocytes are crucial for the effector phase of autoimmunity in the central nervous system. *Brain* 132, 2487–2500. doi:10.1093/brain/awp144.

Milior, G., Lecours, C., Samson, L., Bisht, K., Poggini, S., Pagani, F., et al. (2016). Fractalkine receptor deficiency impairs microglial and neuronal responsiveness to chronic stress. *Brain. Behav. Immun.* 55, 114–125. doi:10.1016/j.bbi.2015.07.024.

Miron, V. E., Boyd, A., Zhao, J.-W., Yuen, T. J., Ruckh, J. M., Shadrach, J. L., et al. (2013). M2 microglia / macrophages drive oligodendrocyte differentiation during CNS remyelination. *Nat. Neurosci.* 16, 1211–1218. doi:10.1038/nn.3469.M2.

Miron, V. E., and Franklin, R. J. M. (2014). Macrophages and CNS remyelination. *J. Neurochem.* 130, 165–171. doi:10.1111/JNC.12705.

Mittelbronn, M., Dietz, K., Schluesener, H. J., and Meyermann, R. (2001). Local distribution of microglia in the normal adult human central nervous system differs by up to one order of magnitude. *Acta Neuropathol.* 101, 249–255. doi:10.1007/s004010000284.

Mondelli, V., Vernon, A. C., Turkheimer, F., Dazzan, P., and Pariante, C. M. (2017). Brain microglia in psychiatric disorders. *The Lancet Psychiatry* 4, 563–572. doi:10.1016/S2215-0366(17)30101-3.

Monson, E. A., Trenerry, A. M., Laws, J. L., MacKenzie, J. M., and Helbig, K. J. (2021). Lipid droplets and lipid mediators in viral infection and immunity. *FEMS Microbiol. Rev.* 45, 1–20. doi:10.1093/femsre/fuaa066.

Montilla, A., Ruiz, A., Marquez, M., Sierra, A., Matute, C., and Domercq, M. (2021). Role of Mitochondrial Dynamics in Microglial Activation and Metabolic Switch. *ImmunoHorizons* 5, 615–626. doi:10.4049/immunohorizons.2100068.

Montilla, A., Zabala, A., Matute, C., and Domercq, M. (2020). Functional and Metabolic Characterization of Microglia Culture in a Defined Medium. *Front. Cell. Neurosci.* 14, 1–11. doi:10.3389/fncel.2020.00022.

Moore, K. J., and Tabas, I. (2011). Macrophages in the pathogenesis of atherosclerosis. *Cell* 145, 341–355. doi:10.1016/j.cell.2011.04.005.

Mundt, S., Mrdjen, D., Utz, S. G., Greter, M., Schreiner, B., and Becher, B. (2019). Conventional DCs sample and present myelin antigens in the healthy CNS and allow parenchymal T cell entry to initiate neuroinflammation. *Sci. Immunol.* 4. doi:10.1126/sciimmunol.aau8380.

Nadjar, A. (2018). Role of metabolic programming in the modulation of microglia phagocytosis by lipids. *Prostaglandins Leukot. Essent. Fat. Acids* 135, 63–73. doi:10.1016/j.plefa.2018.07.006.

Nair, S., Sobotka, K. S., Joshi, P., Gressens, P., Fleiss, B., Thornton, C., et al. (2019). Lipopolysaccharide-induced alteration of mitochondrial morphology induces a metabolic shift in microglia modulating the inflammatory response in vitro and in vivo. *Glia* 67, 1047–1061. doi:10.1002/glia.23587.

Neumann, H., Kotter, M. R., and Franklin, R. J. M. (2009). Debris clearance by microglia: An essential link between degeneration and regeneration. *Brain* 132, 288–295. doi:10.1093/brain/awn109.

Nimmerjahn, A., Kirchhoff, F., and Helmchen, F. (2005). Resting microglial cells are highly dynamic surveillants of brain parenchyma in vivo. *Science* 308, 1314–1318. doi:10.1126/science.1110647.

Nissen, J. C., Thompson, K. K., West, B. L., and Tsirka, S. E. (2018). Csf1R inhibition attenuates experimental autoimmune encephalomyelitis and promotes recovery. *Exp. Neurol.* 307, 24–36. doi:10.1016/j.expneurol.2018.05.021.

Nordmark, G., Kristjansdottir, G., Theander, E., Eriksson, P., Brun, J. G., Wang, C., et al. (2009). Additive effects of the major risk alleles of IRF5 and STAT4 in primary Sjögren's syndrome. *Genes Immun.* 10, 68–76. doi:10.1038/gene.2008.94.

Norton, W. T., and Poduslo, S. (1973). Isolation and Characterization of Myelin. *J. Neurochem.* 21, 147–195. doi:10.1007/978-1-4757-1830-0_5.

Nott, A., Holtman, I. R., Coufal, N. G., Schlachetzki, J. C. M., Yu, M., Hu, R., et al. (2019). Brain cell type–specific enhancer–promoter interactome maps and disease-risk association. *Science* 366, 1134–1139. doi:10.1126/science.aay0793.

Nugent, A. A., Lin, K., van Lengerich, B., Lianoglou, S., Przybyla, L., Davis, S. S., et al. (2020). TREM2 Regulates Microglial Cholesterol Metabolism upon Chronic Phagocytic Challenge. *Neuron* 105, 837-854.e9. doi:10.1016/j.neuron.2019.12.007.

Oren, R., Farnham, A. E., Saito, K., Milofsky, E., and Karnovsky, M. L. (1963). Metabolic patterns in three types of phagocytizing cells. *J. Cell Biol.* 17, 487–501. doi:10.1083/jcb.17.3.487.

Orihuela, R., McPherson, C. A., and Harry, G. J. (2016). Microglial M1/M2 polarization and metabolic states. *Br. J. Pharmacol.* 173, 649–665. doi:10.1111/bph.13139.

Palumbo, S., and Pellegrini, S. (2017). "Experimental In Vivo Models of Multiple Sclerosis: State of the Art," in *Multiple Sclerosis: Perspectives in Treatment and Pathogenesis*, 173–183. doi:10.15586/codon.multiplesclerosis.2017.ch11.

Paolicelli, R. C., Bolasco, G., Pagani, F., Maggi, L., Scianni, M., Panzanelli, P., et al. (2011). Synaptic pruning by microglia is necessary for normal brain development. *Science* 333, 1456–1458. doi:10.1126/science.1202529.

Park, J., Min, J. S., Chae, U., Lee, J. Y., Song, K. S., Lee, H. S., et al. (2017). Anti-inflammatory effect of oleuropein on microglia through regulation of Drp1-dependent mitochondrial fission. *J. Neuroimmunol.* 306, 46–52. doi:10.1016/j.jneuroim.2017.02.019.

Parkhurst, C. N., Yang, G., Ninan, I., Savas, J. N., Yates, J. R., Lafaille, J. J., et al. (2013). Microglia promote learning-dependent synapse formation through brain-derived neurotrophic factor. *Cell* 155, 1596–1609. doi:10.1016/j.cell.2013.11.030.

Patel, J. R., McCandless, E. E., Dorsey, D., and Klein, R. S. (2010). CXCR4 promotes differentiation of oligodendrocyte progenitors and remyelination. *Proc. Natl. Acad. Sci. U. S. A.* 107, 11062–11067. doi:10.1073/pnas.1006301107.

Patsopoulos, N. A., Baranzini, S. E., Santaniello, A., Shoostari, P., Cotsapas, C., Wong, G., et al. (2019). Multiple sclerosis genomic map implicates peripheral immune cells and microglia in susceptibility. *Science* 365. doi:10.1126/science.aav7188.

Plemel, J. R., Manesh, S. B., Sparling, J. S., and Tetzlaff, W. (2013). Myelin inhibits oligodendroglial maturation and regulates oligodendrocytic transcription factor expression. *Glia* 61, 1471–1487. doi:10.1002/glia.22535.

Plemel, J. R., Stratton, J. A., Michaels, N. J., Rawji, K. S., Zhang, E., Sinha, S., et al. (2020). Microglia response following acute demyelination is heterogeneous and limits infiltrating macrophage dispersion. *Sci. Adv.* 6, 1–15. doi:10.1126/sciadv.aay6324.

Pocivavsek, A., Burns, M. P., and Rebeck, G. W. (2009). Low-density lipoprotein receptors regulate microglial inflammation through c-Jun N-terminal kinase. *Glia* 57, 444–453. doi:10.1002/glia.20772.

Poitelon, Y., Kopec, A. M., and Belin, S. (2020). Myelin Fat Facts: An Overview of Lipids and Fatty Acid Metabolism. *Cells* 9. doi:10.3390/cells9040812.

Pont-Lezica, L., Beumer, W., Colasse, S., Drexhage, H., Versnel, M., and Bessis, A. (2014). Microglia shape corpus callosum axon tract fasciculation: Functional impact of prenatal inflammation. *Eur. J. Neurosci.* 39, 1551–1557. doi:10.1111/ejn.12508.

Porporato, P. E., Filigheddu, N., Pedro, J. M. B. S., Kroemer, G., and Galluzzi, L. (2018). Mitochondrial metabolism and cancer. *Cell Res.* 28, 265–280. doi:10.1038/cr.2017.155.

Prinz, M., Masuda, T., Wheeler, M. A., and Quintana, F. J. (2021). Microglia and Central Nervous System-Associated Macrophages mdash from Origin to Disease Modulation. *Annu. Rev. Immunol.* 39, 251–277. doi:10.1146/annurev-immunol-093019-110159.

Prinz, M., and Priller, J. (2014). Microglia and brain macrophages in the molecular age: From origin to neuropsychiatric disease. *Nat. Rev. Neurosci.* 15, 300–312. doi:10.1038/nrn3722.

Prinz, M., and Priller, J. (2017). The role of peripheral immune cells in the CNS in steady state and

disease. *Nat. Neurosci. 2017 202* 20, 136–144. doi:10.1038/nn.4475.

Psachoulia, K., Chamberlain, K. A., Heo, D., Davis, S. E., Paskus, J. D., Nanescu, S. E., et al. (2016). IL4I1 augments CNS remyelination and axonal protection by modulating T cell driven inflammation. *Brain* 139, 3121–3136. doi:10.1093/brain/aww254.

Ransohoff, R. M. (2012). Animal models of multiple sclerosis: The good, the bad and the bottom line. *Nat. Neurosci.* 15, 1074–1077. doi:10.1038/nn.3168.

Ransohoff, R. M. (2016). A polarizing question: Do M1 and M2 microglia exist. *Nat. Neurosci.* 19, 987–991. doi:10.1038/nn.4338.

Rath, M., Müller, I., Kropf, P., Closs, E. I., and Munder, M. (2014). Metabolism via arginase or nitric oxide synthase: two competing arginine pathways in macrophages. *Front Immunol.* 5, 1–10. doi:10.3389/fimmu.2014.00532.

Rawji, K. S., Mishra, M. K., and Yong, V. W. (2016). Regenerative capacity of macrophages for remyelination. *Front. Cell Dev. Biol.* 4. doi:10.3389/fcell.2016.00047.

Ribeiro Xavier, A. L., Kress, B. T., Goldman, S. A., De Lacerda Menezes, J. R., and Nedergaard, M. (2015). A distinct population of microglia supports adult neurogenesis in the subventricular zone. *J. Neurosci.* 35, 11848–11861. doi:10.1523/JNEUROSCI.1217-15.2015.

Robinson, M. D., McCarthy, D. J., and Smyth, G. K. (2009). edgeR: A Bioconductor package for differential expression analysis of digital gene expression data. *Bioinformatics* 26, 139–140. doi:10.1093/bioinformatics/btp616.

Rogulja-Ortmann, A., Lüer, K., Seibert, J., Rickert, C., and Technau, G. M. (2007). Programmed cell death in the embryonic central nervous system of Drosophila melanogaster. *Development* 134, 105–116. doi:10.1242/dev.02707.

Rong, S., Cortés, V. A., Rashid, S., Anderson, N. N., McDonald, J. G., Liang, G., et al. (2017). Expression of SREBP-1c requires SREBP-2-mediated generation of a sterol ligand for LXR in livers of mice. *Elife* 6, 1–17. doi:10.7554/eLife.25015.

Rong, Z., Cheng, B., Zhong, L., Ye, X., Li, X., Jia, L., et al. (2020). Activation of FAK/Rac1/Cdc42-GTPase signaling ameliorates impaired microglial migration response to Aβ42 in triggering receptor expressed on myeloid cells 2 loss-of-function murine models. *FASEB J.* 34, 10984–10997. doi:10.1096/fj.202000550RR.

Rosati, G. (2001). The prevalence of multiple sclerosis in the world: An update. *Neurol. Sci.* 22, 117–139. doi:10.1007/s100720170011.

Rubio-Araiz, A., Finucane, O. M., Keogh, S., and Lynch, M. A. (2018). Anti-TLR2 antibody triggers oxidative phosphorylation in microglia and increases phagocytosis of β-amyloid. *J. Neuroinflammation* 15, 1–13. doi:10.1186/s12974-018-1281-7.

Saliba, D. G., Heger, A., Eames, H. L., Oikonomopoulos, S., Teixeira, A., Blazek, K., et al. (2014). IRF5:RelA interaction targets inflammatory genes in macrophages. *Cell Rep.* 8, 1308–1317. doi:10.1016/j.celrep.2014.07.034.

Sariol, A., Mackin, S., Allred, M. G., Ma, C., Zhou, Y., Zhang, Q., et al. (2020). Microglia depletion exacerbates demyelination and impairs remyelination in a neurotropic coronavirus infection. *Proc. Natl. Acad. Sci. U. S. A.* 117, 24464–24474. doi:10.1073/pnas.2007814117.

Schafer, D., Lehrman, E., Kautzman, A., Koyama, R., Mardinly, A., Yamasaki, R., et al. (2012). Microglia sculpt postnatal neuronal circuits in an activivty and complement-dependent manner. *Neuron* 74, 691–705. doi:10.1016/j.neuron.2012.03.026.Microglia.

Schafer, D., and Stevens, B. (2015). Microglia Function in Central Nervous System Development and Plasticity. *Cold Spring Harb Perspect Biol* 7. doi:10.1016/s1054-3589(08)60887-x.

Schirmer, L., Srivastava, R., and Hemmer, B. (2014). To look for a needle in a haystack: The search for autoantibodies in multiple sclerosis. *Mult. Scler. J.* 20, 271–279. doi:10.1177/1352458514522104.

Schulz, C., Perdiguero, E. G., Chorro, L., Szabo-Rogers, H., Cagnard, N., Kierdorf, K., et al. (2012). A lineage of myeloid cells independent of myb and hematopoietic stem cells. *Science* 335, 86–90. doi:10.1126/science.1219179.

Schuster, S., Boley, D., Möller, P., Stark, H., and Kaleta, C. (2015). Mathematical models for explaining the Warburg effect: A review focussed on ATP and biomass production. *Biochem. Soc. Trans.* 43, 1187–1194. doi:10.1042/BST20150153.

Shemer, A., and Jung, S. (2015). Differential roles of resident microglia and infiltrating monocytes in murine CNS autoimmunity. *Semin. Immunopathol.* 37, 613–623. doi:10.1007/s00281-015-0519-z.

Shen, K., Reichelt, M., Kyauk, R. V., Ngu, H., Shen, Y. A. A., Foreman, O., et al. (2021). Multiple sclerosis risk gene Mertk is required for microglial activation and subsequent remyelination. *Cell Rep.* 34, 108835. doi:10.1016/j.celrep.2021.108835.

Shigemoto-Mogami, Y., Hoshikawa, K., Goldman, J. E., Sekino, Y., and Sato, K. (2014). Microglia enhance neurogenesis and oligodendrogenesis in the early postnatal subventricular zone. *J. Neurosci.* 34, 2231–2243. doi:10.1523/JNEUROSCI.1619-13.2014.

Shimane, K., Kochi, Y., Yamada, R., Okada, Y., Suzuki, A., Miyatake, A., et al. (2009). A single nucleotide polymorphism in the IRF5 promoter region is associated with susceptibility to rheumatoid arthritis in the Japanese population. *Ann. Rheum. Dis.* 68, 377–383. doi:10.1136/ard.2007.085704.

Sierra, A., Encinas, J. M., Deudero, J. J. P., Chancey, J. H., Enikolopov, G., Linda, S., et al. (2010). Microglia Shape Adult Hippocampal Neurogenesis through Apoptosis-Coupled Phagocytosis. *Cell Stem Cell* 7, 1–13. doi:10.1016/j.stem.2010.08.014.Microglia.

Sierra, A., Paolicelli, R. C., and Kettenmann, H. (2019). Cien Años de Microglía: Milestones in a Century of Microglial Research. *Trends Neurosci.* 42, 778–792. doi:10.1016/j.tins.2019.09.004.

Sigurdsson, S., Nordmark, G., Göring, H. H. H., Lindroos, K., Wiman, A.-C., Sturfelt, G., et al. (2005). Polymorphisms in the Tyrosine Kinase 2 and Interferon Regulatory Factor 5 Genes Are Associated with Systemic Lupus Erythematosus. *Am. J. Hum. Genet.* 76, 528–537. doi:10.3987/com-06-s(o)49.

Singh, S., Metz, I., Amor, S., Van Der Valk, P., Stadelmann, C., and Brück, W. (2013). Microglial nodules in early multiple sclerosis white matter are associated with degenerating axons. *Acta Neuropathol.* 125, 595–608. doi:10.1007/s00401-013-1082-0.

Slavin, A., Ewing, C., Liu, J., Ichikawa, M., Slavin, J., and Bernard, C. C. A. (1998). Induction of a multiple sclerosis-like disease in mice with an immunodominant epitope of myelin oligodendrocyte glycoprotein. *Autoimmunity* 28, 109–120. doi:10.3109/08916939809003872.

Sloane, J. A., Batt, C., Ma, Y., Harris, Z. M., Trapp, B., and Vartanian, T. (2010). Hyaluronan blocks oligodendrocyte progenitor maturation and remyelination through TLR2. *Proc. Natl. Acad. Sci. U. S. A.* 107, 11555–11560. doi:10.1073/pnas.1006496107.

Smith, K. J., Kapoor, R., and Felts, P. A. (1999). Demyelination: The role of reactive oxygen and nitrogen species. *Brain Pathol.* 9, 69–92. doi:10.1111/j.1750-3639.1999.tb00212.x.

Solaini, G., Baracca, A., Lenaz, G., and Sgarbi, G. (2010). Hypoxia and mitochondrial oxidative metabolism. *Biochim. Biophys. Acta - Bioenerg.* 1797, 1171–1177. doi:10.1016/j.bbabio.2010.02.011.

Spangenberg, E., Severson, P. L., Hohsfield, L. A., Crapser, J., Zhang, J., Burton, E. A., et al. (2019). Sustained microglial depletion with CSF1R inhibitor impairs parenchymal plaque development in an Alzheimer's disease model. *Nat. Commun.* 10, 1–21. doi:10.1038/s41467-019-11674-z.

Spiteri, A. G., Ni, D., Ling, Z. L., Macia, L., Campbell, I. L., Hofer, M. J., et al. (2022). PLX5622 Reduces Disease Severity in Lethal CNS Infection by Off-Target Inhibition of Peripheral Inflammatory Monocyte Production. *Front. Immunol.* 13, 1–16. doi:10.3389/fimmu.2022.851556.

Stephan, A. H., Barres, B. A., and Stevens, B. (2012). The complement system: An unexpected role in synaptic pruning during development and disease. *Annu. Rev. Neurosci.* 35, 369–389. doi:10.1146/annurev-neuro-061010-113810.

Stienstra, R., Netea-Maier, R. T., Riksen, N. P., Joosten, L. A. B., and Netea, M. G. (2017). Specific and Complex Reprogramming of Cellular Metabolism in Myeloid Cells during Innate Immune Responses. *Cell Metab.* 26, 142–156. doi:10.1016/j.cmet.2017.06.001.

Strachan-Whaley, M., Rivest, S., and Yong, V. W. (2014). Interactions between microglia and T cells in multiple sclerosis pathobiology. *J. Interf. Cytokine Res.* 34, 615–622. doi:10.1089/jir.2014.0019.

Sun, D., Yu, Z., Fang, X., Liu, M., Pu, Y., Shao, Q., et al. (2017). Lnc RNA GAS 5 inhibits microglial M2 polarization and exacerbates demyelination . *EMBO Rep.* 18, 1801–1816. doi:10.15252/embr.201643668.

Tada, B. Y., Ho, A., Matsuyama, T., and Mak, T. W. (1997). Reduced Incidence and Severity of Antigen-induced Regulatory Factor-1. *J Exp Med* 185, 231–238.

Takaoka, A., Yanai, H., Kondo, S., Duncan, G., Negishi, H., Mizutani, T., et al. (2005). Integral role of IRF-5 in the gene induction programme activated by Toll-like receptors. *Nature* 434, 243–249. doi:10.1038/nature03308.

Tamura, T., Yanai, H., Savitsky, D., and Taniguchi, T. (2008). The IRF family transcription factors in immunity and oncogenesis. *Annu. Rev. Immunol.* 26, 535–584. doi:10.1146/annurev.immunol.26.021607.090400.

Tanabe, S., Saitoh, S., Miyajima, H., Itokazu, T., and Yamashita, T. (2019). Microglia suppress the secondary progression of autoimmune encephalomyelitis. *Glia* 67, 1694–1704. doi:10.1002/glia.23640.

Tepavčevič, V., Kerninon, C., Aigrot, M. S., Meppiel, E., Mozafari, S., Arnould-Laurent, R., et al. (2014). Early netrin-1 expression impairs central nervous system remyelination. *Ann. Neurol.* 76, 252–268. doi:10.1002/ana.24201.

Thomas, A., Charbonneau, J. L., Fournaise, E., and Chaurand, P. (2012). Sublimation of new matrix candidates for high spatial resolution imaging mass spectrometry of lipids: Enhanced information in both positive and negative polarities after 1,5-diaminonapthalene deposition. *Anal. Chem.* 84, 2048–2054. doi:10.1021/ac2033547.

Thompson, A. J., Baranzini, S. E., Geurts, J., Hemmer, B., and Ciccarelli, O. (2018). Multiple sclerosis. *Lancet* 391, 1622–1636. doi:10.1016/S0140-6736(18)30481-1.

Tierney, J. B., Kharkrang, M., and La Flamme, A. C. (2009). Type II-activated macrophages suppress the development of experimental autoimmune encephalomyelitis. *Immunol. Cell Biol.* 87, 235–240. doi:10.1038/icb.2008.99.

Tokizane, K., Konishi, H., Makide, K., Kawana, H., Nakamuta, S., Kaibuchi, K., et al. (2017). Phospholipid localization implies microglial morphology and function via Cdc42 in vitro. *Glia* 65, 740–755. doi:10.1002/glia.23123.

Tremblay, M. Ě., Lowery, R. L., and Majewska, A. K. (2010). Microglial interactions with synapses are modulated by visual experience. *PLoS Biol.* 8. doi:10.1371/journal.pbio.1000527.

Ueno, M., Fujita, Y., Tanaka, T., Nakamura, Y., Kikuta, J., Ishii, M., et al. (2013). Layer v cortical neurons require microglial support for survival during postnatal development. *Nat. Neurosci.* 16, 543–551. doi:10.1038/nn.3358.

Vainchtein, I. D., Vinet, J., Brouwer, N., Brendecke, S., Biagini, G., Biber, K., et al. (2014). In acute experimental autoimmune encephalomyelitis, infiltrating macrophages are immune activated, whereas microglia remain immune suppressed. *Glia* 62, 1724–1735. doi:10.1002/glia.22711.

Van den Bossche, J., Baardman, J., Otto, N. A., van der Velden, S., Neele, A. E., van den Berg, S. M., et al. (2016). Mitochondrial Dysfunction Prevents Repolarization of Inflammatory Macrophages. *Cell Rep.* 17, 684–696. doi:10.1016/j.celrep.2016.09.008.

Van den Bossche, J., O'Neill, L. A., and Menon, D. (2017). Macrophage Immunometabolism: Where Are We (Going)? *Trends Immunol.* 38, 395–406. doi:10.1016/j.it.2017.03.001.

van der Poel, M., Ulas, T., Mizee, M. R., Hsiao, C. C., Miedema, S. S. M., Adelia, et al. (2019). Transcriptional profiling of human microglia reveals grey–white matter heterogeneity and multiple sclerosis-associated changes. *Nat. Commun.* 10, 1–13. doi:10.1038/s41467-019-08976-7.

Van Horssen, J., Dijkstra, C. D., and De Vries, H. E. (2007). The extracellular matrix in multiple sclerosis pathology. *J. Neurochem.* 103, 1293–1301. doi:10.1111/j.1471-4159.2007.04897.x.

Vandenbroeck, K., Alloza, I., Swaminathan, B., Antigüedad, A., Otaegui, D., Olascoaga, J., et al. (2011). Validation of IRF5 as multiple sclerosis risk gene: Putative role in interferon beta therapy and human herpes virus-6 infection. *Genes Immun.* 12, 40–45. doi:10.1038/gene.2010.46.

Vandesompele, J., De Preter, K., Pattyn, F., Poppe, B., Van Roy, N., De Paepe, A., et al. (2002). Accurate normalization of real-time quantitative RT-PCR data by geometric averaging of multiple internal control genes. *Genome Biol.* 3, RESEARCH0034. doi:10.1186/gb-2002-3-7-research0034.

Vats, D., Mukundan, L., Odegaard, J. I., Zhang, L., Smith, K. L., Morel, C. R., et al. (2006). Oxidative metabolism and PGC-1β attenuate macrophage-mediated inflammation. *Cell Metab.* 4, 13–24. doi:10.1016/j.cmet.2006.05.011.

Villoslada, P., Alonso, C., Agirrezabal, I., Kotelnikova, E., Zubizarreta, I., Pulido-Valdeolivas, I., et al. (2017). Metabolomic signatures associated with disease severity in multiple sclerosis. *Neurol. Neuroimmunol. NeuroInflammation* 4. doi:10.1212/NXI.0000000000000321.

Voet, S., Prinz, M., and van Loo, G. (2019). Microglia in Central Nervous System Inflammation and Multiple Sclerosis Pathology. *Trends Mol. Med.* 25, 112–123. doi:10.1016/j.molmed.2018.11.005.

Volobouеva, L. A., Emery, J. F., Sun, X., and Giffard, R. G. (2013). Inflammatory response of microglial BV-2 cells includes a glycolytic shift and is modulated by mitochondrial glucose-regulated protein 75/mortalin. *FEBS Lett.* 587, 756–762. doi:10.1016/j.febslet.2013.01.067.

Vukovic, J., Colditz, M. J., Blackmore, D. G., Ruitenberg, M. J., and Bartlett, P. F. (2012). Microglia modulate hippocampal neural precursor activity in response to exercise and aging. *J. Neurosci.* 32, 6435–6443. doi:10.1523/JNEUROSCI.5925-11.2012.

Wake, H., Moorhouse, A. J., Jinno, S., Kohsaka, S., and Nabekura, J. (2009). Resting microglia directly monitor the functional state of synapses in vivo and determine the fate of ischemic terminals. *J. Neurosci.* 29, 3974–3980. doi:10.1523/JNEUROSCI.4363-08.2009.

Wakselman, S., Béchade, C., Roumier, A., Bernard, D., Triller, A., and Bessis, A. (2008). Developmental neuronal death in hippocampus requires the microglial CD11b integrin and DAP12 immunoreceptor. *J. Neurosci.* 28, 8138–8143. doi:10.1523/JNEUROSCI.1006-08.2008.

Wang, S., Liu, R., Yu, Q., Dong, L., Bi, Y., and Liu, G. (2019). Metabolic reprogramming of macrophages during infections and cancer. *Cancer Lett.* 452, 14–22. doi:10.1016/j.canlet.2019.03.015.

Warburg, O. (1956). On the origin of cancer cells. *Science* 123, 309–314. doi:10.1126/science.123.3191.309.

Watanabe, M., Toyama, Y., and Nishiyama, A. (2002). Differentiation of proliferated NG2-positive glial progenitor cells in a remyelinating lesion. *J. Neurosci. Res.* 69, 826–836. doi:10.1002/jnr.10338.

Weiss, M., Blazek, K., Byrne, A. J., Perocheau, D. P., and Udalova, I. A. (2013). IRF5 is a specific marker of inflammatory macrophages in vivo. *Mediators Inflamm.* 2013. doi:10.1155/2013/245804.

Weiss, M., Byrne, A. J., Blazek, K., Saliba, D. G., Pease, J. E., Perocheau, D., et al. (2015). IRF5 controls both acute and chronic inflammation. *Proc. Natl. Acad. Sci. U. S. A.* 112, 11001–11006. doi:10.1073/pnas.1506254112.

Weissert, R. (2013). The immune pathogenesis of multiple sclerosis. *J. Neuroimmune Pharmacol.* 8, 857–866. doi:10.1007/s11481-013-9467-3.

West, A. P., Brodsky, I. E., Rahner, C., Woo, D. K., Erdjument-Bromage, H., Tempst, P., et al. (2011). TLR signalling augments macrophage bactericidal activity through mitochondrial ROS. *Nature* 472, 476–480. doi:10.1038/nature09973.

Wlodarczyk, A., Holtman, I. R., Krueger, M., Yogev, N., Bruttger, J., Khorooshi, R., et al. (2017). A novel microglial subset plays a key role in myelinogenesis in developing brain. *EMBO J.* 36, 3292–3308. doi:10.15252/embj.201696056.

Xue, J., Schmidt, S. V., Sander, J., Draffehn, A., Krebs, W., Quester, I., et al. (2014). Transcriptome-Based Network Analysis Reveals a Spectrum Model of Human Macrophage Activation. *Immunity* 40, 274–288. doi:10.1016/j.immuni.2014.01.006.

Yamasaki, R., Lu, H., Butovsky, O., Ohno, N., Rietsch, A. M., Cialic, R., et al. (2014). Differential roles of microglia and monocytes in the inflamed central nervous system. *J. Exp. Med.* 211, 1533–1549. doi:10.1084/jem.20132477.

Yan, J., Pandey, S. P., Barnes, B. J., Turner, J. R., and Abraham, C. (2020a). T Cell-Intrinsic IRF5 Regulates T Cell Signaling, Migration, and Differentiation and Promotes Intestinal Inflammation. *Cell Rep.* 31, 107820. doi:10.1016/j.celrep.2020.107820.

Yan, J., Peter Bengtson, C., Buchthal, B., Hagenston, A. M., and Bading, H. (2020b). Coupling of NMDA receptors and TRPM4 guides discovery of unconventional neuroprotectants. *Science* 370. doi:10.1126/science.aay3302.

Yang, S., Qin, C., Hu, Z. W., Zhou, L. Q., Yu, H. H., Chen, M., et al. (2021). Microglia reprogram metabolic profiles for phenotype and function changes in central nervous system. *Neurobiol. Dis.* 152, 105290. doi:10.1016/j.nbd.2021.105290.

Yang, Z., and Ming, X. F. (2014). Functions of arginase isoforms in macrophage inflammatory responses: Impact on cardiovascular diseases and metabolic disorders. *Front. Immunol.* 5, 1–10. doi:10.3389/fimmu.2014.00533.

Yeo, W., and Gautier, J. (2004). Early neural cell death: Dying to become neurons. *Dev. Biol.* 274, 233–244. doi:10.1016/j.ydbio.2004.07.026.

Yin, Y., Henzl, M. T., Lorber, B., Nakazawa, T., Thomas, T. T., Jiang, F., et al. (2006). Oncomodulin is a macrophage-derived signal for axon regeneration in retinal ganglion cells. *Nat. Neurosci.* 9, 843–852. doi:10.1038/nn1701.

Yoshida, Y., Yoshimi, R., Yoshii, H., Kim, D., Dey, A., Xiong, H., et al. (2014). The Transcription Factor IRF8 Activates Integrin-Mediated TGF-β Signaling and Promotes Neuroinflammation. *Immunity* 40, 187–198. doi:10.1016/j.immuni.2013.11.022.

You, Y., and Gupta, V. (2018). The extracellular matrix and remyelination strategies in multiple sclerosis. *eNeuro* 5, 2–5. doi:10.1523/ENEURO.0435-17.2018.

Zabala, A., Vazquez-Villoldo, N., Rissiek, B., Gejo, J., Martin, A., Palomino, A., et al. (2018). P2X4 receptor controls microglia activation and favors remyelination in autoimmune encephalitis. *EMBO Mol. Med.* 10, e8743. doi:10.15252/emmm.201708743.

Zalc, B. (2018). One hundred and fifty years ago Charcot reported multiple sclerosis as a new neurological disease. *Brain* 141, 3482–3488. doi:10.1093/brain/awy287.

Zhan, L., Fan, L., Kodama, L., Sohn, P. D., Wong, M. Y., Mousa, G. A., et al. (2020). A mac2-positive progenitor-like microglial population is resistant to csf1r inhibition in adult mouse brain. *Elife* 9, 1–22. doi:10.7554/eLife.51796.

Zhang, L., Ji, L., Tang, X., Chen, X., Li, Z., Mi, X., et al. (2015). Inhibition to DRP1 translocation can mitigate p38 MAPK-signaling pathway activation in GMC induced by hyperglycemia. *Ren. Fail.* 37, 903–910. doi:10.3109/0886022X.2015.1034607.

Zhang, Y., Chen, K., Sloan, S. A., Bennett, M. L., Scholze, A. R., O'Keeffe, S., et al. (2014). An RNA-sequencing transcriptome and splicing database of glia, neurons, and vascular cells of the cerebral cortex. *J. Neurosci.* 34, 11929–11947. doi:10.1523/JNEUROSCI.1860-14.2014.

Zhao, J., Bi, W., Xiao, S., Lan, X., Cheng, X., Zhang, J., et al. (2019). Neuroinflammation induced by lipopolysaccharide causes cognitive impairment in mice. *Sci. Rep.* 9, 1–12. doi:10.1038/s41598-019-42286-8.

Zhou, Y., Zhou, B., Pache, L., Chang, M., Khodabakhshi, A. H., Tanaseichuk, O., et al. (2019). Metascape provides a biologist-oriented resource for the analysis of systems-level datasets. *Nat. Commun.* 10. doi:10.1038/s41467-019-09234-6.

Zrzavy, T., Hametner, S., Wimmer, I., Butovsky, O., Weiner, H. L., and Lassmann, H. (2017). Loss of "homeostatic" microglia and patterns of their activation in active multiple sclerosis. *Brain* 140, 1900–1913. doi:10.1093/brain/awx113.